Hydrometeorological Triggers of Debris Flows.

Evolution of the temporal occurrence of debris flows between 1900 and 2008.

Diplomarbeit

Eingereicht am

Institut für Alpine Naturgefahren,

Universität für Bodenkultur, Wien

Betreuer

Univ. Prof. DI Dr. nat. techn. Johannes HÜBL

Co-Betreuer

Ass. Prof. DI Dr. nat. techn. Roland KAITNA

Martin BRAUN

Wien, November 2014

Eidesstattliche Erklärung

Hiermit versichere ich, die Diplomarbeit mit dem Titel „Hydrometeorological Triggers of Debris Flows“ eigenständig und nach bestem Wissen und Gewissen verfasst zu haben. Es wurden keine weiteren, bis auf die von mir im Literaturverzeichnis angeführten Quellen verwendet, die in der vorliegenden Arbeit als solche gekennzeichnet sind. Sämtliche abgeleiteten Quellen wie Datensätze oder Illustrationen wurden als solche hervorgehoben.

Declaration of Authorship

I hereby certify, that the master thesis with the title “Hydrometeorological Triggers of Debris Flows” is to the best of my knowledge and belief the result of my own investigations and is composed by myself unless stated otherwise in the text. All content derived from the work of others, including graphs and data sets has been specifically acknowledged.

_____

Martin Braun

Acknowledgement

First of all I want to thank my Supervisor Johannes Hübl for giving me the opportunity to write my thesis on this interesting topic and providing valuable constructive remarks at critical stages of the thesis. The numerous anticipatory brain-storming sessions with my Co-Supervisor Roland Kaitna were invaluable for writing this thesis as well as his unconditional support to stay at the right track with everything.

I also want to give credit to Matto Berti from the Department at Biological, Geological, and Environmental Sciences at the University of Bologna for sharing his rainfall detection algorithm with me and giving me examples on how to utilise it for my research. Acknowledgement also goes to ZAMG and the National Hydrographic Service for providing rainfall and temperature data.

Moreover I want to thank Renate Kepplinger and Verena Auberger for assisting me in proof reading the thesis. Of course the sole responsibility for the content lies with the author.

Special thanks to my PhD supervisors at the departments of economics and social sciences for giving me the flexibility for investigating this topic besides my other tasks as well as to the secretaries Monika Stanzer, Eva Motsch and Eva Lanz for supporting me in administrative matters. Numerous colleagues and lecturers provided helpful input throughout my studies and while writing this thesis.

I am also grateful to my parents whose support made my studies possible and to Oyuna for her emotional support. Lastly I want to thank my extended family and all my friends for helping me getting through difficult times.

Abstract

The main factor responsible for triggering debris flows is rainfall. The triggering mechanism however is a complex combination of causal factors which can be modelled by process-based models for intensively surveyed catchments. To date it is not possible to conduct a large-scale analysis for thousands of debris flows with sufficient information about relevant parameters to make substantiated general statements about their triggering behaviour. This problem can be overcome with the aid of well-established empirical approaches which help to describe factors of interest. In this study the evolution of the temporal occurrence of debris flows during the last one hundred years and the corresponding hydrometeorological triggers of debris flows are investigated and empirical relationships derived. The basis for this analysis is a database of all debris flow events documented by local authorities as well as data of daily precipitation and temperature from public meteorological station networks. The specific goal of the thesis was to identify potential shifts in debris-flow occurrence over the last > 100 years and to determine intensity-duration thresholds for debris flow triggering. Finally, a Bayesian approach was used to analyse the effects of different precipitation parameters on debris flow triggering probability. Results are comparable to the range of former studies and show that the distance of a precipitation gauge to the event is critical for identifying threshold conditions. It also shows that frequentist approaches are sensitive to the completeness of a hazard inventory as well as to the method of identification of triggering event rainfall or utilisation of a rainfall detection algorithm. The outcomes of this study contribute to a better understanding of the reaction of torrential watersheds to rainfall and aid developing more reliable debris flow forecasting tools for early warning.

Kurzfassung

Regen ist eine der Hauptursachen für das Auslösen von Muren. Der Auslösemechanismus ist jedoch von einem komplexen Zusammenspiel von verschiedensten kausalen Faktoren abhängig, die üblicherweise mit Hilfe von prozessbasierten Modellen adäquat beschrieben werden können. Solche Modelle können meist nur für gut dokumentierte Einzugsgebiete verwendet werden. Bis zum jetzigen Zeitpunkt ist es nicht möglich, alle notwendigen Informationen für eine großangelegte Untersuchung tausender Muren durchzuführen, was notwendig wäre um eine fundierte, generelle Beschreibung des Auslösemechanismus zu tätigen. Mit Hilfe von etablierten empirischen Herangehensweisen kann diesem Problem begegnet werden. Um die Auftretenshäufigkeit und Evolution von Muren im Hinblick auf hydrometeorologische Auslöser für die letzten hundert Jahre zu analysieren, wurden empirische Zusammenhänge auf Basis von Niederschlags-Intensitäts-Diagrammen genutzt und mit anderen häufigkeitsbasierten Herangehensweisen kombiniert. Für den vorliegenden Zeitraum (1900-2008) ist es zudem notwendig, zumindest die Temperatur als Indikator für Klimawandeleffekte zu berücksichtigen um potenzielle Veränderungen der Auftretenshäufigkeit mit klimatischen Veränderungen vergleichen zu können. Das Hauptziel der Arbeit ist daher, Primärdaten zu Niederschlag, Temperatur und Naturgefahren zu analysieren, generelle und klimawandelbedingte Trends herauszuarbeiten und Niederschlags-Intensitäts-Grenzwerte zu ermitteln. Abschließend wurde eine mit Hilfe des Theorems nach Bayes eine Untersuchung der Effekte von verschiedenen Niederschlagsklassen auf die Auftretenswahrscheinlichkeit vorgenommen. Die Ergebnisse wurden mit bereits publizierten Arbeiten verglichen und eine Sensitivitätsanalyse durchgeführt. Sie bewegen sich im Spektrum von vorhergehenden Studien und zeigen, dass vor Allem der Abstand einer Messstation zur Mure ein wichtiger Faktor in Bezug auf die Validität der Ergebnisse ist. Ferner wurde gezeigt dass deskriptive, häufigkeitsbasierte Methoden einen homogen erhobenen Ereigniskatalog voraussetzen und abhängig davon sind, wie ein Regenereignis definiert ist bzw. welcher Algorithmus angewandt wird um Regenereignisse zu identifizieren.

Table of Contents

1 Introduction

Gravitational mass-movements such as avalanches, landslides and floods pose a continuous threat in mountainous areas. Because the underlying physical processes cannot be modelled for DFs without thorough investigation of site conditions and collection of specific parameters through field work and/or evaluation with geo-information systems (GIS), it stands for reason to use other means of evaluation for larger sets of data. Therefore a quantitative empirical approach oriented at hazard frequency (also called *frequentist* approach) is used taking into account that for this thesis a dataset consisting of both a very large temporal spectrum of 100 years as well as a large geographic spectrum covering most parts of mountainous Austria accounting for many different catchments with a high diversity of mostly unknown catchment parameters. Such an approach provides a viable solution to possibly find common indicators and trends of CC impacts on DFs. Especially with respect for providing a first approach to find patterns for hydrometeorological triggers for a large part of the Austrian Alps, well-established empirical approaches can be utilised to at least partly overcome the problem of lacking data and accurate historical resolution.

The main parameter for the initiation of DFs is precipitation (more specifically: rainfall), but in the context of a study taking into account potential climatic shifts a combined approach for considering rainfall as well as temperature and connect this information to DF inventories where possible.

There are two main objectives to be covered by the thesis at hand:

1. How did the temporal occurrence of DFs evolve in Austria?

Connected to this question are the following secondary objectives:

   a. Are there seasonal shifts occurring in events triggered?
   b. Is it possible to assess the development of occurrence rates and magnitudes for the last 100 years?

Since triggering of DFs is mainly connected to rainfall:

2. What can the examination of rainfall data tell us with regard to triggering mechanisms of DFs? Therefore several important secondary questions arise:
   a. What is the percentage of events triggered by precipitation (thunderstorms and frontal systems)?
   b. Can seasonal shifts be determined with regard to these systems and can threshold values for frontal rainfall be determined?
   c. Which patterns exist between magnitude, frequency, precipitation thresholds and seasonality over time?

To answer the questions within the scope of a master thesis in this rather broad context mentioned in the *Introduction*, there is a brief description of the study area, scope and available data in *Study Scope* some of the relevant information needed for conducting a proper study as well as information omitted (e.g. other empirical approaches, which could not be verified because of lacking data) will be explained in the chapter *Theoretical Background*, which will explain the basics of precipitation formation, classification and relevant parameters as well as delineate DFs in the context of other hazards. As a foundation for the study relevant aspects of CC, available DF data and the role of CC on such hazards will be described as well as approaches for dealing with uncertainties and extremes. While the *Data preparation* section will describe how the data was prepared for this thesis-project, the *Methods* present an overview of the methods used for this study, the *Results* show the main findings separated into analyses of primary data, of shifts and an empirical approach on DF initiation followed by a *Discussion and Conclusion*. An aggregated comprehensive overview of the study results is provided in the respective appendices.

After the end of each chapter an emphasised section summarizes the main findings and limitations on a by-chapter basis.

2 Study Scope

With regard to gravitational mass movements, Austria – besides Switzerland – has a special position in Europe. About two thirds of the country consist of mountainous regions the most part of which are being the European Alps. From a meteorological point of view, the Alps are a climatically transitional region. They are part of a major atmospheric circulation source area influenced by three major regimes: the Atlantic Ocean, the Mediterranean Sea and the climate of continental Europe. Generally, the Austrian part of the Alps can be split into four climatic regions: The northwest, northeast, southwest and southeast (Matulla et al., 2003).

The study area consisted of all DFs occurring in the Republic of Austria from 1900 until 2008, which are indicated by the red hexagons in the map in Figure 1.

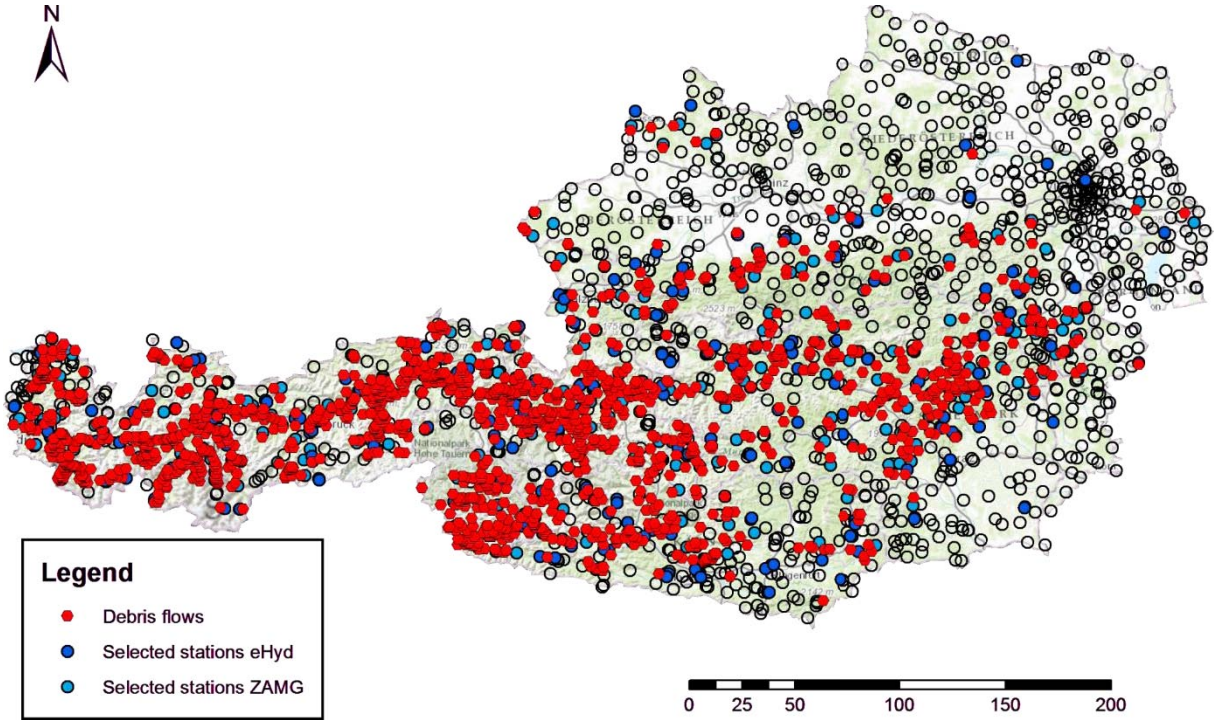

Figure 1: Illustration of all events and the meteorological stations considered for analysis. While the red hexagons depict the 2,412 events investigated, the dark blue circles show eHYD stations measuring daily precipitation. The light blue circles represent the ZAMG stations additionally used for analysis. The translucent circles with a black outline show all stations examined for suitability but not used for analysis

In total, 2,412 documented DF events and data distributed over a region of approximately 80,000 km² were available for investigation. A worldwide unique debris flow event database (EDB, provided by IAN) was merged together with two public datasets of daily precipitation data, data from the Zentralanstalt für Meteorologie und Geodynamic (ZAMG) and from the Hydrographic Service of Austria ("eHYD-data"). From the EDB only DFs with assigned daily dates were considered. Precipitation data was provided for 1,649 meteorological stations. The high number for precipitation gauges results in

the fact that some stations were moved 1 to 9 times during their lifetime. In this case ZAMG stations were assigned a new name, whereas eHYD-stations kept the same iD and just the coordinates changed.

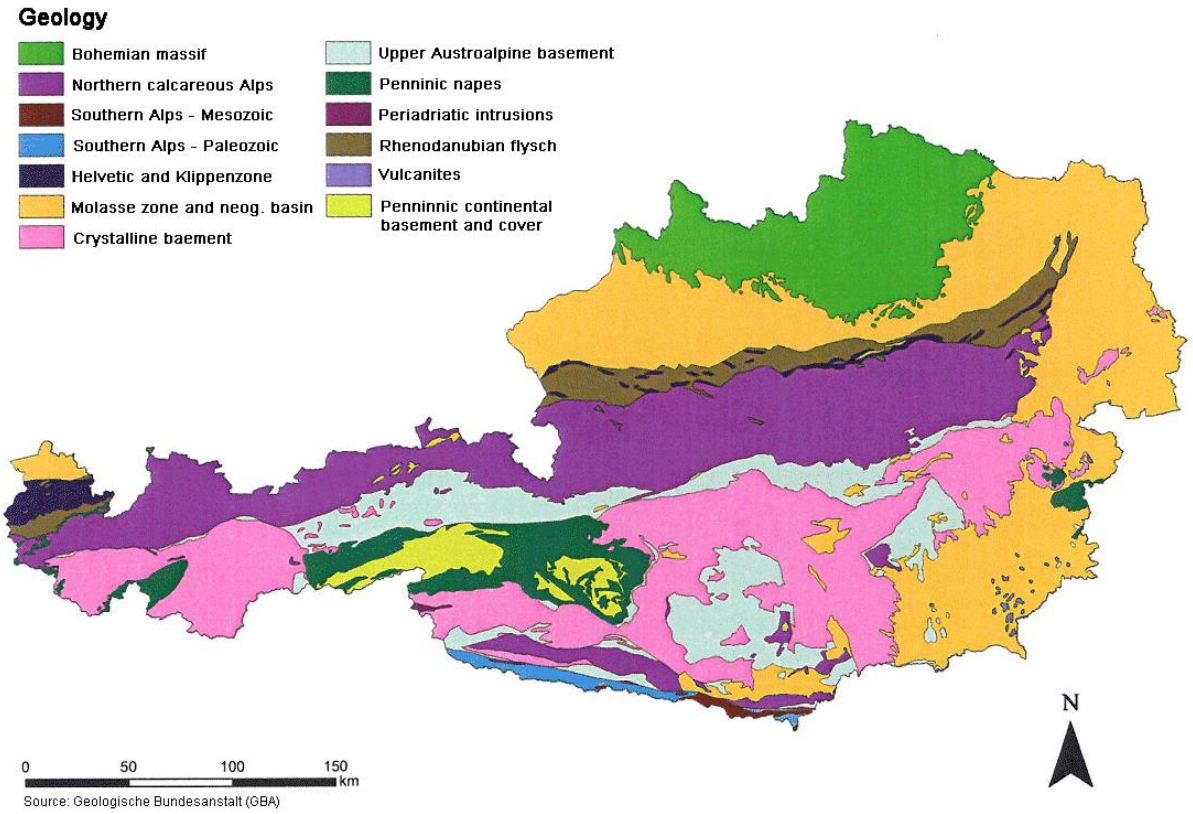

Figure 2: Geologic zones of Austria (modified after Sauer et al., 1992; Sitter, 2010)

When overlaying the map of DFs with the geologic map of Austria the majority of DFs occur in high alpine catchments. As a previous study showed that DFs are dominating in the Penninic napes, the Crystalline basement, the Upper Austroalpine basement, and Northern calcareous Alps (cf. Table 1). The table below summarises the study conducted by Sitter (2010).

Geological unit	Percentage of debris-like processes [%]	Total Number of processes
Bohemian Massif	0.4	236
Northern calcareous Alps	*21.0*	*919*
Helvetic and Klippenzone	14.1	71
Molasse zone and neogene basin	6.3	254
Crystalline basement	*30.3*	*1,198*
Upper Austroalpine basement	*26.7*	*797*
Penninic napes	*39.3*	*216*
Rhenodanubian flysch	5.5	344

Table 1: Influence of geological conditions on DF like processes (data from Sitter, 2010). *Roughly 95 % of DF occur in four geological units: northern calcareous Alps, crystalline basement, upper austroalpine basement, and penninic napes.*

While the Molasse and the Flysch zone would favour DF-like processes, the relief energy available in these zones is too low and provides a limiting factor for transport processes. In the Bohemian Massif

though, the relief energy would increase again but granite and gneiss are a limiting factor for debris input.

The abovementioned dominant geological units for gravitational mass movements are mainly situated at the main Alpine ridge and mainly cover southern Vorarlberg, Tyrol, Salzburg, Styria, and Carinthia with about one third of the catchments. Especially the high relief in this area as well as the geological substrate in this area, which is very susceptible to weathering are dominant factors for such processes.

Out of 1,649 precipitation gauges, 452 were utilised for investigating 2,034 DF events from a database of 2,412 DFs occurring from 1900-2008. The numbers of DFs investigated are lower, when the distance of the nearest station (nearest neighbour precipitation gauge) is limited.

3 Theoretical Background

Like most hazardous processes, gravitational mass movements are occurring through an interrelation of various causal relationships determined by long-term climatic and geophysical impacts, catchment morphology, event history (mainly defined by basic and variable disposition), antecedent conditions and short-term climatic parameters (Fuchs and Keiler, 2006).

All of these can help to describe different *aspects* of gravitational mass movements. Whereas the long-term processes such as glacial retreat, debuttressing effects or climatic impacts on geomorphic parameters (such as the lithological characteristics; Rickenmann, 1999) are responsible for the basic disposition (with the long-term climatic conditions having an effect on geomorphic as well as ecosystem conditions influencing the potential sediment availability), short-term effects influence the variable disposition and thus the overall load on the system which can lead to mass movements when a certain load-threshold is exceeded. In other words, while short-term effects usually decide if single DFs can be triggered, long-term effects can affect DF behaviour on a regional to continental scale. It is not yet known how climatic tipping points could change the basic disposition.

Additionally to the conditions mentioned, social dimensions also play a major role in risk perception. This is not only true for considerations about changing risk in future climatic conditions, but also when examining the history with gravitational mass movements, where thinning-out of time series providing information about past events is a major problem which has to be dealt with using specialised approaches.

During the last decades, systematic inventories of gravitational mass movements and important parameters associated with their occurrence have started, but only about 100 of 1,000 (10 %) torrential catchments being equipped with monitoring instruments (Sitter, 2010). As especially data from smaller catchments is lacking, approaches like dendrogeomorphic, stratigraphic, lichenometric or other are necessary to inventorise the abovementioned processes (Stoffel, 2010).

The thesis at hand is based on such an inventory of historic events that was compiled at the Institute of Mountain Risk Engineering (Hübl et al., 2011, 2008). The inventory was compiled using two historical chronicles (Brixner chronicle and Stiny chronicle) and as well as hazard reports by governmental institutions, and also newer information such as newspaper articles, technical reviews, as-build drawings, hazard reports and information from departments of the Austrian Torrent and Avalanche control. Background information about the EDB is provided in detail in a thesis by Sitter (2010), whereas the most relevant information about the data used for this study is provided in Chapter 4: *Data Preparation and Methods*.

In this thesis, the focus will be mainly on precipitation, since – amongst other factors – precipitation has by far the biggest influence on the characteristics of DF occurrence and magnitude. Associated parameters will be also considered because the initiation of DFs is a result of a complex interaction of climatic factors and the geophysical processes mentioned above on different temporal and spatial scales.

For clarification, a division into main climatic factors and secondary climatic factors was made. The main climatic factors describe the major parameters of interest in this thesis and secondary climatic factors are associated ones, which were not fully be integrated in this work.

3.1 Gravitational Mass Movements

Figure 3 is showing the number of people reportedly being affected by natural disasters globally. However, it only depicts a broad classification of events regarding the international dimension making the classification not appropriate for the subject under study here: in this data base DFs are either counted under hydrological or geophysical hazards depending whether the mass movement is dry or wet without a consistent rule (i.e., there is a distinction by water content, but it is not explained further. Apparently debris flows which are part of geophysical hazards have less water content; CRED, 2009). It is expected that disasters of the climatological and meteorological category will also increase throughout the world, because mountainous areas belong to rather susceptible areas globally (The World Bank, 2005). For a more consistent approach it seems desirable to use the category mass movement and subsume all DFs as wet mass movement in this data base.

Disaster subgroup	**Definition**	**Disaster Main Types**
Geophysical	Events originating from solid earth	Earthquake, Volcano, Mass movement (dry)
Meteorological	Events caused by short-lived/small to meso scale atmospheric processes (in the spectrum from min. to days)	Storm
Hydrological	Events caused by deviations in the normal water cycle and/or overflow of bodies of water caused by wind set-up	Flood, Mass Movement (wet)
Climatological	Events caused by long-lived/meso to macro scale processes (in the spectrum from intra-seasonal to multi-decadal climate variability)	Extreme Temperature, Drought, Wildfire
Biological	Disaster caused by the exposure of living organisms to germs and toxic substances	Epidemic, Insect Infestation, Animal Stampede

Table 2: EM-DAT disaster definition and classification (Guha-Sapir et al., 2011)

Table 2 shows an overview how disasters are categorised by the UN and by EM-DAT, including a short definition and typical phenomena (Guha-Sapir et al., 2011). Here DFs belong to the hydrological category because of their water content; however these events do not seem representative for the current study, since only disastrous types of hazards are reported in this database instead of aiming at a complete inventory. EM-DAT uses the United Nation definition of a disaster being a "serious disruption of the functioning of society, causing widespread human, material, or environmental losses which exceed the ability of the affected society to cope using only its own resources" (United Nations, 1992, s.p.). Since disasters are commonly perceived as realization of hazards which exceed the response capacity of a society (Coppola, 2011), DFs will be strongly underrepresented.

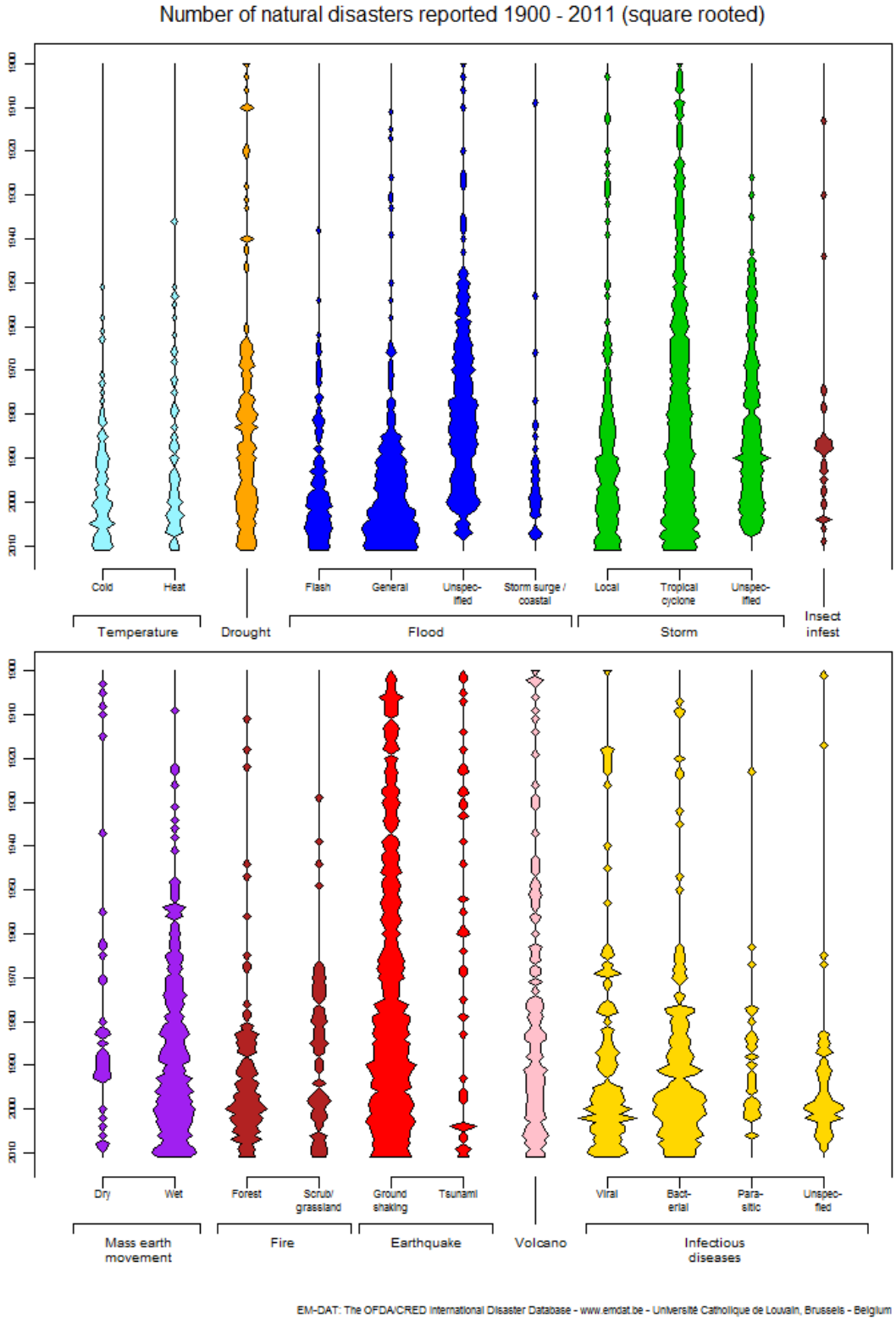

Figure 3: Number of disasters reported between 1900 and 2011 (square rooted; CRED, 2009). *Time-related underreporting further back in times is clearly visible*

Compared to the previous decade the number of people affected as well as the number of people killed by disasters in Europe decreased while the number of events and the monetary damage inflicted increased. Globally the trend is not so clear. During the last decade hazards in Europe seem to be

underreported (cf. colour-coded Table 3 showing no trends). On the other side, when looking into yearly damage statistics the overall trend is clear. While a first guess would be that there is just neither a clear signal nor climatic influence in frequency and occurrence of gravitational mass movements, this thesis aims at thoroughly investigating this topic.

	№ of Events	Killed [1,000 people]	Total Affected [1,000 people]	Damage [Billion USD]
World 1900-1984	171	39,342	4,928	2.09
World 1985-1994	136	8,293	3,356	2.52
World 1995-2004	204	9,095	2,468	2.52
World 2005-2014	169	8,512	2,979	1.54
Europe 1900-1984	35	15,472	10	0.73
Europe 1985-1994	16	706	21	1.05
Europe 1995-2004	23	618	18	1.33
Europe 2005-2014	4	17	1	n.a.

Table 3: Numbers of events, people killed and affected as well as damage inflicted in the last three decades and in the period before (Categories dry and wet mass movements, i.e. Avalanche, debris flow, landslide, rockfall, subsidence, and unspecified CRED, 2009)*. The table is colour coded showing larger values in red, and smaller values in green.*

When examining the Austrian EDB, the cumulative curves for all mountain-related hazards do not show a significant change in hazard occurrence but rather increase linearly since 1960 (cf. Figure 4). Before the 1960ies less events were counted, however, it cannot be excluded that this scaling break is caused by under-reporting in the time before 1960. DFs amount to about 10% of all mountain-related hazards in Austria.

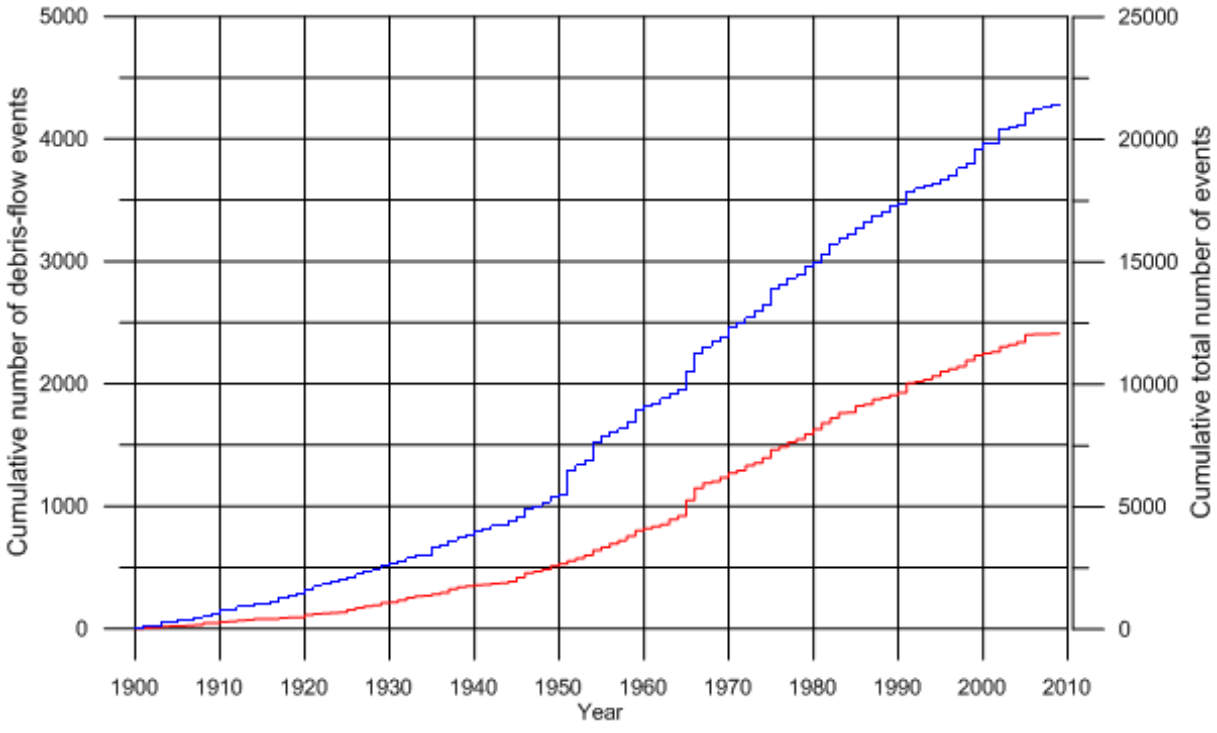

Figure 4: Cumulative curves for the total number of events from the EDB (21437, blue line) and DFs (2412, red line) from 1900 to 2009 (data taken from EDB)

For the European Union, there is an overall increase of natural disasters (EEA, 2012) as depicted in Figure 5. After comparison with EM-DAT data, the trend for hydrological hazards excluding floods (with DFs being a sub group in the EEA report) is unclear.

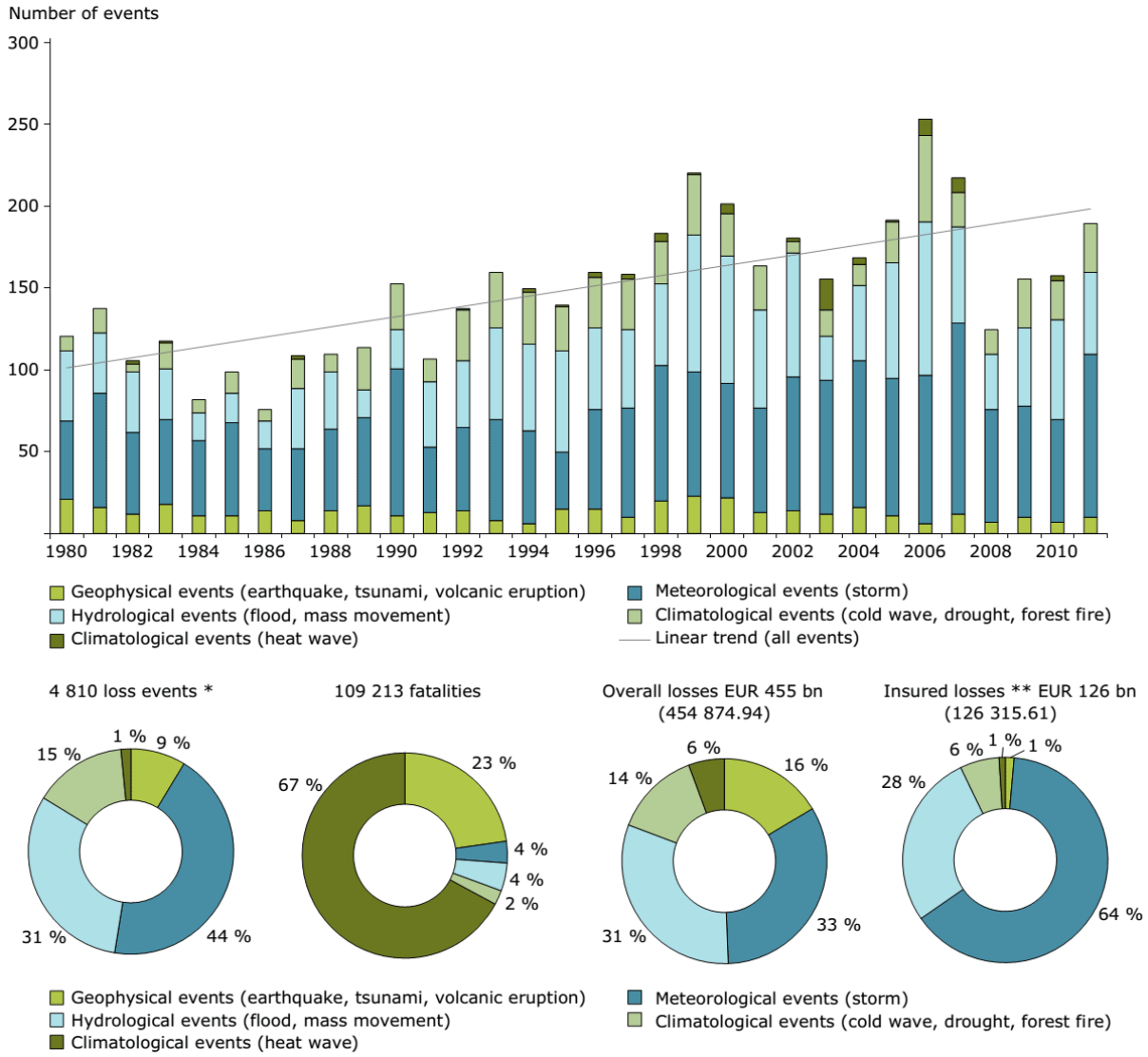

Figure 5: Natural disasters in EEA member countries (1980-2011; EEA, 2012)

Because the EDB is the most extensive hazard inventory currently available in Austria, it will subsequently be used as reference database in the thesis.

This historical inventory of hazardous events was compiled according to the 3W-standard (what, when, where) defined during the INTERREG-project DISALP (DIS-ALP, 2007; Hübl et al., 2008). Following these standards, the process group (water-related, snow-related, slump, glide) and the associated process (eleven processes related to the process group) as well as the name of the catchment, the geographic location including coordinates, and the date of the event (as specific as possible) were incorporated into the database. Where possible, the event magnitude and triggering conditions were also added. The event magnitude was compiled from run-out area, spatial extent, deposition heights and

qualitative indicators and categorised into five different classes: small, medium, large, extremely large, and unknown (cf. Figure 6). Category "unknown" was used for events where no or not enough corresponding information was assigned in the respective database entry.

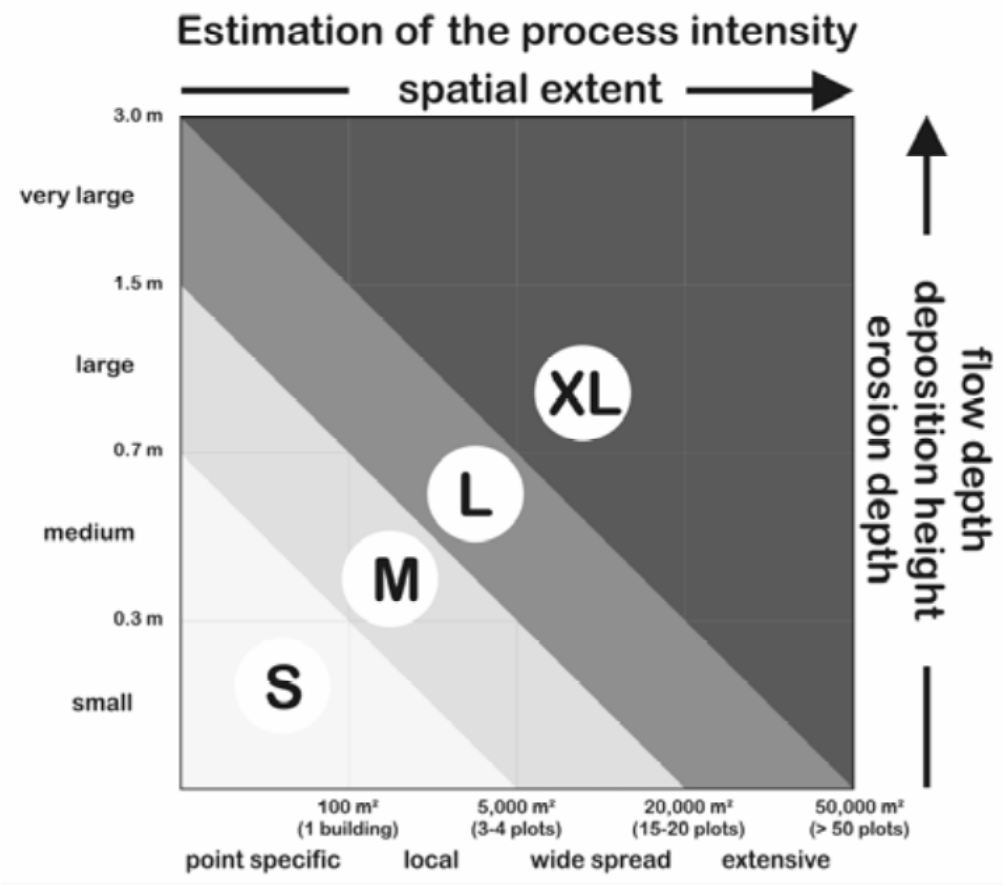

Figure 6: Process magnitude classification used in the EDB provided by the Institute of Mountain Risk Engineering (Hübl et al., 2011)

3.1.1 Dominant catchment processes in Austria

In Austria, two general types of dominant processes were distinguished on a catchment basis: *Fluvial* and *DF-like* hazard processes. Additionally, some catchments which were not clearly attributable to one type of process are termed indifferent catchments.

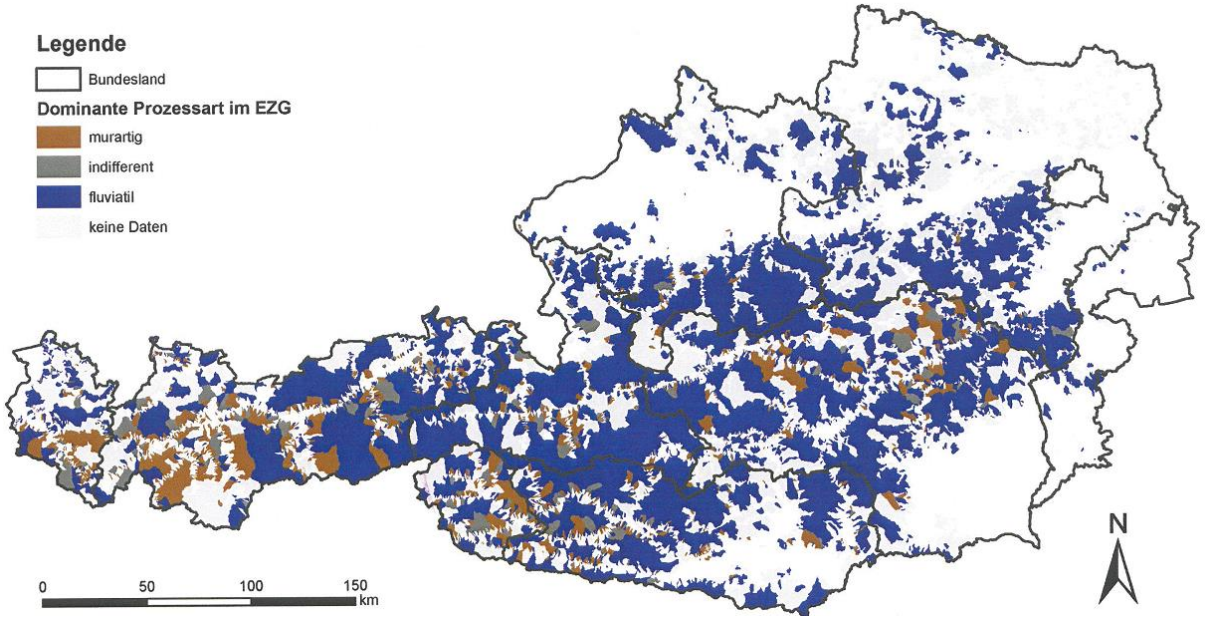

Figure 7: Dominant catchment processes in Austria (Sitter, 2010)

Figure 7 shows the dominant catchment processes in Austria, with DFs depicted in brown (Hübl et al. (2011) We see that DF like processes only occurred in catchments < 80 km², with 95 % of catchments prone to DFs are < 15 km². Bigger catchments thus showed predominantly fluvial behaviour.

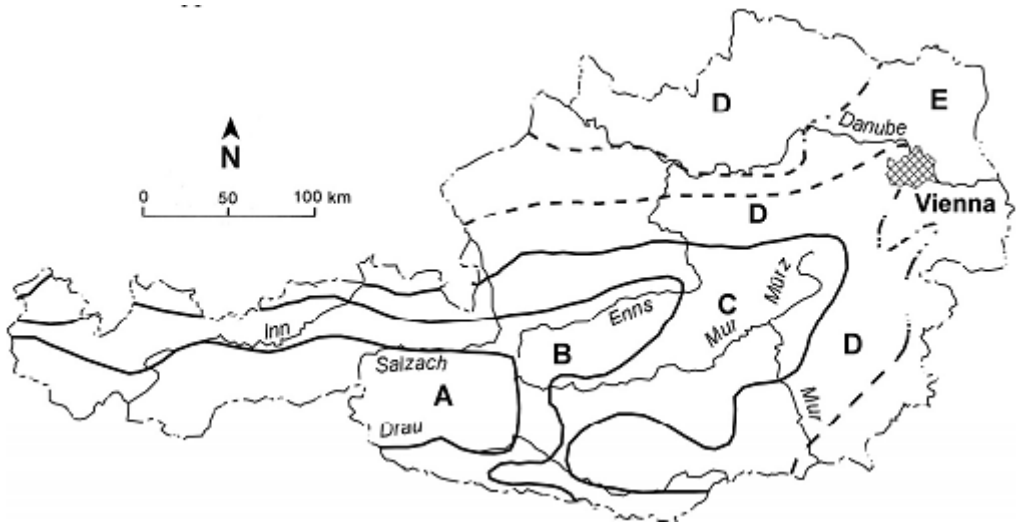

Figure 8: Overview of torrent zones in Austria (Embleton-Hamann, 2007)

The pattern for catchments prone to DFs was already analysed by Kronfellner-Kraus (1984) and showed that the catchments can be classified by maximum debris-load which is determined by the orographic characteristics on a large-scale: zones with large and dangerous debris stores are located in zones of highest relief (zone A in Figure 8; highest DF occurrence), while triggering factors for torrential hazards in zones B and C are more complex. According Kronfellner-Kraus' study Austria can be subdivided into five zones (Figure 8 and Table 4).

Zone	Observed maximum debris loads (G. KRONFELLNER-KRAUS, pers. comm.)	Percentage of torrent types (for explanation see text) based on AULITZKY (1986)		
		Types 1+2	Type 3	Type 4
A	> 100,000m³, exceptionally < 1 000 000m³	81	19	-
B	100,000 – 200,000m³	64	35	1
C	< 60,000m³	33	55	12
D	< 20,000m³	10	68	22
E	Loess gullies up to several thousand m³; other torrents up to several hundred m³	-	65	35

Table 4: DF zonation (from Embleton-Hamann, 2007). *Torrent types follow classification defined by Aulitzky (1986) with Type 1 being the most dangerous (high occurrence of DF, not obeying the laws of hydraulics). Type 2 are torrents with high debris content (mainly obeying laws of hydraulics), type 3 torrents with some debris content, and type 4 are torrents without significant debris load.*

Bertrand et al. (2013) emphasize that the most dangerous torrent catchments are the ones that regularly produce DFs. This is because the sediment volumes transported by DFs are two to three orders of magnitude higher than the volumes transported by floods (Mao et al., 2009) and that peak discharges are also considerably higher (Hungr et al., 2001), the combination of both leading to high impact forces in the run-out zone.

3.1.2 Melton number

The Melton ruggedness index or ruggedness number (Melton, 1957) is a dimensionless number which is a good overall measure for describing the drainage evolution of a catchment. It was found that this number is also related to the occurrence and intensity of geomorphic hazards in general. First it was used to describe basin dynamics with no specific context to gravitational mass movements, but later on it was increasingly used as an index if a catchment is more or less prone to geomorphic hazards especially those connected with sediment or water mobilisation and slope erosion (Slaymaker, 2010). This was further examined by Korvanen and Slaymaker (2008) who could prove a relationship of the Melton ruggedness index with debris fan slope as well as an inverse relationship between the latter and catchment area. Overall, they proved a direct relation of this index with gravitational mass movements as well as inverse catchment area (Rickenmann, 2009).

$D_d \left[\frac{km}{km^2}\right]$	H_t [m]	R	Coupling	Geomorphic process	Incidence of hazards
>10	>1,000	>10	High	DFs	High
1-10	300-1,000	ca. 1	Intermediate	Fluvial	Intermediate
<<10	>>1,000	<1	Low	Mass movements	High

Table 5: Characteristics described by the Melton ruggedness number (Slaymaker, 2010). *D_d... drainage density; H_t... basin relief; R... Melton ruggedness index*

In this context, the results of a study from Hübl et al. (2008) are supported by other research which shows that high-mountain valleys are much likelier to have DFs as prevalent processes, because they consist of smaller, more rough catchments where the initiation of DFs is much more likely than in a large, mid-slope catchment, which is dominated by fluvial processes (Bertrand et al., 2013). Bertrand states that the Melton index and the fan slope are the most important parameters indicating DF

occurrence (Hübl et al., 2011) Bertrand shows an overview of how the Melton ruggedness index can serve as an indicator in connection to drainage density and basin relief (denoted as *"coupling"* in Table 5).

3.1.3 Further classification

Because the Melton index is not more than a roughly empirically validated indicator for geomorphic process prevalence, other variables are used to describe a hazard in more detail. Table 6 summarizes important characteristics of DF-like processes in contrast to fluvial processes for better distinction. In the following sub-chapter important characteristics of DFs are described in detail.

Displacement type	**Fluvial**		**Debris-DF like**	
Name	Flow	Fluviatile sediment transport	DF like sediment transport	DF
Process type	Clear water flood	Weak sediment transport	Strong sediment transport	DF
Flow behaviour	Newtonian	Newtonian	Close to Newtonian	Non-Newtonian
Volumetric sediment concentration	negligible	0-2 %	20-40 %	>40 %
Max. grain size	mm to cm	Up to dm diameter	Up to m	Up to m
Density	About 1,000 kg/m³	<1,300 km/m³	1,300-1,700 km/m³	>1,700 kg/m³
Determination of clear water runoff possible	Yes	Restricted	No	No
Rating curve feasible	Yes	Yes	No	No
Q_{total}/Q_{flood}	1	1-1.4	1.4-3.5	>3.5
Viscosity [Pa]	0.001-0.01	0.01-0.2	0.2-2	>2
Shear strength	none	none	none	present
Main acting forces	Turbulence, tractive stress	Turbulence, tractive stress	Buoyancy, turbulence, tractive stress, dispersive pressure	Buoyancy, dispersive pressure, viscous and frictional forces
Distribution of sediment in the profile	Solids near the sole (creeping, saltating) and suspended matter distributed cross-sectionally	Solids near the sole (creeping, saltating) and suspended matter distributed cross-sectionally	Solids and suspended matter distributed cross-sectionally	Solids distributed cross-sectionally
Sorting of deposited sediment	present	present	not frequent	none
Decomposition of depositions	Yes	Yes	Yes/no	No
Damage through	Water and suspended matter	Water, suspended matter and rubble	Solids and water	Mainly solids (in interaction with water)

Table 6: Properties of processes occurring in torrential catchments (Hübl, 2006)

3.2 Debris Flows

The information and classification methods mentioned in the previous section are of good help for processing field investigations, for example when trying to classify a hazard in a consistent way to include it into a hazard inventory. This section describes accompanying parameters of interest in the context of mountain risk engineering in a more detailed way.

As van Steijn (1996), Hungr et al. (2005) and others have shown, DF activity in a certain area can be described with regard to frequency (i.e. the number of occurrences of DFs) and/or magnitude (i.e. the size of a DF event).

Currently, no long-term analysis of the entire event data available in the EDB in correlation to aforementioned parameters exists in Austria. Thus, the aim is to bridge this gap in climate-related information for DFs. In the Austrian Alps such processes are mainly occurring in small catchments (Aulitzky, 1980; Hübl et al., 2011). Since most DFs flow down torrential gorges and leave their marks, catchments with a general disposition towards a certain process can be identified by silent witnesses (Kaitna and Hübl, 2013).

For engineering hazard mitigation it is important to know certain process characteristics, like peak flow depth and mean velocity, however, often basic information like dominant process type as well as frequency of occurrence and magnitude of the event (Mazzorana et al., 2012) are rarely available (Fuchs et al., 2013, 2012).

DFs are mainly initiated by mobilisation of sediment stored in channels, which can be induced by channel erosion or through shallow landslides through the sudden input of large amounts of water both of which is directly influenced by rainfall, which can be intense or long-term rainstorm, sudden snowmelt, rain-on-snow events, or the sudden release of water from glaciers (glacier lake outburst floods; GLOF) or blockage and release, e.g. by dammed lakes. Whereas the initiation process depends on antecedent and initial conditions the structure of the process mainly depends on the location (cf. Figure 9) and morphology.

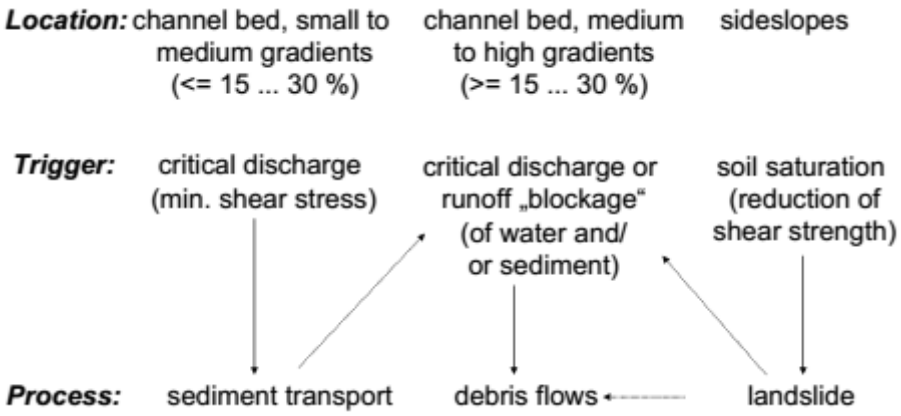

Figure 9: Dependence of a process from location (Rickenmann, 2009)

Figure 9 illustrates the role which location plays with regard to gravitational mass movements and shows some of the causal processes that are involved in DF formation.

3.2.1 Interactions of processes in torrents

A DF consists of a mixture of sediment, water, and occasionally woody debris. Because of its high content of sediment of various sizes and its unsteady and non-uniform flow behaviour, complex interactions between the liquid and solid phases yield high impact forces and high flow velocities. These dynamics are the results of multiscale interactions between the climate system and the geomorphology of a catchment. Often the DF process is divided into three zones: Initiation, transit, and deposition zone.

In the *initiation zone* (source area), the relief, the nature of the surface and subsurface, general vegetation cover and climatic factors are critical parameters, which are effective a priori, meaning that they are acting over very long time-scales and therefore usually considered as constant. Triggering conditions are weather related impacts (i.e. short-term characteristics of a changing climate) or disturbances of the processes mentioned above, which can occur through human activity or other geophysical processes (e.g. earthquakes).

In the *transit zone* (DF track), critical parameters are the inclination and cross section as well as the nature of the soil, terrain roughness, vegetation (dependent on previous erosion, LULUCF[1] and generation changes) and the availability of material. The latter depends on the history of the channel, like e.g. if a large DF event occurred recently it is very unlikely that another large DF is initiated, under a *ceteris paribus* assumption (in this case: other parameters within the system under consideration are constant).

[1] Land use, land-use change, and forestry

Finally there is the *deposition zone*, where the shape and height of the debris fan is influenced again by relief, but also by ground cover and potential obstacles e.g. houses or infrastructure. Because of precipitation being the main trigger it can occur suddenly, which makes it hard to develop early warning systems (De Blasio, 2011; Rickenmann, 2009).

Figure 10: DF zonation (Zone 1 = initiation zone, zone 2 = transition zone, zone 3 = deposition zone), and an illustrative example of the development of a DF (Konagai et al., 2007; Takahashi, 2007).

Not only process parameters in respective DF zones are relevant; DFs as a whole have different characteristics in terms of density and flow behaviour: in contrast to sediment-laden flows such as debris floods there is a harder-to-describe interaction between the liquid and solid phases, where the fluid and all sizes of particles can travel with equal speed (cf. example in Figure 10). Also, it can consist of more sediment than water (by volume). Compared to mud flows, DFs consist of coarser, granular and sometimes stonier particles having a significant impact on the flow behaviour. Very coarse DFs, which are common in alpine areas especially where glacial moraine deposits exist (Rickenmann, 2009; Steijn, 1996) with quicker dewatering occurring after deposition (Pierson, 1980; Rodine and Johnson 1976; cited in Costa, 1984) than e.g. in mudflows (Rickenmann, 2009). Figure 11 shows a comparison of the main characteristics of DFs and water flows. In this respect, a DF is a sub-category of a hyperconcentrated flow. It generally has lower water content and is coarser than mud flows or lahars (Rickenmann, 2009).

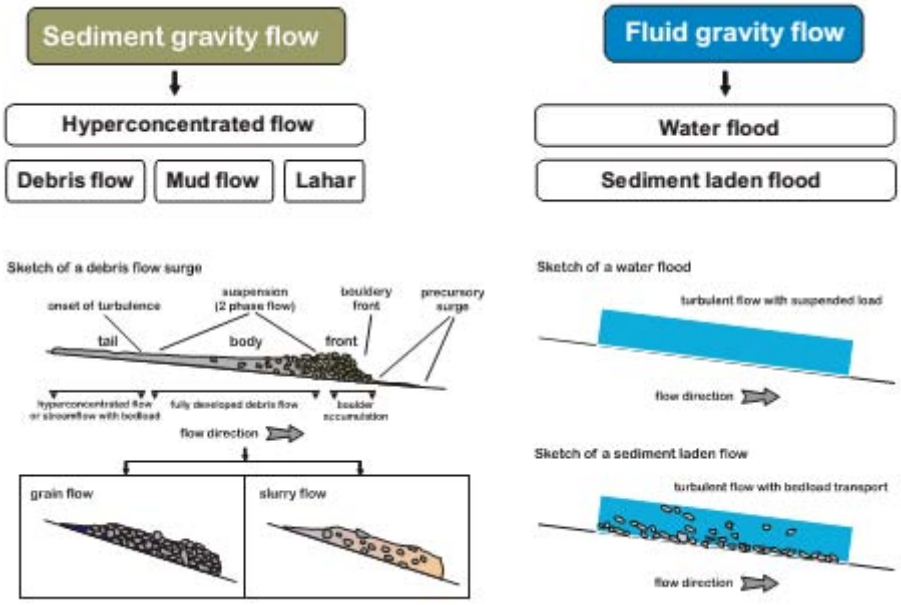

Figure 11: Main characteristics of DFs and water floods (Rickenmann, 2009)

A study conducted by the Austrian Research Centre for Forests (BFW; cf. Andrecs and Hagen, 2010) showed, that the most important parameters with regard to DF occurrence are such derived from precipitation followed by geological and topographic conditions. Andrecs' and Hagen's study tried to elaborate an easy-to-use decision guidance for practitioners, which is in line with state-of-the-art research (Mazzorana et al., 2012) and undermines the importance of precipitation for DF initiation.

Importance	Definition
0	No relevance
1	Small relevance (There is an influence, which is negligible compared to the dominant process)
2	Small to medium relevance
3	Medium relevance (Neglecting this parameter adds considerably to uncertainty)
4	Strong relevance
5	Highest relevance (Critical parameter)

Table 7: Definition of the respective importance type determined through expert consultation (Andrecs and Hagen, 2010)

The focus of the study carried out by the BFW was to develop a method to identify the reaction of different DFs to variables specified in Table 8 and to determine the absolute importance of parameters in the context of CC. Table 8[2] summarizes the main results with respect to DFs with a relative importance of a process with respect to process-relevant variables, the importance of an aggregated variable determined by consultation of international experts and an absolute variable as a rounded product of absolute variable importance and relative parameter importance (derived from the average

[2]Relative importance in brackets include additional consideration of indirect effects. Absolute importance is the rounded value of variable importance times the relative parameter importance.

relevance of a parameter for a whole process), defining the absolute importance of a parameter within the whole process.

DF	Variable	Importance	Parameter	Importance	
		Abs.		Rel.	Abs.
	Precipitation	4.5	Intensity	5	23
			Cumulative	4.5	20
			Temporal distribution	3	14
			Spatial distribution	3	14
			Type (solid/liquid)	1.5	7
	Geology, Soil	4	Properties of loose substrate	5	20
			Infiltration	5	20
			Water storage capacity	5	20
			Thickness of loose substrate	4 (3)	16 (12)
			Basic substrate (bedrock)	2 (4)	8 (16)
	Topography	3.75	Terrain slope	5	19
			Channel slope	5	19
			Channel morphology	4	15
			Topography	3.5	13
			Catchment area	1 (2)	4 (8)
	Land use	2.75	Infiltration	5	14
			Structural measures	4	11
			Water storage capacity	4	11
			Type of use	3	8
			Surface reorganisation	0-3	0-8
			Surface roughness	1.5	4
	Vegetation	2.75	Water storage capacity	5	14
			Infiltration	5	14
			Forest cover	5	14
			Evapotranspiration	4	11
			Erosion protection	3	8
			Surface roughness	3	8
			Interception	2	6
	Wind	2	Wind speed and direction – Forest cover	(2.5)	(5)
			Wind speed – soil	(2.5)	(5)
	Temperature	1.75	Temperature – air	4	7
			Temperature – subsoil	3	5
	Global radiation	1	Global radiation – vegetation	2	2
			Global radiation – soil	1.5	2

Table 8: Perceived relevance of different parameters (Andrecs and Hagen, 2010). *The parameter "importance" is defined in Table 7.*

In this study precipitation was identified as the most critical process with crucial parameters being precipitation intensity, cumulative precipitation as well as temporal and spatial distribution of precipitation to some extent. Besides this, also geological and topographic parameters play an important role in DF triggering.

Besides rainfall, which is described in the sub-chapters below, also other factors not considered in Andrecs and Hagen's (2010) study like snowmelt, glacier lake outburst floods, volcanic eruptions or earthquakes can lead to initiation of partly catastrophic DFs. While the latter three play a rather minor

role in the Austrian Alps, GLOF can provide an increased threat in other parts of the European Alps and were investigated in different studies (Huggel et al., 2003, 2002).

The most common triggers of DFs in the Alpine region are high-intensity, short-duration rainstorms or low-intensity, long-duration precipitation events (Bollschweiler and Stoffel, 2010; Guzzetti et al., 2008, 2007; Stoffel, 2010; Stoffel et al., 2011). There is an extensive body of studies conducted to derive empirical triggering rainfall thresholds considering i.e. the duration, intensity, cumulative and antecedent precipitation.

3.2.2 Magnitude-frequency relationships

Different formulas to empirically derive future DF event magnitude have been proposed in literature (Table 9):

Formula	N	Source
$M = KA_C 100 J_C$	1,420	(Kronfellner-Kraus, 1987, 1984)
$M_a = 150 A_C (100 J_f - 3)^{2.3}$	15	(Hampel, 1977)
$M = 27000 A_C^{0.78}$	~65	(Rickenmann, 1995; Zeller, 1985)
$M = L_C (110 - 250 J_f)$	82	(Rickenmann and Zimmermann, 1993)
$M_a = 13600 A_C^{0.61}$	551	(Takei, 1980)
$M_a = 29100 A_c^{0.67}$	64	(D'Agostino et al., 1996)
$M_a = 70 A_C J_C^{1.28} I_G$	84	(D'Agostino and Marchi, 2001)

Table 9: Empirical relationships describing the Maximum (M) or average (M_a) event magnitude of DFs and/or torrential floods (Bergmeister et al., 2009; Rickenmann, 2009)

A problem of empirical formulae for magnitude estimation is that catchment characteristics are not adequately represented and one has to be careful with transferring these empirical relationships to other study areas. With current knowledge about magnitude-frequency relationships it is not possible to transfer data gained from one catchments to another one. An analysis including the qualitative information on event magnitude exceeds the scope of this thesis, but would pose an interesting option for subsequent analysis and connection with the data elaborated here. An additional investigation would take into account catchment sizes, which were already used by Sitter (2010) for analysis and could make it possible to investigate the event magnitude of DFs with regard to rainfall intensity (Malamud et al., 2004)

Magnitude-frequency relationships can only be used with confidence for the catchment where it has been derived, because there are very high differences with varying location (Crozier, 2010). Furthermore, derivations for future conditions are difficult since the system state of a channel network can change after a period of increased DF occurrence (Crozier and Preston, 1999), as well as through changes of climatic framework conditions. In a broader sense this means that first-time DFs (DFs which were triggered in a catchment where no records of DF activity existed before), are less a reliable indicator of climatic influence in triggering conditions than the reactivation or increase of existing movements.

Because detailed information for relevant catchment parameters were not available, magnitude-frequency relationships can only be analysed according to the magnitude classes described earlier. With catchment information available a more in depth-analysis could merge information about precipitation and temperature with other parameters for DF such as magnitude-frequency relationships or testing of applicability of empirical relationships.

As described in Malamud et al. (2004) such information can be used to fit DF inventories to frequency density distributions and extrapolate available data. Subsequently, also a power law for magnitude-frequency relationships for the dataset at hand can potentially be developed.

3.3 Main climatic factors

When investigating rainfall thresholds for Austria, it has to be kept in mind that especially due to orographic effects and diverse topography there is a high variability of climatic factors which can heavily affect a generalised statement about thresholds for the whole country. This means that even though it is of high interest to determine an overall triggering threshold for Austria it has to be used with caution since regions of homogenous geology and meteorological conditions are not bound by national borders. After all, Austria consists of regions of different orographic characteristics and the central Alps have different precipitation conditions than the southern and the northern alpine foothills. While the geological heterogeneity can be roughly derived from Figure 2 presented in Chapter 2, the meteorological heterogeneity is illustrated through climate graphs such as the one depicted in Figure 12.

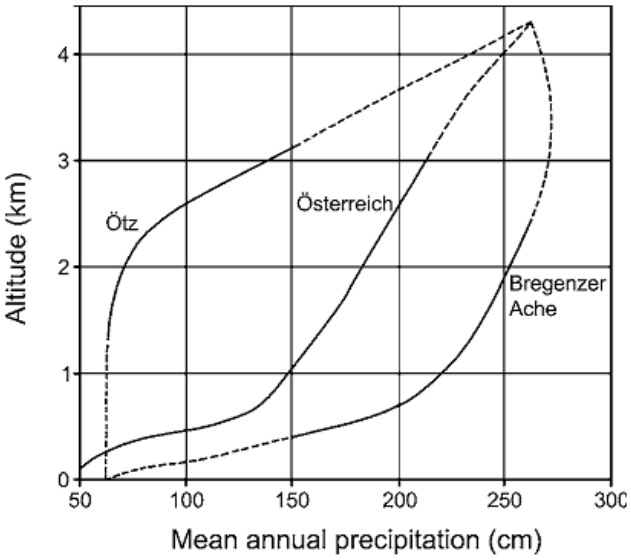

Figure 12: Illustration of the variability of mean annual precipitation in Austria. Such variability is also true for other climatic factors (Lauschet 1976; after Barry, 2008)

Since most DF events can be directly attributed to precipitation conditions it is important to look at the different characteristics of precipitation, which have to be considered in our study. The four variables of main interest are the following:

- Event rainfall: i.e. the duration of pronounced rainfall, which has led to a DF – hereafter called TER (triggering event rainfall; due to the partly different nomenclature used in literature), denoting the cumulative sum of triggering rainfall [mm].
- Rainfall duration, which means the duration of a rainfall event in days [mm/d], or in hours [hrs] [mm/h]
- Rainfall intensity, meaning the cumulative amount of rainfall per temporal unit – in our case daily rainfall, or

- Antecedent rainfall conditions being the sum of total rainfall before an event including TER, but also considering less intense conditions with prior wetting of the soil substrate, which can act as an agent for creating a slip surface for a land slide creating a DF in succession (or similar).

3.3.1 Convective precipitation

Convective precipitation manifests itself in short-duration, heavy rain fall events, which typically have a duration of up to few hours of varying intensity on a sharply delimited, small-scale area being below 10 km². Convective precipitation develops when humid air masses are lifted into a potentially unstable stratification or missing inversion. This can lead to the development of *Cumulus congestus* clouds or *Cumulonimbus* type clouds. The latter can have a considerable vertical extent of up to 30 km up to the Tropopause, while the cells of the cloud have a life time of 30 to 60 min. (Klose, 2008). Because of the Bergeron-Findeisen process such clouds can develop very large drops and thus lead to high precipitation events (Kappas, 2009).

During recent years, research increasingly used radar rainfall-data as a supplement or alternative to traditional rain gauge measurements. With radar data helps to spatially and temporally resolve rainfall like local convective precipitation events with much higher precision. Potential applications are e.g. to use quarter-hourly data and average values for catchments connected with other information such as solar radiation and wind speed (Sene, 2010). The downside of radar measurements is, that it is only available since a few years and for some regions are poorly covered because of radar shadowing.

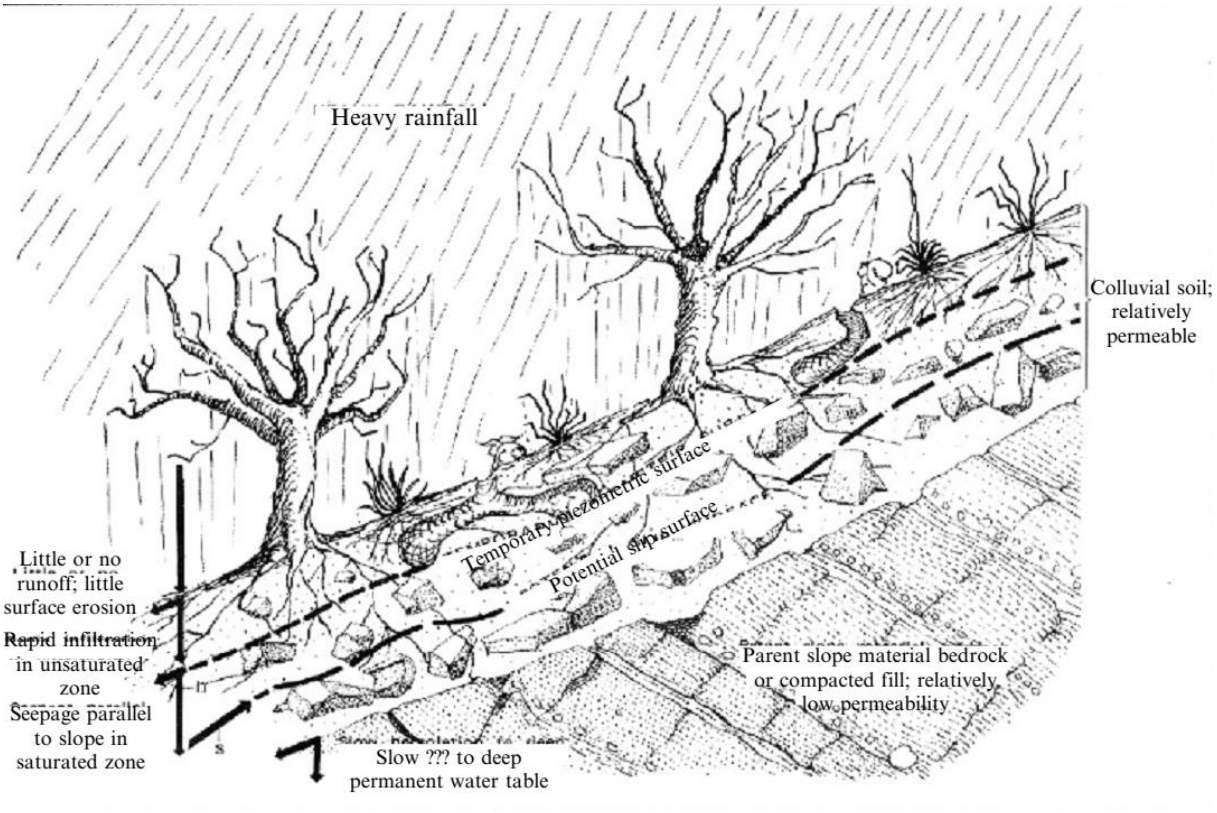

Figure 13: Processes involved when heavy precipitation occurs (Campbell, 1975)

Convective rainfall is the main factor for heavy rain in general. The latter is defined by the WMO (World Meteorological Organisation) as rainfall exceeding 50 mm in 24 h. For Austria definitions provided by Wussow 1933 and Schimpf (1970; both mentioned in Weinmeister, 1994) are often used. The criterion for heavy precipitation defined by Wussow is a function of time without spatial differentiation and is defined by:

Equation 1

$$h_n \geq \sqrt{5t - \frac{t}{24}^2} \; [mm]$$

With *t* denoting the duration in hrs.

Schimpf studied precipitation for 713 rainfall gauges and defined four functions for Austria, which consider regional effects by using the maximum annual daily rainfall as a selection criterion for the formulas below:

Criterion: Avg. daily rainfall [mm]	**h_n**	**h_n: 1h [mm]**
25	$h_n = 6.49t^{0.1855}$	13.9
35	$h_n = 4.85t^{0.2715}$	14.7
45	$h_n = 3.89t^{0.3365}$	15.4
55	$h_n = 3.25t^{0.3891}$	16

Table 10: Empirical estimation of heavy precipitation (Schimpf, 1970; mentioned in Weinmeister, 1994)

For our dataset, regional effects are restricted to the location of the rain gauge. Therefore potential measuring errors and uncertainties have to be considered. Important aspects are described in form of the process flow chart below.

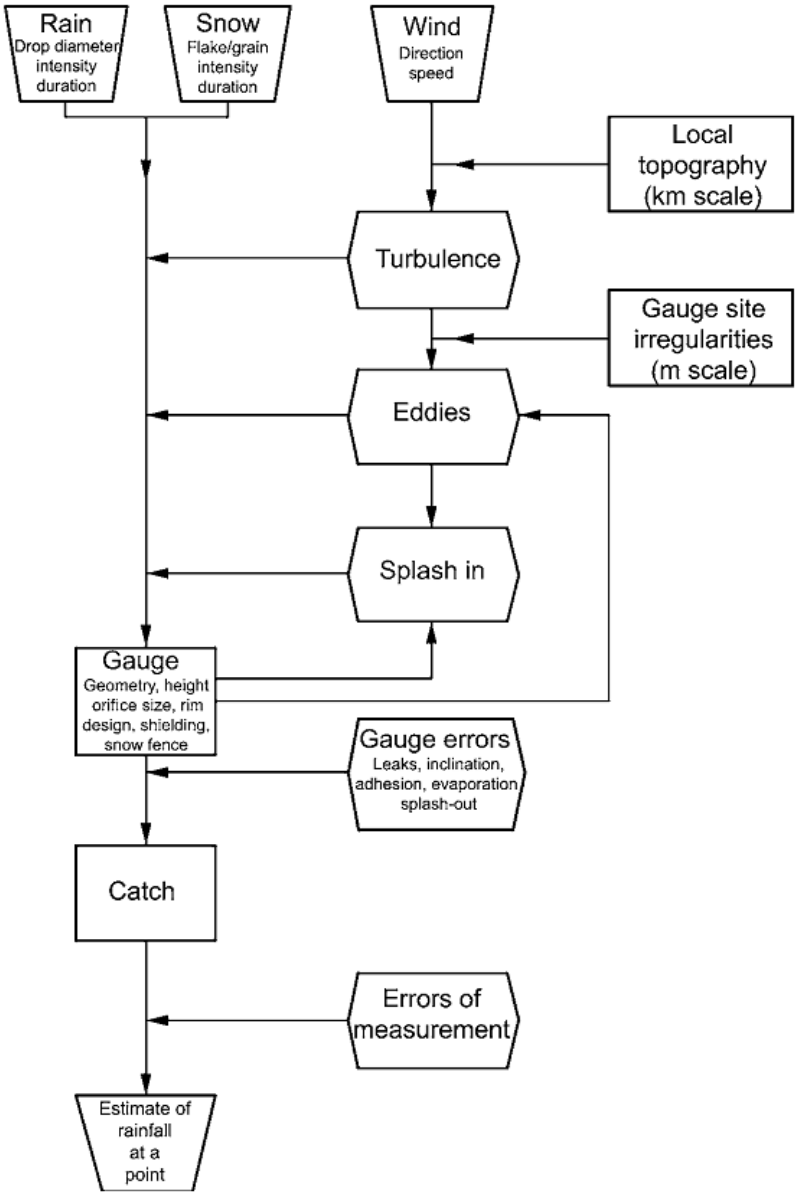

Figure 14: Schematic illustration of potential uncertainties in precipitation gauging (Rodda, 1967).

It is clear that an intensity-duration approach will always incorporate the uncertainties described in Figure 14, and that a statistical approach characterising DF occurrence will always neglect the

processes illustrated in Figure 13. Because of the lack of data it is very difficult to describe these uncertainties in (statistical) models. In the analysis at hand quantile statistics will be used for assessing heavy precipitation.

3.3.2 Advective precipitation

Advective or frontal precipitation consists of long-lasting persistent rainfalls. Advective precipitation occurs, when air masses are moved horizontally and when either warm air masses are lifted above cold ones (warm front) or colder air masses are pushed under warmer ones (cold front). This leads to precipitation events that can last several hrs and show a small and rather constant precipitation intensity. The horizontal extent is larger than 1,000 km² in many cases in contrast to advective precipitation (Bronstert et al., 2002).

3.3.3 Orographic precipitation

Orographic precipitation is caused by a vertical uplift of air masses due to a topographic barrier. Because the orographic component usually is weak, the combination with cyclonic of convective processes is necessary, where the orographic barrier can act as a triggering mechanism for heavy rainfall (Whittow, 2000). Orographic precipitation is by definition part of advective precipitation.

Most of the studies investigating DF only distinguish between convective precipitation and antecedent rainfall. When data resolution is high enough it is advisable to additionally differ between convective and advective precipitation since convective precipitation can usually last from several min. up to an hour while convective precipitation lasts from hrs to several days, while antecedent rainfall is in most cases chained precipitation of several fronts.

Such a distinction is useful to separate the pattern of high intensity rainfall from long-term rainfall and to investigate different characteristics of DFs triggered by different kinds of rainfall. In the *Results* section, these aspects are being accounted for through dividing precipitation into intensity and duration classes as well as through investigating probabilities for intensity, duration, TER, and antecedent rainfall.

3.4 Secondary climatic factors

3.4.1 Other Hydrometeors

Hydrometeors are not only comprised of the forms of precipitation mentioned above, but also include solid and liquid water droplets which are suspended in the atmosphere as clouds or fog, particles raised by wind buoyancy (blowing gusts of snow), as well as liquid or solid water particles deposited on the surface (such as dew, deposition of fog, hoar, rime and glaze. They especially play an important role in mountain climate and weather and can influence precipitation measurements considerably (Barry, 2008).

3.4.2 Rain-on-snow events

Especially in Alpine areas as well as in mountainous areas in general rain-on-snow events have an influence on the initiation of DFs.

Current research is to date mainly focusing on the Swiss Alps, where the comparably high population density with regard to other mountainous areas throughout the world as well as increased scientific interest in CC impacts has led to greater efforts to study and predict DFs in this context.

A large amount of DFs triggered in 1987 was initiated due to a blockage of water beneath perennial snow patches, where snow melt was considered to be the main causal factor for DF occurrence. This melting was followed by a subsequent warm rainfall event. This combination of snowmelt and intense rainfall has led to over 600 DFs during summer 1987 (Rickenmann and Zimmermann, 1993). Also after the “avalanche winter”, which brought vast amounts of snow and thus a period of high avalanche occurrence in the winter 1999 to the European Alps was followed by increased snow melt events in the following years, since the high amount of snow was preserved due to microclimatic conditions. Following (Bardou et al., 2003) concluded that a large number of DFs was triggered in a large number of alpine catchments, part of which was likely to be triggered by the antecedent climatic relationship to snow precipitation and the first summer thunderstorms. Also snow avalanche deposits have been identified as a proximal cause for increased DF activity (Bardou and Delaloye, 2004). Also studies focusing on other areas confirm these developments (Blodgett et al., 1996; Carson, 2002; Harris et al., 1997).

3.5 Characteristics of precipitation

3.5.1 Extreme rainfall events

Rare extremes can be assessed by classic extreme value theory, using well-established distribution models like Gumbel, Weibull, etc. In practical application there are two main issues described by Teegavarapu (2012): (1) Non-stationarity, and (2) changes with respect to extreme event intensity and occurrence. Normally extreme value quantiles are computed for different periods of time. To do this it has to be assumed that non-stationarity within these periods is negligible. Otherwise statistical models have to be used, where parameters vary over time to describe the temporal evolution of rare events (Teegavarapu, 2012), which makes analysis more complex. A good overview of how to statistically deal with extreme and rare events is given by Kropp and Schellnhuber (2011).

In contrast to heavy precipitation analysis mentioned before, in the context of CC it is of high interest to use indices for extreme precipitation, which are more practical and rather easy to use in large datasets. Such indices can be either based on percentiles (e.g. 90 % or 99 %-percentile, 10 % or 1 % percentile), absolute values (e.g. maximum rainfall intensity), threshold (days with a minimum of 10 mm daily precipitation) or duration (e.g. TER, Sillmann and Roeckner, 2007).

3.5.2 Antecedent rainfall

Antecedent rainfall constitutes a pre-dispositioning factor for the initiation of soil slips which can subsequently lead to DFs and its definition is of high importance for this study. Especially in soils with a low permeability, antecedent rainfall can be important because it significantly reduces soil and increases pore water pressure. The time intervals, which have been taken under consideration for this thesis are 1-10 mm TER (duration of pronounced rainfall, which has led to a DF) as well as 15 and 30 days of antecedent precipitation (Aleotti, 2004). The definition of antecedent and TER is illustrated in Figure 25.

3.6 Climate Change Implications for Gravitational Mass Movements

Various studies have investigated the link between regional climate models (RCMs) and hydrology: because of the projected higher surface temperature, it is expected that the macro-scale hydrological cycle will be also enhanced[3] (Bates et al., 2008). Because a rise in global temperature, leads to an increased global evaporation and evapotranspiration (Trenberth and Dai, 2014; Wentz et al., 2007), it will additionally alter the global hydrologic regime and the regional climatic regime in Austria among all temporal scale (Zechmeister-Boltenstern, 2014).

Even though meaningful global CC projections are available, analysis of the meso-scale impacts with respect to gravitational mass movements (for regional or local predictions) are difficult, because they can vary considerably depending on the region (Dobler et al., 2010). Especially in the Alps strong altitudinal gradients have a remarkable influence on atmospheric, hydrospheric, cryospheric, and ecological conditions. In the last decades this influence lead to trends three times higher than on global average (Dobler et al., 2010). The water cycle of the Alps is characterised by orographic effects, reduced evapotranspiration rates because of generally lower temperatures and an additional feedback through water storage in ice. The changes projected by the IPCC (Bates et al., 2008; cf. also Figure 16; IPCC, 2014) and recent studies shot that CC will have a considerable influence on the complex dynamics of runoff genesis in Alpine watersheds (APCC, 2014; Eckhart, 2012; Horton et al., 2006).

[3] Shifting magnitude and timing of hydrological events; increases in surface atmospheric moisture with regional differences, substantial interannual do decadal-scale variations with a global upward trend; changes of precipitation patterns and increases of heavy precipitation events in high latitudes; reduced snow cover and widespread melting.

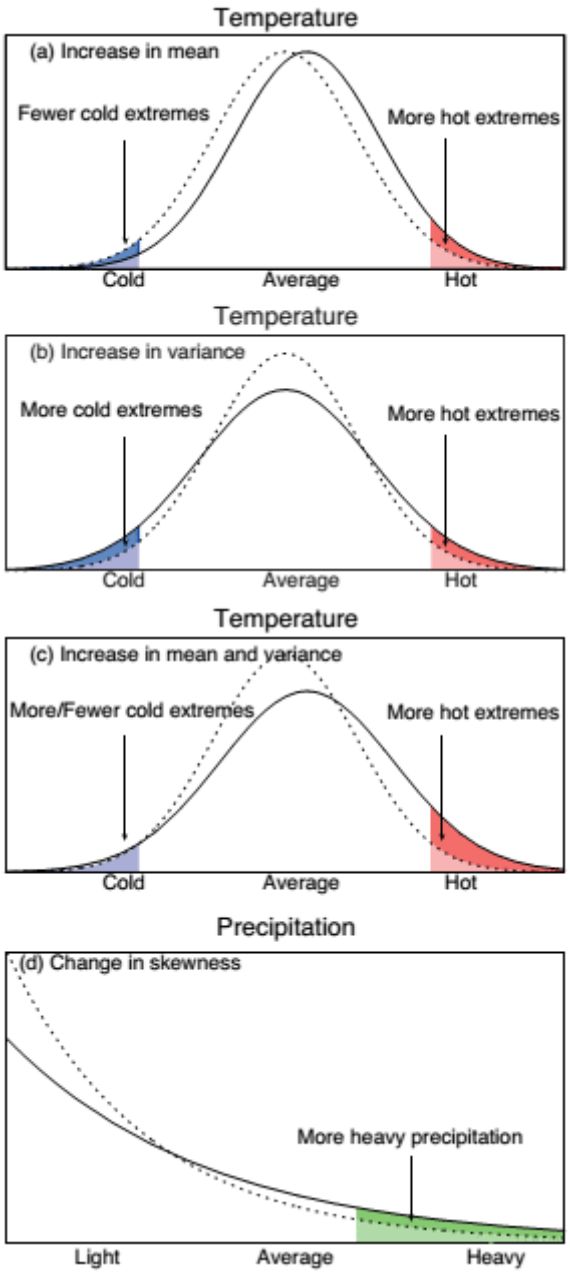

Figure 15: Illustration of increase in mean, variance and skewness of climatic events (IPCC, 2014).

Nevertheless, general or coupled general circulation models (CGCMs, GCMs) help us to assess future developments through utilisation of information from the past on large scales. These models include several assumptions deduced from the expected concentration of greenhouse gases (GHG) and aerosols. Although GCMs have a fine temporal resolution of 30 min to a few hrs, provided simulations with a horizontal resolution of about 150-500 km are too coarse on a spatial scale (Groppelli et al., 2011a, 2011b), creating the need for implementing additional approaches for downscaling. This can be done with the aid of statistical or dynamic downscaling. Because regional circulation models are more and more available, dynamic downscaling is becoming more popular. RCMs use the data provided by GCMs and incorporate meso-scale geographical features, such as topography or land use, land use change and forestry (LULUCF). Naturally, the largest uncertainties of this approach result from

the assumptions underlying the GCM scenario as well as the structure of the model. To minimise these uncertainties, different sets of RCMs incorporating extracted common CC signals and combination of different ensembles of GCMs are being utilised.

For an exhaustive information base to assess the future, a comprehensive analysis of the historical data at hand is necessary to assess recent impacts of CC on DFs, but also to utilise this data to improve early warning systems and thereby improve vulnerability reduction (de Perez et al., 2014).

Changes in temperature and precipitation have been linked to changes in glacier mass balance and terminus position, which is especially true for high mountain regions, but indirect effects on geomorphological processes are not yet well known. Especially areas with a strong relief are strongly influenced by the angle and aspect of the slope as well as the sediment input and supply of slope moisture. These processes then evolve in downslope direction (Keiler et al., 2010).

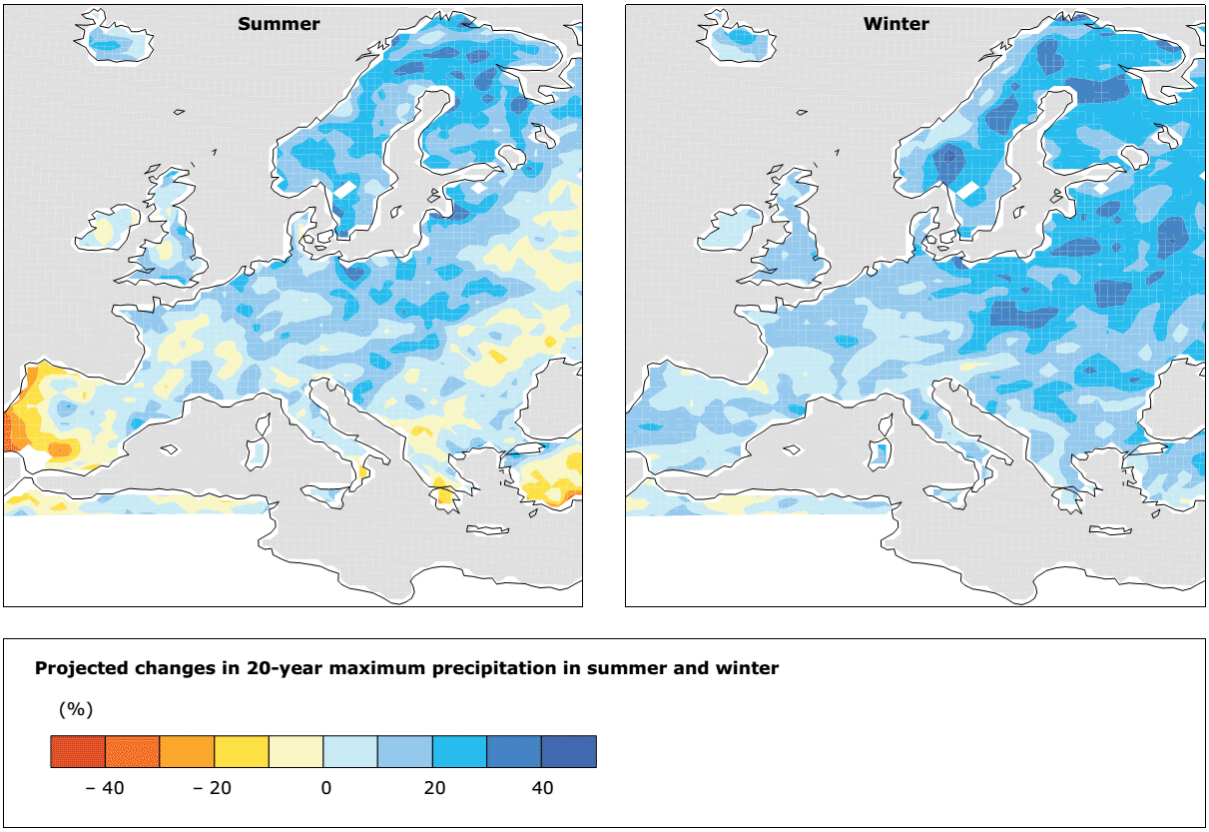

Figure 16: Consecutive wet days (EEA, 2012)

Future shifts in climate will probably be affected by a restructuring of atmospheric circulation cells on a global, synoptic-scale cell (Lionello et al., 2008). Variation in alpine climate is closely linked to the North Atlantic Oscillation (NAO; Keiler et al., 2010). The NAO is the main determinant of storm-tracks across Europe as well as temperature anomalies and is generally close to the Arctic Oscillation (AO; Ambaum et al., 2001; Deser, 2000) and influenced by the thermohaline circulation. Changes in

precipitation will likely affect the north south difference in precipitation, leading to increased precipitation in the north and to decrease in the south (Figure 16).

3.7 DFs and Climate Change

CC in mountainous areas is expected to have an increased effect on slope instability and DFs amongst other hazards. This is particularly true for elevated regions in higher latitudes. It is obvious that land global land area warms faster than water and that continentality of climatic factors will probably increase[4]. Previous research also has well-established the fact, that mountainous areas will be more strongly affected with rises in mean temperature, but also experience even more frequent extreme temperature and precipitation than for the global averages as was illustrated by Liggins et al. (2013), for the European Alps, the Andes, Himalaya, Pyrenees, Caucasus and the New Zealand Alps (Figure 17). In a recent study Huggel et al. (2012) hinted that major ice and rock avalanches in Alaska could constitute a causal impact of CC, while there also seems to be a trend in slope instability in Asia, like with the famous Kolka-Karmadon event, where a rock avalanche led to a glacier lake outburst flood causing a DF leading to more than 100 casualties.

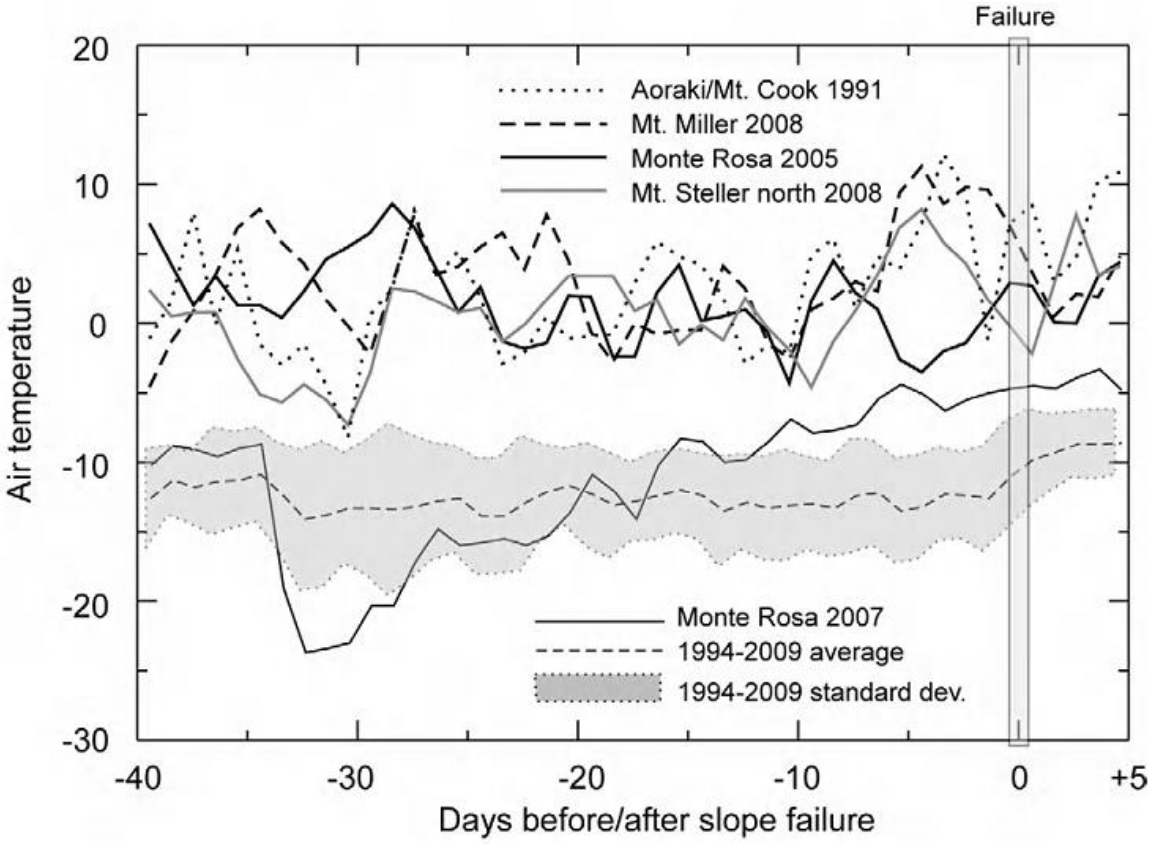

Figure 17: Air temperatures at selected sites in mountainous areas and averages from 1994-2009 (Huggel et al., 2013).

Changes in all aspects of precipitation will affect flood regimes globally (Reynard, 2007), especially mountains (Barry, 2008) with – from a standpoint of investigating climatic shifts – are temporally

[4] Increasing temperature ranges over landmasses, increasing extreme weather events. The aridity of dry regions and the humidity of wet regions is projected to increase, causing positive feedbacks in meteorological conditions.

coupled to DF occurrence (Teegavarapu, 2012). Especially potential shifts in warm/wet days can lead to an increase of DF activity.

When studying CC effects on DFs, it is important to look at the different time scales on which CC influences slope stability. Figure 18 illustrates the spectrum of effects with regard to their time scale (Huggel et al., 2012).

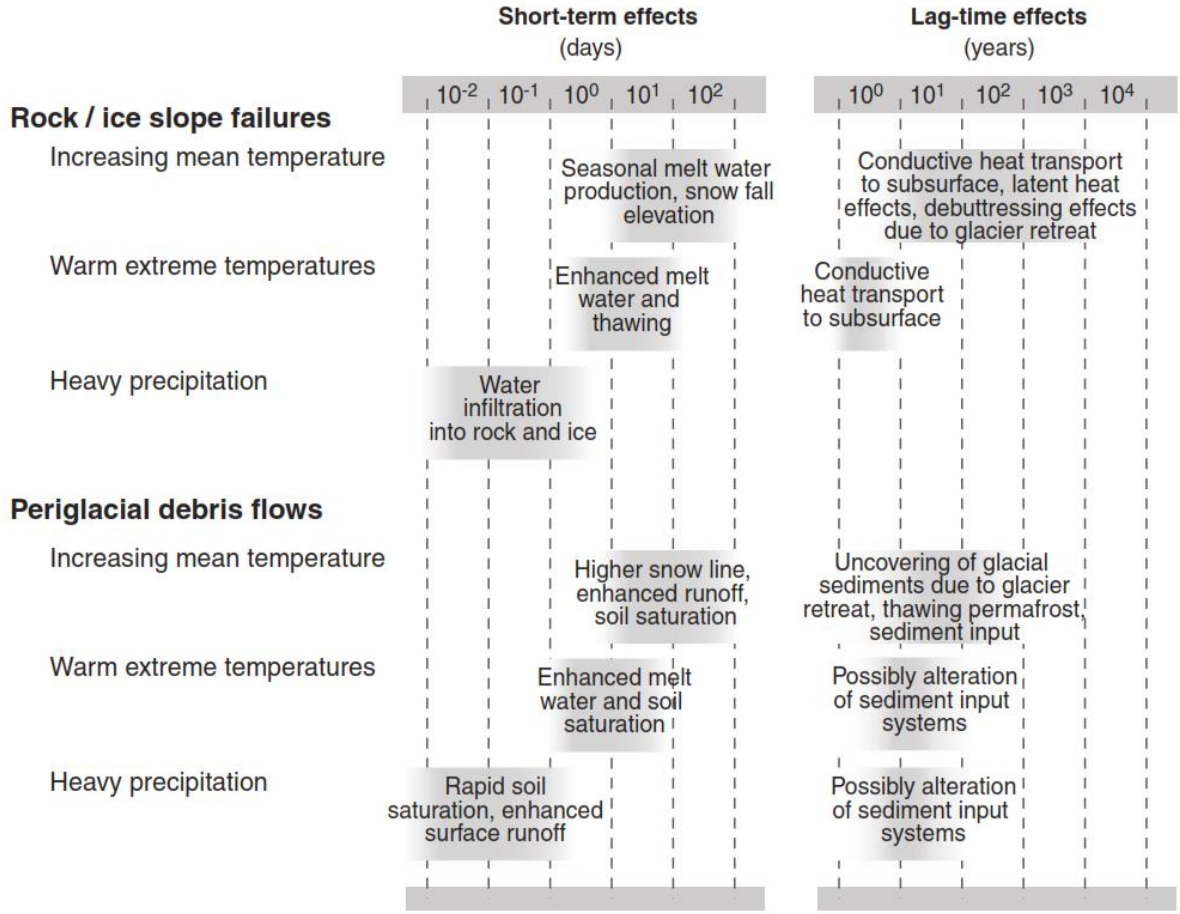

Figure 18: Time horizons of effects influencing gravitational mass movements (Huggel et al., 2012)

3.7.1 Short-term effects

The following parameters are important parameters where CC can play a considerable role in affecting DF triggering conditions.

Increase in precipitation totals

Wetter antecedent conditions can cause that there is less rainfall needed to achieve critical water content. If there is a reduction in soil capillary suction this subsequently leads to a reduction in cohesion. Generally, high water tables can lead to a reduction in shear strength. Wetter conditions also lead to an increased weight of the soil layer. Increased bulk density causes a decrease in shear strength/stress ratio in cohesive material. For longer periods of time higher water tables lead to the

situation that critical water content is reached much faster and much more frequent during rainfall events. Precipitation totals also cause an increased river discharge (Crozier, 2010).

Increase in rainfall intensity causes that infiltration is more likely to exceed subsurface drainage rates causing a rapid building-up of perched water tables. DFs can be triggered, because the effective normal stress is leading to a reduction in shear strength. But also increased through-flow causes increased seepage and drag forces, particle detachment and piping. Piping removes underlying structural support and usually enhances drainage until blockage occurs (Crozier, 2010).

Another CC-related effect could be the shift in cyclone tracks and meso- to macro-scale weather systems. This could lead to DFs or to an increase in DFs at site which were unaffected or less affected before. In this case slopes would rapidly adjust to the new framework conditions, probably leading to a severe increase in frequency and possibly in magnitude. More frequent wetting and drying cycles, as expected for some regions in Europe would lead to an increase of fissuring and to a widening of joint systems, a reduction in cohesion and rock mass joint friction (Fischer et al., 2006).

As outlined in the current and previous IPCC reports an increased variability in precipitation and temperature is to be expected. This leads to a set of effects for DFs: A reduction in antecedent water conditions through evapotranspiration could lead to a lower antecedent water status requiring more rain to trigger DFs. Transformative processes affecting continuous and discontinuous permafrost could lead to glacier down-wasting, debuttressing effects of the underlying soil, reduction in cohesion in jointed rock masses, debris and soil (Gobiet et al., 2013; Huggel et al., 2012; Stoffel and Huggel, 2012).

More rapid snow melt would affect runoff and infiltration and thus build up pore water pressure and strength reduction. Also, a reduction in glacier volume would cause a removal of lateral support to valley side slopes (Crozier, 2010).

Another component which is not considered much in current literature is an increase in wind speed and duration. This would lead to an increase in evapotranspiration rates causing a reduction of soil moisture, especially when high wind-speed events occur. This leads to enhanced drying and cracking, providing additional weak points for following rainfall events (Crozier, 2010).

DFs are mainly initiated by mobilisation stored in channels induced by channel or through shallow landslides through the sudden input of large amounts of water both of which is directly influenced by rainfall which can be intense or long-term rainstorm, sudden snowmelt, rain-on-snow events, of the sudden release of water from glaciers (GLOFs) or dammed lakes (Fischer et al., 2006). The most common triggers of DFs in the Alpine region are high-intensity, short-duration rainstorms or low-intensity, long-duration precipitation events. An increase of rainfall intensity due to CC therefore fosters increase of DF frequency.

3.7.2 Long-term effects

Conductive heat transport can occur on a decadal range, where e.g. permafrost thawing processes can alter the system state, while debuttressing effects can take place in a range from decades to millennia on a large spatial scale. Also unloading of ice due to glacier melt-off can have effects on similar time scales (e.g. for sediment input are occurring at the scale of decades while effects on seismicity are at the scale of thousands of years; Huggel et al., 2012).

Glacier retreat and/or debuttressing effects can alter the system state in a way that large-scale, catastrophic DFs can be triggered as occurred in the Kolka-Karmadon through initiation of a rock-ice avalanche, which caused the DF (Huggel et al., 2012; Stoffel and Huggel, 2012).

Regardless of the time scale, it is likely that variables influencing DF-initiation are influenced by CC by going through a tipping-point behaviour. This has been assessed as being likely for some sites (e.g. Huggel et al., 2012). With regard to climatic tipping points the recent IPCC report substantiates the supposition that thresholds for a radical change in system behaviour – at least for temperature – could be lower than anticipated before, while the systemic behaviour of other climatic signals are difficult to assess (IPCC, 2013). Additionally, to the uncertainties of evaluating such signals with respect to DFs previous research also shows that geomorphic thresholds affect DF initiation in a non-linear way (Phillips, 2003). This can possibly lead to more extreme DFs in the future. The interaction of these processes with climatic shifts is currently not well enough understood, thus it is difficult to make a specific assertion about exact system conditions for a site under investigation.

In periglacial areas sediments exposed by glacier retreat can remain on side for several decades before being mobilised by landslides of DFs. For these processes different lag times have been observed in other studies (Huggel et al., 2012).

3.7.3 Cryospheric and periglacial phenomena

Increasing problems related to gravitational mass movements with respect to permafrost soils occurred in Austria in the recent years (Krainer, 2007). Especially buildings in skiing and hiking areas were affected by freeze-thawing processes and subsidence effects, while down valley people and structures are increasingly threatened by such hazards (Huggel et al., 2012). With regard to interdependencies between permafrost and DFs particularly, catchment characteristics are of importance. Thawing of the ice in permafrost soils can lead to destabilisation of slopes where previously ice worked as cohesive material and thus lead to a greatly increased input of sediment in general and to settling processes in areas with a low inclination (Gobiet et al., 2013). On steep slopes the hydraulic conductivity as well as the slope stability are influenced negatively, where thawed permafrost can act as active layer for sliding processes (Kellerer-Pirklbauer and Kaufmann, 2007).

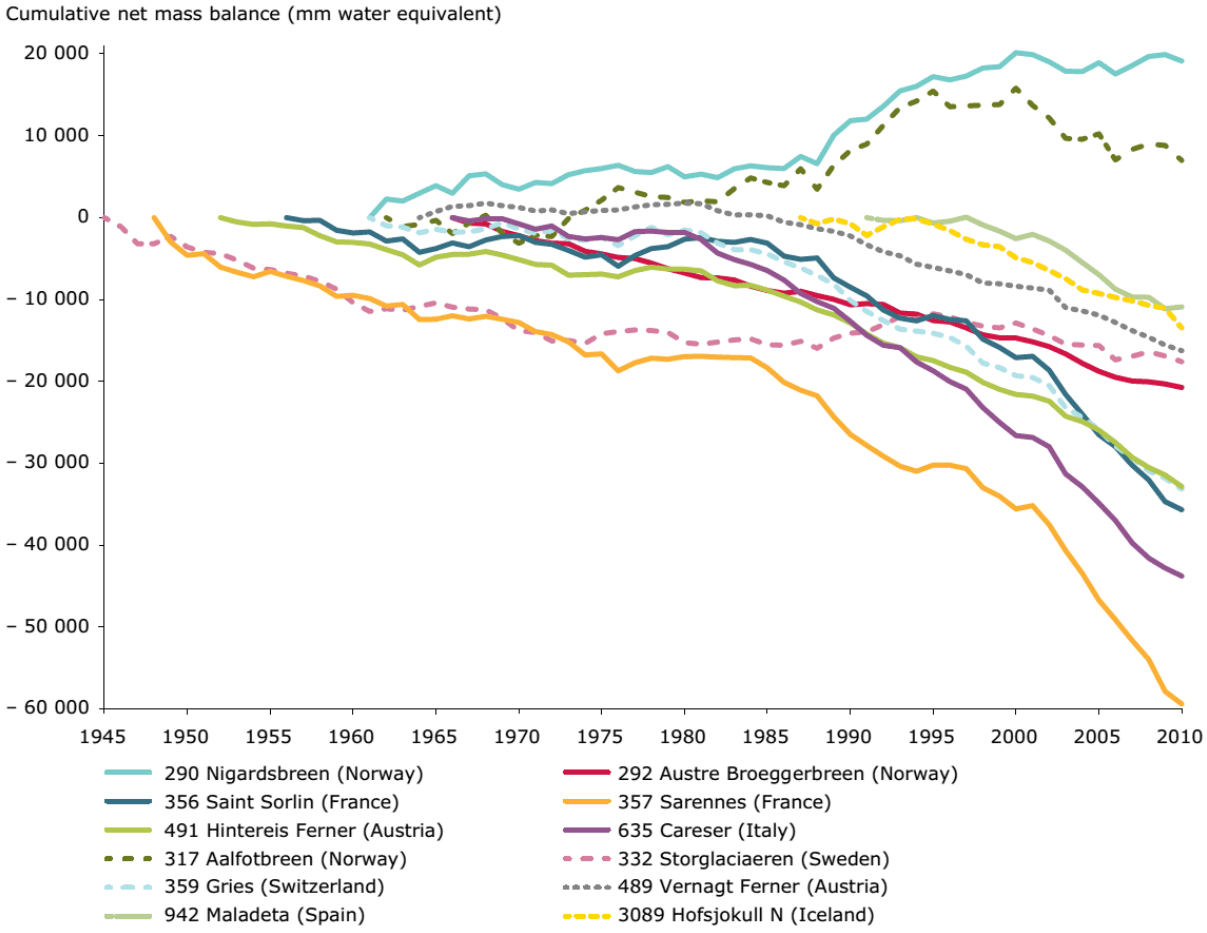

Figure 19: Cumulative net mass balance of selected European glaciers (EEA, 2012)

CC can alter the hydrologic regime in mountainous areas and especially the thermal regime of glaciers (Figure 19), which will have an impact on permafrost soils and periglacial areas, leading to an increased sediment availability increasing the overall disposition for a longer time scale (e.g. Figure 20 shows that many of the DFs triggered in the "landslide year" 1987 in central Switzerland had initiation zones in recently deglaciated areas (Rickenmann and Zimmermann, 1993). Although it is expected that this

disposition will decrease after several events, process-understanding of DFs in periglacial areas is yet not well known and analyses of triggering conditions scarce (Dramis et al., 1995; Fischer et al., 2006; Haeberli, 1992; Harris and Gustafson, 1993; Rebetez et al., 1997). These dynamics take place in the order of decades or more, because it takes a long time for a CC signal to penetrate into the glacier or permanently frozen soil, even when air temperatures would be affected already. Because long-term changes in glacier extent, volume and mass of these glaciers which are globally driven by climatic and oceanographic conditions their mass balance will change. As stated in the report of the Arctic Monitoring and Assessment Programm (AMAP, 2011) runoff will probably increase in the next decades but will ultimately decline, because reductions in glacier area will outweigh the effect of rapid melting. This will lead to a decrease in runoff and is also true for mountainous Regions in Europe (Huggel 2014, talk[5]).

Figure 20: Example of DF initiation in periglacial areas (Rickenmann and Zimmermann, 1993; Rickenmann, 2009).

Another phenomenon associated with periglacial processes are glacial lake outburst floods (GLOFs). They can occur if water is being dammed in moraine-dammed lakes, while below these dams there are in many cases ideal conditions for DF triggering. Steep gradients and readily available material with a wide grain size distribution can result in extremely large events if the dammed lake should break (Haeberli, 1983).

[5] Presentation of the contribution of the IPCC Working Group 2 to the Fifth Assessment Report at: 15. Österreichischer Klimatag, Innsbruck, Austria, 02-04. April 2014.

3.8 Empirical rainfall thresholds

The investigation of hydro-meteorological thresholds through statistical analysis has been conducted in a wealth of studies before and is a common method used on a regional scale (Caine, 1980; Guzzetti et al., 2007; Wieczorek and Glade, 2005). Rainfall thresholds are part of approaches in modelling DF occurrence, which can be subdivided into the following categories (Berti et al., 2012):

- Thresholds based on physical processes building upon numeric simulation models. These models usually define various relationships between rainfall and other hydrologic variables (Crosta, 1998; Montgomery and Dietrich, 1994; Terlien, 1998; Wilson and Wieczorek, 1995)
    - Process based
    - Conceptual models
- Empirical models, based on an historical investigation of the relationship between rainfall and the occurrence of DFs (Caine, 1980; Campbell, 1974; Crozier and Glade, 1999)
    - Historical DF inventories
    - Statistical data

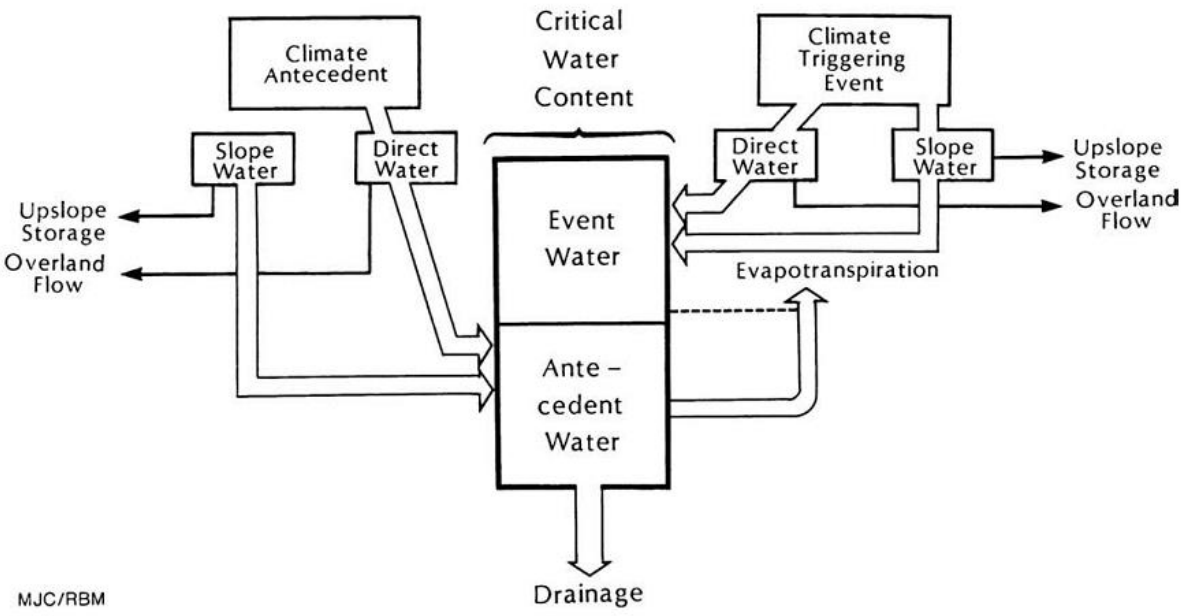

Figure 21: Example of a hydro-climatic landslide triggering model (Crozier, 2010)*, i.e. a conceptual model. These processes are also valid for DF initiation.*

Furthermore, the empirical investigation of rainfall thresholds can be grouped into the following categories: Thresholds considering rainfall intensity (mm per time unit, as don in ID-threshold analysis), event rainfall length (i.e. duration of a rainfall event), thresholds including antecedent conditions for DF initiation (e.g. antecedent rainfall) or cumulative rainfall (i.e. cumulated rainfall over a defined event duration, TER), thresholds including other conditions (e.g. antecedent discharge, storms and the

like). Although there are different approaches in the specificities, the most common approach here are intensity-duration relationships (Tablebi et al., 2010).

Also because the exact physical processes of DFs are not well described in the literature yet, models examining empirical thresholds are more commonly used in general (Aleotti, 2004; Crozier, 2010). This relationship can be further optimised by the usage of mean annual precipitation or the TER (in the literature also referred to as critical cumulative rainfall (Aleotti, 2004), which is used in the thesis at hand.

Since our analysis includes a large part of Austria, the pluviometric characteristics of antecedent rainfall shows large variability with regard to duration (between 1 and 40 days[6]) and the mean triggering intensity (between 1.09 and 129 mm). Sub-daily rainfall is not resolved and thus represents a neglected part in the analysis which has to be accounted for.

Figure 22 shows rainfall thresholds defined in previous studies and will serve as a comparison for the Austrian thresholds which were identified in this work.

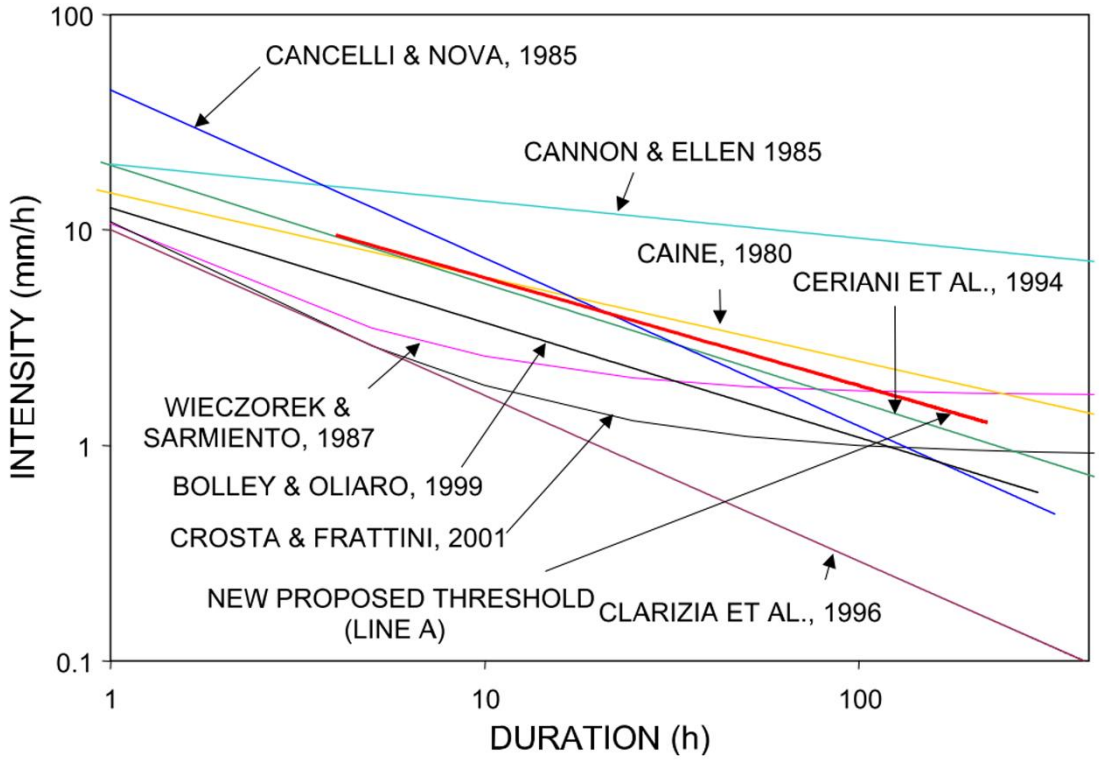

Figure 22: Intensity-duration thresholds determined in other studies for different study scopes (Aleotti, 2004).

Usually, the term "threshold" means the minimum or maximum (critical) level of a quantity needed to induce a certain process (Reichenbach et al., 1998).

[6] For the results section antecedent rainfall of max 30 days was considered.

While all of the abovementioned methods and elements described in Chapters 3.1 to 3.3 can be used to some extend for a limited number of catchments to make a first assumptions about parameters relevant for DF characteristics, they do not provide a feasible path for the large-scale analysis intended, mainly because consistent and detailed catchment data and characteristics could not be acquired. A thorough investigation for magnitude frequency relationships proves difficult, when the data available only describes DF magnitudes in rather broad classes. Because of this, the focus will be on descriptive statistics and the usage of methods in probability theory.

As described in Chapters 3.4 to 3.10 different precipitation characteristics can be separated through means of descriptive statistics for better understanding and subsequently be used with applications of probability theory. In this case Bayes' theorem was used for 1D and 2D analysis of characteristics of interest (as described in the Methods *section). While temperature and precipitation extremes as well as thawing-effects could be described, additional information would be needed for a concise evaluation of potential climatic effects in the cryosphere.*

A combination of the frequency, precipitation and temperature data at hand with meteorological, geological and special parameters would provide a possibility for a follow-up investigation.

4 Data Preparation and Methods

For subsequent analysis information from three data bases was connected to analyse potential effects on DF initiation and patterns of DF occurrence

Through collaboration with the Forest Service for Torrent and Avalanche Control in Austria (WLV – Wildbach- und Lawinenverbauung) an extensive event database (EDB) was compiled at the Institute of Mountain Risk Engineering at Boku University Vienna. With 631 stations from ZAMG and 1,018 stations from eHYD, there is also exhaustive data available for meteorological and climatological parameters. The potentially usable stations for all events are 1,649 precipitation gauges in total.

4.1 Precipitation Data

4.1.1 eHYD-Data

The Hydrographischer Dienst (eHYD) provided 1,018 datasets of daily precipitation measurement and data from 663 stations reporting average daily temperature[7]. The data generally begins with information in variable numbers of headers providing information about station name, iD-Numbers, coordinates and likewise. This header is then followed by two columns denoting the time in dd.mm.yyy hh:mm:ss format and the average temperature or the precipitation in two significant digits respectively. Because some of the stations were moved up to seven times in their history of existence, the lengths of the meta-information in the header varies and thus a routine was needed to attribute the daily measurement to the respective coordinate.

4.1.2 ZAMG-Data

The Zentralanstalt für Meteorologie und Geodynamik (ZAMG) provided 631 datasets of daily measurement with each consisting of geographical coordinates, height, date, daily precipitation, minimum daily temperature, maximum daily temperature, snow fall and pressure.

4.2 EDB (Event Database)

The EDB of the Institute of Mountain Risk Engineering is a worldwide unique database of mountain hazards occurring in Austria. In the version used for this study there was a total of 28,075 events of mountain hazard processes with 21,437 events which had daily information available including 2,412 DFs within the period between 1900 and 2009 . 2,125 DF events had a magnitude class attributed (with classification according to Figure 6). Therefore subsequently the term "*all events*" will denote events from the whole dataset of dated DFs (2,412), while "*magnitude assigned*" will denote DFs from the 2,125 dataset. It is important to differentiate between these two, because the practically usable amount of DFs in both approaches results in different probabilities.

[7] In nearly all cases temperature data was from a station, where precipitation data was already available.

Because of compatibility issued the EDB was exported into *.CSV-values. The geo-coordinates were transformed from BMN M28, BMN M31, BMN M34 respectively into ETRS98 in ArcGIS, and later on merged with the rest of the respective data in MatLab for further processing.

4.3 Data formats for MatLab processing

To ease data analysis all the coordinates of the measurements in eHYD, ZAMG and all the event-coordinates in the EDB were transformed into the ETRS89-format and checked in ArcGIS.

Several entries contained typographical or other errors, but could be identified through the station name, while some of the stations were located too far outside of Austria. Because the MatLab default format for dates is days since the year zero (with 01.01.0000 being represented by the value 000001), a routine had to be written in C for fast back and forth transformations, because the MatLab-algorithm couldn't cope with the large amount of data in an feasible way.

After pre-processing, the station measurements from the raw data files (examples cf. Appendix 2 – Raw data file examples) could be transformed into a matrix of the following format:

[Station Number] [Beginning of measurement] [End of measurement] [X coordinate]

[Y coordinates] [Z coordinates] [Day of measurement] [Variable]

With variable being rain or temperature, while the data from the EDB was transformed as follows:

[Event-iD] [X coordinate] [Y coordinates] [Date of occurrence]

This then provided the main corpus for most calculations, enabling fast logical indexing for geospatial analysis and differentiation by date or season. The station number and event-iD helped to keep the link to the original data in case some inconsistencies would be found.

For analysis of precipitation with respect to DFs for each event the nearest active gauging station was sought and the data was sorted in a different way for subsequent seasonal analysis and the investigation of Bayesian rainfall thresholds. The sorting was executed through creating a matrix described by an X-index for the respective nearest station found and a Y-index consisting of a time series starting with 01.02.1872 and ending with 31.05.2013. This was done separately for precipitation and temperature with Figure 20 illustrating the resulting data file.

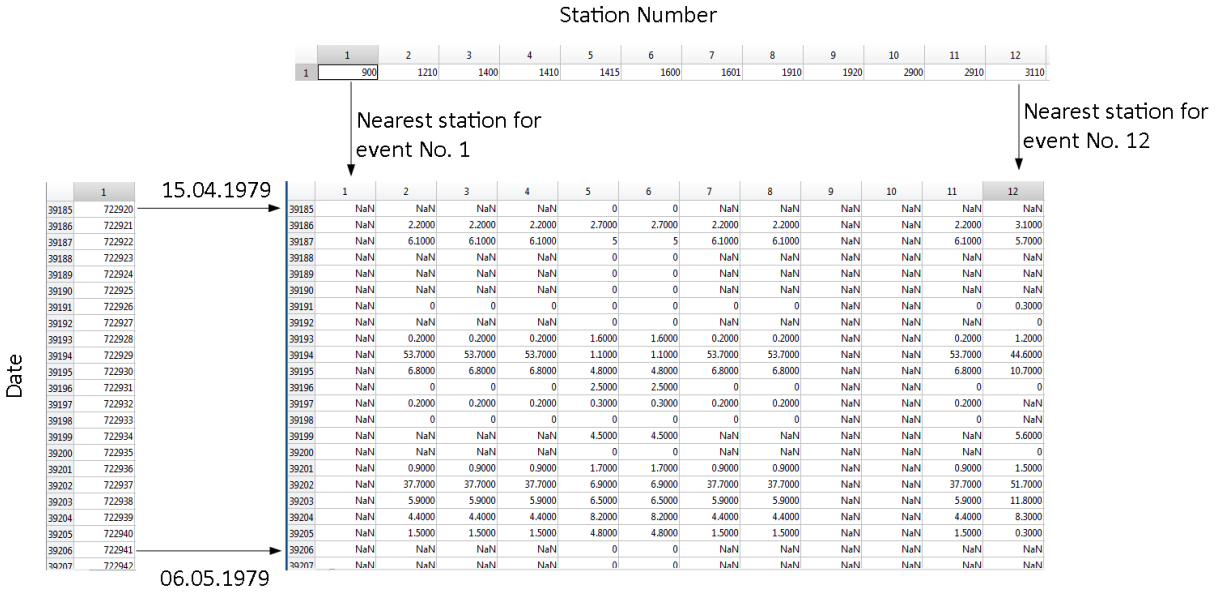

Figure 23: Final data sorting for the main analysis. Data is aggregated in a matrix where rows can be filtered by date with a row index and columns sorted by a station index. Thus data can be filtered quickly with selecting station and date ranges (the respective indices of the date and station vectors are referenced to the matrix indices). There is one matrix for temperature data and one for precipitation data

This format allowed to quickly extract time series for a given interval or station. Through logical indexing it is possible to make analyses e.g. for seasonal variations or different decades which makes it the core file for all subsequent analyses.

4.4 Data validation (root mean square error of prediction)

The root mean square error (RMSEP), which is also called the root mean square deviation is being used frequently to assess the difference between values which were predicted by a model or algorithm and values actually observed. In our case the observed values are deduced from manual definition of TER.

Generally spoken, the RMSEP aggregates residual values into a single measure of predictive power:

Equation 2

$$RMSEP = \sqrt{\frac{\sum_{i=1}^{n}\left(X_{Obs,i} - X_{model,i}\right)^2}{n}} = \sqrt{\frac{\sum_{i=1}^{n} d_i^2}{n}}$$

The RMSEP of a model prediction with respect to the estimated variable X_{model} is defined as the square root of the mean squared error:

Where X_{obs} is observed values and X_{model} is modelled values at time/place i, d are the differences.

This RMSEP values can be used to distinguish model performance in a calibration period with that of a validation period as well as to compare the individual model performance to that of other predictive models (Bras, 1990).

When calibrating the rainfall detection algorithm the first idea would be to use R^2 for evaluating calibration result, because R^2 is highly dependent on the range of a dataset. As shown in Figure 24, this measure is always higher if the spread of the data is lager, since it is a measure evaluating the spread of a dataset in a given linear fit. While the fit on the left (range 10 to 20) has an R^2 of 0.90, the fit on the right has an R^2 of just 0.625 (range 13-17 of the same dataset; Davies and Fearn, 2006).

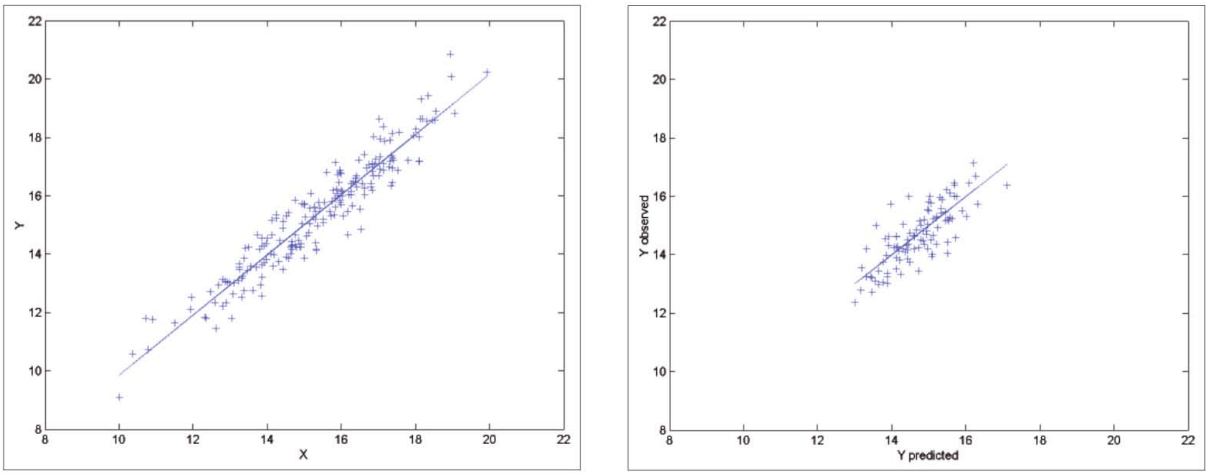

Figure 24: Effect of the data range on calibration (Davies and Fearn, 2006).

A good measure of the goodness of a calibration is the standard error of prediction (SEP). It quantifies the variability of the difference between the predicted values (provided by the detection algorithms) and the reference values from the validation (i.e. manual definition of TER for the whole DF dataset). The best way is to use the squared differences, because with this method it does not matter if the difference is negative or not (Davies and Fearn, 2006).

In this study the relative RMSEP was used to calibrate a rainfall detection algorithm with TER-data derived from known event rainfall for the debris flows from EDF and look for possibilities from rainfall between 1-10 mm and 1-10 days. The relative RMSEP shows the RMSEP on a scale between 0 and 100 %.

4.5 Triggering event rainfall and derivation of rainfall thresholds

4.5.1 Triggering event rainfall

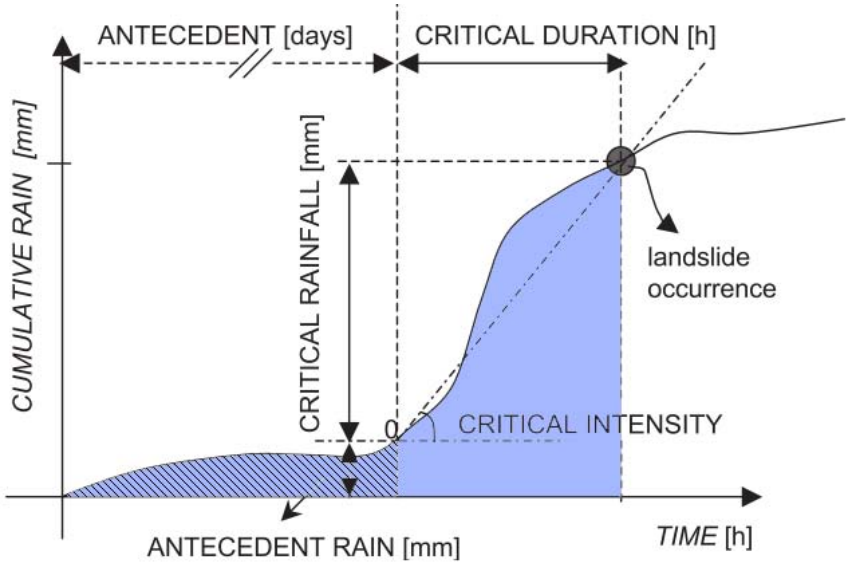

Figure 25: Defining the TER, described as critical rainfall in Aleotti (2004). *The blue non-hatched area shows TER, the hatched area shows an additional proportion considered for antecedent rainfall (in my analysis antecedent rainfall is hatched area + blue area).*

As can be seen in Figure 25, TER is the amount of rainfall from a point in time where the curve for cumulative precipitation shows a pronounced increase in rainfall intensity until the triggering event. In well-defined cases such an increase should show a clearly visible break in the slope of the cumulative curve. Some studies use the term antecedent rain as defined in Aleotti (2004), while others shift the end to the time of DF initiation. In the latter case antecedent rainfall would include the time period of critical rainfall. For consistency the antecedent rainfall as used in this thesis means: Time period starting at the primal occurrence of continuous rainfall until the initiation of the DF. This means that the critical duration is included in our definition of antecedent rainfall. Because we only investigate daily rainfall data, this decision should not significantly affect calculations or results.

4.5.2 Rainfall thresholds

Studies show that DFs often evolve from small soil slips and caused e.g. by strong embankment on hill slopes, disadvantageous road cuts and unfavourable drainage conditions for surface water (Aleotti, 2004; Jones et al., 2000; Nakamura, 2000). Terrain roughness plays a vital role with regard to drainage conditions and the probability of DF initiation (Similarly to the parameters identified in Andrecs and Hagen, 2010).

Aleotti (2004) found that the distance of the rain gauge to the event is also critical for determining thresholds. He showed that the mutual pairwise distance between gauges in a given area for hourly precipitation verb missing a direct relation between the maximum difference in rainfall intensity and

the distance between the respective gauges now the sentence gets too long can be proven affecting the significance of a measurement with regard to the TER at site. For a distance between 5 and 10 km there is a greater relation between maximum rainfall intensity difference and distance, while it decreases in ranges being greater than 10 km. An additional difficulty is, that rainfall differences not only depend on the distance, but furthermore on e.g. elevation, aspect and its general position affected by micro and meso-meteorological variability. Because of the long time-scales, four ways of examination were used in this work: No limit on nearest station distance, max 30 km, max 20 km, and max 10 km. The results of this approach are shown in the Results section and discussed subsequently.

Analyses were made for TER, rainfall intensity, rainfall duration and two lengths of antecedent rainfall (in one case antecedent rainfall of max. 15 days was considered, in another case it was 30 days). Because rainfall intensity was identified as the most influential variable, subsequently ID-relationships were investigated.

4.5.3 Intensity-duration relationships

Most ID thresholds follow a simple power law, while some also add a constant as y-intercept variable. Therefore, the following equation represents a general and widely used approach representing the whole spectrum of these power-law relationships (Guzzetti et al., 2007):

Equation 3

$$I = c + a \cdot D^{\beta}$$

Where I denotes the rainfall intensity, D its duration and c, α, and β are parameters. While c represents the intercept variable, β is the exponent describing an inverse power law relationship while α represents the (nonlinear) gradient. The parameter β can be valid for about up to four orders of magnitude, but for very short or very long durations it usually becomes difficult to justify the causal relationship which is assumed through using this equation.

This implies that global thresholds, or thresholds for very large areas usually describe somewhat lower levels below which debris flows should not occur. Subsequently regional thresholds are larger, but local thresholds usually have the highest values. This scaling relationship is also apparent in the data at use here, where very large areas are affected by an averaging effect, since the station usually represents a precipitation gauge somewhere in the valley where rainfall is not as strong as in orographically pronounced terrain (in addition to temporal averaging, where daily means are not representative of storm rainfall).

In this thesis the ID-relationships computed were mainly compared to the findings stated in Guzzetti et al. (2008, 2007) and Aleotti (2004).

Because of the large data set ID-relationships are computed for different durations while Equation 3 is only used as a descriptor for fitting a power law to the ID-curves ascertained in this thesis.

4.6 Frequency Analysis

For investigating processes of change there are two moments which were interesting in the context of this thesis. One was if and how DF occurrences are affected over time in general and the second question, which is deduced from the first was which part of such processes can be explained by influences of CC.

4.6.1 Kernel Density Estimation (KDE)

To detect possible significant long-term changes in DF occurrence DFs with known intensities (on a magnitude scale from 1 to 4) and at least monthly time designation were regarded. Thus, 2,526 DF phenomena from the EDB could be used with monthly accuracy ranging from 1008 up to 2008. Because of data thinning the KDE results were cropped to 1800-2008 (2,519 DFs were finally considered in the KDE).

For a better representation of the data the average magnitude of the events per year was calculated (cumulated magnitude divided by number of occurrences) to determine if there is an overall shift in DF frequency. Here it has to be kept in mind, that a common problem in time series is that less data is available the farther back in time a phenomenon is investigated. We can clearly see this problem in the KDE-Figure in the Results-section where a more or less consistent inventorisation started around the year 1910, with nearly annual reporting of DF events.

The estimated kernel density at one point of time is defined through the following formula

Equation 4

$$f_h(x) = \frac{1}{h}\sum_{i=1}^{n} K\left(\frac{x - x_i}{h}\right)$$

There are a number of functions available for KDE. The one used here was normal (Gaussian) KDE, which is frequently used to assess the frequency of occurrence of natural hazards (Mudelsee et al., 2003).

Consistency of the data set

To determine if the uncertainties in the data set are small enough a sensitivity analysis by introducing some random noise was conducted. This showed that even when adding noise up to twice the uncertainty (two sigma) to the time series, the results remained unchanged. This leads to the conclusion that the trends are robust with regard to uncertainties. To determine if climate variability had an impact on the trends detected, homogenized precipitation data mentioned earlier in this

chapter was analysed. Precipitation for each season (DJF, MAM, JJA, and SON) was treated separately. In this data, trends in the occurrence of the 30-year means could be detected (cf. Chapter 5.2, Analysis of Precipitation).

For assessing time-dependent DF occurrences and the detection of significant changes the earlier mentioned KDE method was employed. For analysing the data in this thesis a Gaussian kernel K was used to weigh the observed event dates as well as the number of DFs and to calculate the occurrence rate with the following formula:

Equation 5

$$\lambda(t) = \sum_{i=1}^{n} K\left(\frac{1}{h}(T - t_i)\right)$$

While n… Number of DFs, K… Gaussian kernel, t… time of the occurrence of event i, h… band width.

The selection of the bandwidth h was guided by cross-validation. The confidence bands at 90% were estimated by using a bootstrapping technique: N simulated DF events were taken from T(i) with replacement and simulated λ was calculated.

According to this, the following null hypothesis H_0 "constant occurrence rate" was stated:

Equation 6

$$\frac{\sum_{i=1}^{n} \frac{T_i}{N} - \left(\frac{t_u + t_l}{2}\right)}{\frac{(t_u - t_1)}{\sqrt{12N}}}$$

With t_u being the upper bound of the observation interval (year 2008) and t_l the lower bound (year 1910).

4.6.2 Analysis of Climatic Shifts

Analysis of climatic shifts was mainly conducted through the use of linear regression analyses. While for precipitation the annual mean and maximum values were investigated, for temperature the annual maximum temperature as well as the 95 % percentile were analysed.

Additionally, a composite index was formulated describing the humidity in combination with temperatures. To achieve this 10 % and 90 % percentiles for annual temperature and humidity were used respectively to construct the following indices: warm/wet (90 % percentile temperature and 90 % percentile precipitation), warm/dry (90 % percentile temperature and 10 % percentile precipitation), cold/wet (10 % percentile temperature and 90 % percentile precipitation), and cold/dry (10 % percentile temperature and 10 % percentile precipitation). Days meeting these criteria were summed up annually, so that changes can be analysed using regression.

4.7 Bayesian Analysis

A Bayesian approach was used to analyse meteorological trigger conditions of all dated DF events in the EDB. This section explains the method and its advantages compared to conventional probability techniques in detail. The analysis is guided by pioneering work of Berti et al. (2012) who introduced this method to identify trigger conditions for shallow landslides in Italy and provided valuable help for data analysis through providing an example of a rainfall detection algorithm.

4.7.1 One-dimensional Bayesian Analysis

Equation 7

$$P(A|B) = \frac{P(B|A)P(A)}{P(B)}$$

In this formula P(B|A) stands for the conditional probability of B given that A occurs. In our case this refers to the probability of observing a rainfall event of magnitude B under the condition that the landslide event A occurs. P(A) denotes the prior probability.

Example

As an example of the procedure applied we can use hypothetical data which was adapted from a randomly selected station from the data set. For illustrative purposes the number of debris flows was increased as well as higher precipitation values added[8].

N	Duration [days]	Intensity [mm/day]	DF
1	**2**	**30.85**	**Yes**
2	4	3.4	No
3	3	3.9	No
4	3	22.9	No
5	**10**	**23.5**	**Yes**
6	2	4.0	No
7	**2**	**17.4**	**Yes**
8	7	20.0	No
9	6	4.1	No
10	**6**	**22.4**	**Yes**

Table 11: Example of precipitation-gauge data (own creation).

Table 11 shows an example of detected rainfalls with ten detected rainfall events where four of them resulted in DFs leading to a P(A) of 4/10= 0.40. The probabilities for Intensity <20 mm would be calculated as follows: P(B|A)=P(Intensity<20|A)=1/4= 0.25 and P(B)= P(Intensity<20)=5/10= 0.50.

[8] It has to be noted, that landslide possibilities in the real datasets are by far smaller because of the length of the time series

This means that one out of three DFs in our mini-dataset were triggered by a precipitation intensity of < 20 mm/day and that 5 out of 10 rainfall events detected had an intensity of < 20 mm/day. The resulting DF probability – following Equation 7 – is P(A|B)= P(A|Intensity<20) = 0.25*0.40/0.50= 0.20. For intensity >=20 mm we would obtain analogously P(B|A)= 0.75, P(A)= 0.4, and P(B) = 0.50 with the result P(A|B)= 0.6.

Figure 26 shows the results of this approach.

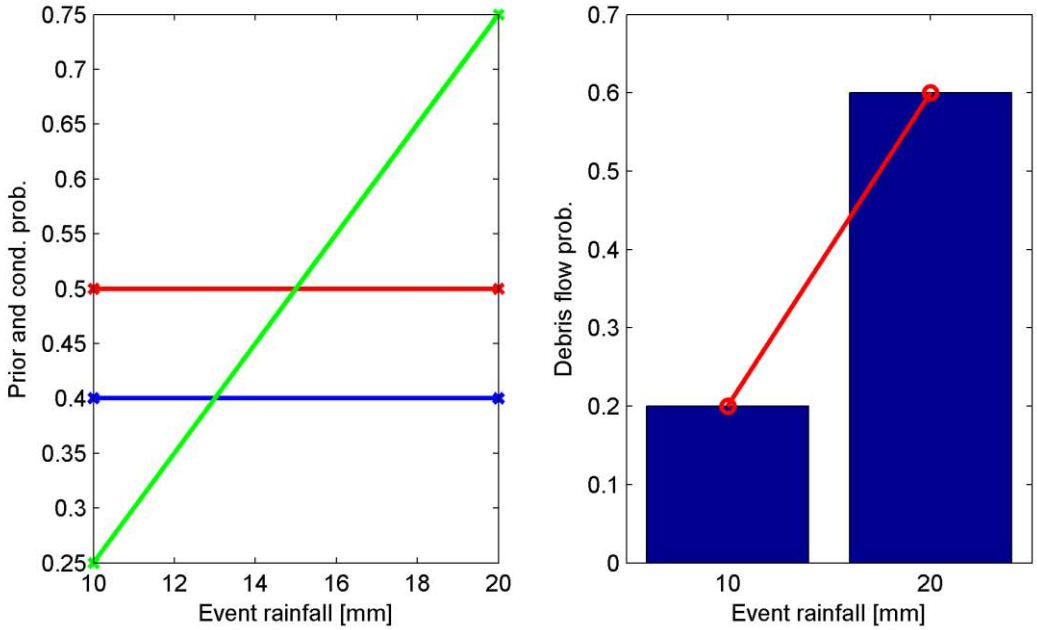

Figure 26: (a) shows prior DF probability P(A) in blue, marginal probability P(B) in red, and likelihood P(B|A) in green; (b) shows the posterior probability P(A|B).

4.7.2 Two-dimensional Bayesian Analysis

Instead of interpreting singular propositions for A with respect to evidence B it is advisable to use the information gained from computing posterior probabilities to combine parameters of interest for different characteristics. We can examine more than one effect by looking at a slightly more expanded version of Bayes theorem:

Equation 8

$$P(A_j|B) = \frac{P(B|A_j)P(A_j)}{\sum_{i=1}^{n} P(B|A_i)P(A_i)}$$

According to Bras (1990) the important feature of this equation is, that the researcher can either express his/her experience in the form of $P(A_j)$ or – as in our case – probability classes of specific states of nature, before even any sample has been taken. In our case it helps us to incorporate the wealth of data measured by the meteorological stations at hand and incorporate the information into the

conditional probabilities of our samples given certain states of nature (our classes). With this in mind, the above equation can be expressed in Brass's sense:

Equation 9

$$P(state|sample) = \frac{P(sample|state)P(state)}{\sum_{all\ states} P(sample|state)P(state)}$$

Thus, above can be simplified into this form:

Equation 10

$$\frac{P(B_j|A)P(A)}{P(B_j)}$$

By doing so it is possible to obtain the conditional probabilities for a space defined by two criteria.

Example (cont.)

When looking at the previous example from Table 11 it is also possible to compute the DF probability for specified intervals, e.g. rainfall smaller than 20 mm, and >20 mm as well as different duration, e.g. 0-4.5 days and 4.5 to 10 days (we can denote intensity classes as $B_{i.}$ and duration classes as $B_{.j}$). This can be illustrated as follows:

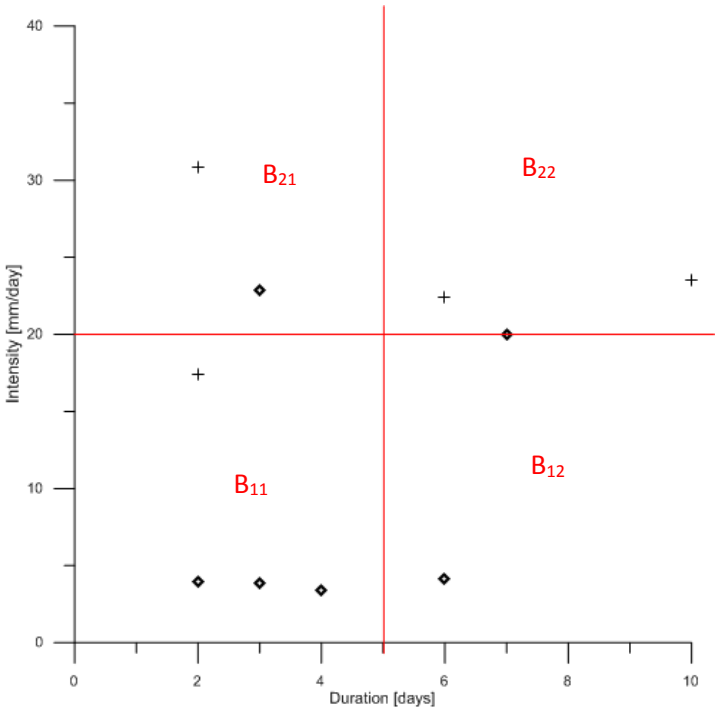

Figure 27: Example of 2D Bayesian analysis

In the class of intensity from 0 to <20 mm and duration from 0 to < 4.5 days one out of 4 rainfall events resulted in a DF. According to Equation 10 we have P(B|A)= 1/4 = 0.25 and P(B)= 4/10 = 0.40. The prior

DF probability is P(A) = 4/10 = 0.40; the posterior DF probability according to the equation is thus $P(A|B_{11}) = 0.25 \cdot \frac{0.40}{0.40} = 0.25$.

If we repeat this for the other sectors of Figure 27, then we obtain: $P(A|B_{21})$= 0.50, $P(A|B_{12})$= 0, and $P(A|B_{22})$= 0.67. This information is illustrated in the Figure below.

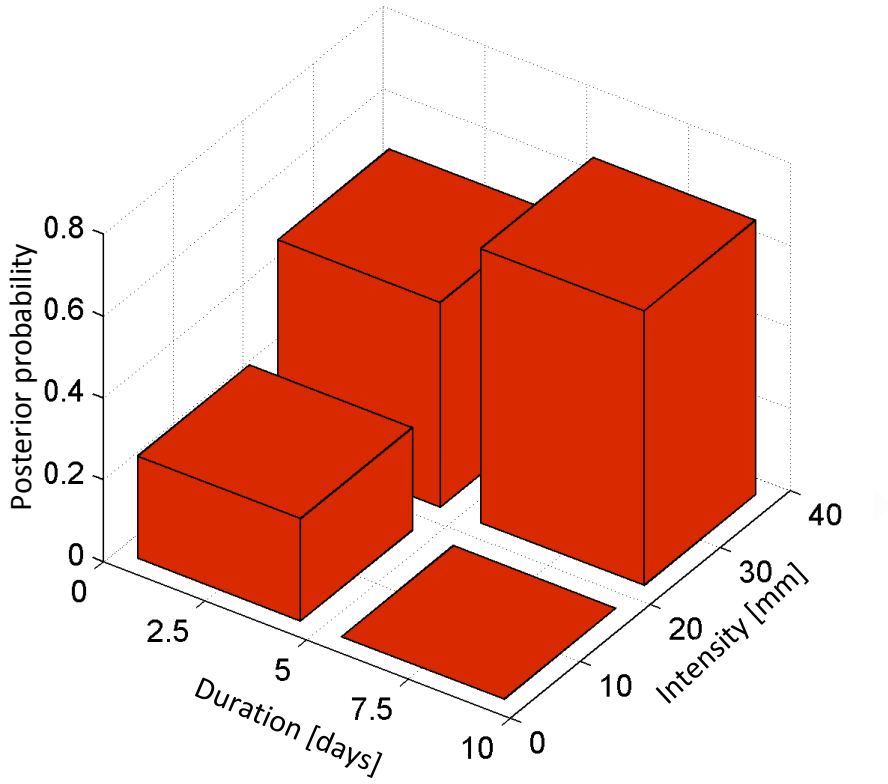

Figure 28: Histogram of conditional probabilities for different duration-intensity classes

4.7.3 Uncertainty Estimation

The probabilities of DFs increase with the "extremeness" of an event, but this rise is irregular to some extent, because the data is unevenly distributed. At the highest values the parameters seem to decrease mainly due to two factors: The computed probabilities of extreme events are affected by a lack of significance due to low sample sizes. Bins with a low amount of data may be not informative enough to be significant and a small variation in the number of DF events could result in a considerably different probability. To account for the impact of this uncertainty the 95 % confidence interval from a Poisson distribution fit representing possible counting errors in the number of DFs was computed (Berti et al., 2012; Naylor et al., 2009) and considered throughout all the computing routines to define the confidence interval for the DF probability (dashed lines in Figure 29). As can be further seen in Figure 29, the upper confidence limit increases strongly with the severity of the event.

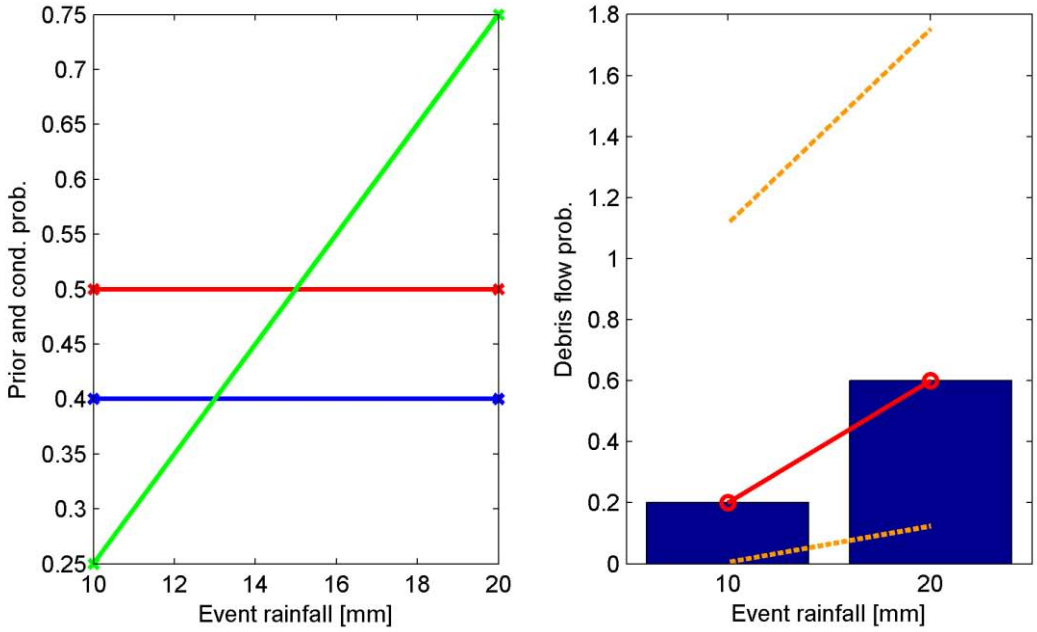

Figure 29: Illustration of prior probability, marginal probability, and conditional probability (Figure 26a) and posterior probability (Figure 26b) computed from example data in Table 11.

Another reason for this uncertainty calculation is that there is a bias introduced through the definition of the TER. While TERs are truncated at the occurrence date of the DF, the non-triggering rainfall continues until the end of the rainfall. Because of this it could happen, that DFs triggered by a long-term rainfall event are counted in another bin, because they have occurred before the end of the rainfall. In combination with other effects this bias may explain the observed trend of DF probability associated to extreme events (Berti et al., 2012).

For one-dimensional (1D) Bayesian analysis the probability can be analysed by estimating the 95% confidence bounds from Poisson counting errors with respect to the number of landslides within a precipitation or duration interval respectively. This procedure is described by (Naylor et al., 2009) for frequency-magnitude distributions in earthquake evaluation and can be applied for any counting errors of histogram data, where power laws play a role. For extreme value analysis it is common to assume power laws in the context of natural hazard occurrence.

Calculation of the confidence bounds is performed as follows: The counting errors are accounted for in the computation of P(A) and for P(B|A). Therefore the total count of DF-triggering precipitation is fitted to a Poisson distribution at α=0.05. Then also the count of all triggering rainfall in range is fitted resulting in the following values:

Variable	Count	Poisson fitted lower bound	Poisson fittet upper bound
P(A)	4	1.0899	10.2416
P(B|A) at TER< 20 mm	1	0.0253	5.5716
P(B|A) at TER>= 20 mm	3	0.6187	8.7673

Table 12: Fitting results showind the upper and lower bount at a confidence of 95 %

Each of these results is then included instead of the counted number, e.g. P(A|B) at the lower bound for TER < 20 mm would be $\frac{\frac{0.0253}{1.0899}\frac{1.0899}{10}}{\frac{5}{10}}$.

Basically, this means that counting errors for the amount of debris flows as well as counting errors for TER are considered.

All of the data available in this study incorporate uncertainties and contain artefacts. While the EDB is potentially biased through over- and underreporting, partially missing data as well as an unclear definition if the coordinate was the DF fan or in the release zone, meteorological data in many cases does not yield a consistent time series, but incorporates a lot of data gaps which cannot be included in the cumulative precipitation graphs. Partially, also the special of temporal information provided is wrong due to input errors (eHYD) or wrong coordinates (ZAMG). However, because of the quantity of data potential impacts on the quality of results are deemed negligible.

In comparison to the example for Bayesian analysis provided in the* Methods*-section it is much harder to make a classification and thus to train an algorithm for TER for real-world data. This is the most sensitive aspect of an analysis relying on Bayes' theorem.

A Bayesian approach gives the possibility to analyse data in a consistent and principled way. The theoretical framework is well proven and was already used in similar contexts (Landslides, Berti et al., 2012; Guzzetti et al., 2007; CC and precipitation, Tebaldi et al., 2005, 2004). The disadvantage is that there is no such rule to select a prior, but depends on the author's estimation on how to classify the prior. In combination with the sample size, this can heavily influence posterior distributions and possibly affect results adversely when compared to frequentist methods (though the problem of data thinning is present in most approaches).

5 Results

From its structure the results section basically follows the research design as detailed in the methods section.

5.1 Analysis of Primary Data

5.1.1 Intensity-Duration Relationships

At first ID relationships were analysed to acquire some basic characteristics regarding debris-flow thresholds for *all events* and to identify potential effects of debris flow magnitude class in conjunction with precipitation data.

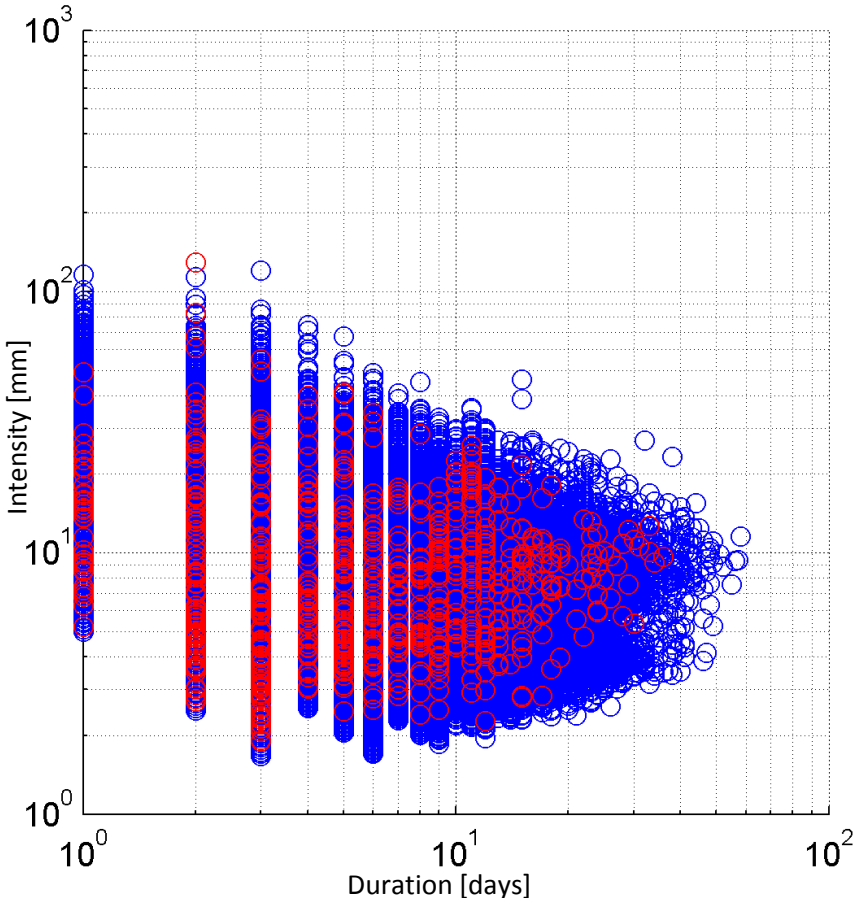

Figure 30: Intensity-duration diagram of all TER (red; n=862) and the whole spectrum of data (blue; n=2,818,619 potential TERs)

Figure 30 depicts the ID-plot of precipitation that actually triggered DFs (in red) as well as data of all rainfall events recorded by any station of the data set shown in blue. The definition of TER is explained in section 4.5.1; rainfall were detected through using a rainfall detection algorithm described in Berti et al. (2012). While the red circles in the figure above show actual TER for event-data (training data for the algorithm), the subsequently detected potential TERs are shown in blue. We see that there exists

a high variability for precipitation triggering DFs throughout the whole area of Austria, with trend of decreasing intensity with increasing duration. However, the data varies over more than one order of magnitude, limiting it's predictive power.

The TER-data for triggering DF was subsequently used to acquire more detailed information about the influence of different DF magnitudes. Plots for different magnitudes are shown in *Appendix 1 – Evaluation of climatic parameters*, here a plot of triggering events (n=862) is shown together with three threshold curves (median threshold; lower and upper 10 % percentile). The 10%- and 90%- percentile as well as the median were calculated from 1-day and 10-day rainfalls and then extrapolated. Thus the lower dashed line in Figure 31 provides a rather good minimum precipitation threshold for the whole dataset. But it is visible that extreme DFs can occur as illustrated with red circles. This is just a preliminary analysis for the subsequent investigation of Bayesian thresholds possibilities.

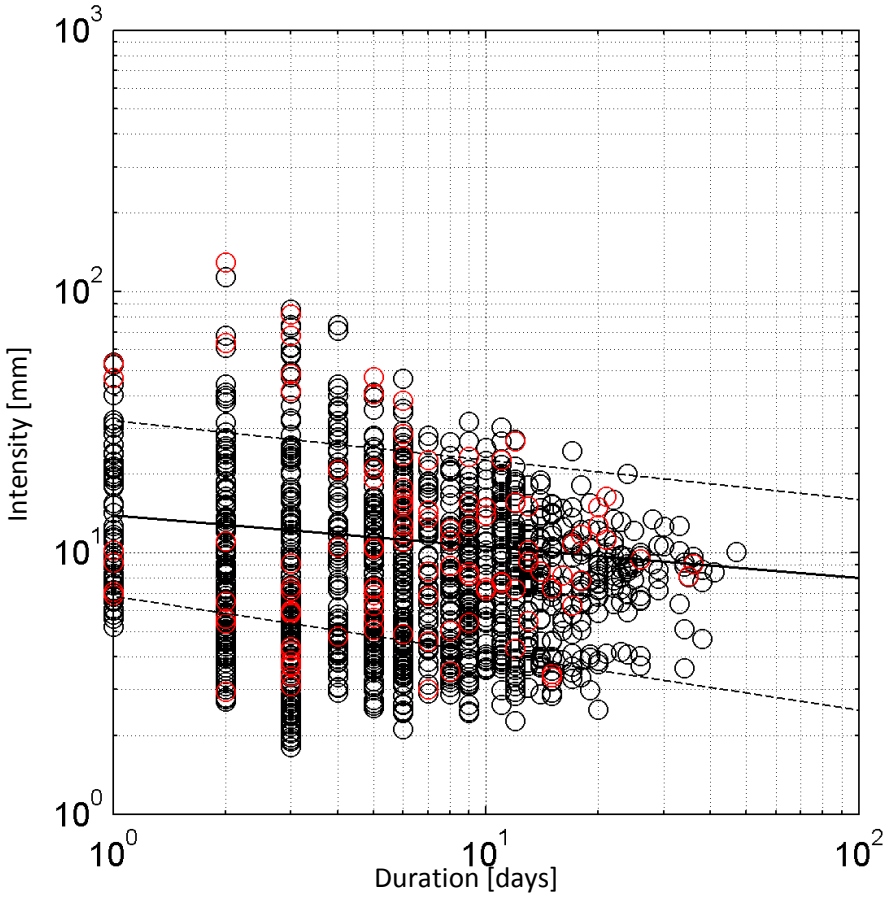

Figure 31: Intensity-duration diagram of all event with an assigned date (black, all events*), events with a magnitude 4 (red, sub-set from dataset with* magnitude assigned*) for comparison and triggering events with median threshold curve (black middle), lower 10 % percentile (black dashed lower), and upper 10 % percentile (black dashed upper).*

The number of DFs for investigation was further reduced, because not all active rain gauges provided meaningful information to train the rainfall detection algorithm. Out of the usable DFs about 94 % had a magnitude class assigned which is about 72.8 % of the total DF dataset. The magnitudes are relatively

well distributed – it is visible that DFs of magnitude class 2 are reported the most, probably because magnitude 1 has less impact on settlements. Naturally, the number then diminishes with increasing magnitude, with extreme DFs (magnitude 4) contributing to about 5.1 % of the whole dataset available. Table 13 summarises this information

Date assigned (1910-2008)	2,412 (max. 2,034 usable data)	100 % (84.3 %)
Gauge measuring TER available	2,125 (max. 1,861 usable data)	88.1 % (77.2 %)
Magnitude assigned	1,756	72.8 %
Magnitude 1 (small)	471	19.5 %
Magnitude 2 (medium)	790	32.8 %
Magnitude 3 (large)	372	15.4 %
Magnitude 4 (extreme)	123	5.1 %

Table 13: Overview of the DFs for different sets of data considered in the analyses.

5.1.2 Analysis of Precipitation

For the analysis three data bases were provided: (1) the EDB from the Institute of Mountain Risk Engineering, (2) measurements from meteorological stations from ZAMG and (3) precipitation measurements from the national hydrographic service (eHYD). At first, precipitation was analysed to prepare the dataset for investigation of potential climatic shifts with regard to the occurrence of DFs.

The data set was homogenised and the seasonal means as well as maxima were computed to detect overall trends. For a first orientation, statistical measures of tendency were used to investigate annual shifts in precipitation data regressing throughout the whole dataset. For investigation of precipitation thresholds an algorithm provided by M. Berti (pers. Communication) was adapted to the MatLab routines developed for this thesis project. Finally, also long-term antecedent precipitation was computed for two ranges – one for 15 days and another one to investigate possible long term effects of antecedent precipitation of 30 days.

Annual means and maxima were investigated for each season. This means that for each year the maximum was extracted from the dataset for each season and the mean for all data of one season in a year. Subsequently seasons will be denoted as follows: DJF – December, January, February; MAM – March, April, May; JJA – June, July, August and SON – September, October, November. It can be seen that the overall regression of the overall climate in Austria is shifting towards less overall precipitation and thus a drier environment in general (cf. Figures for average precipitations and precipitation maxima as well as composite temperature/precipitation indexes stated in *Appendix 1*). If we look at the precipitation maxima, it is obvious from the same regression approach, that there is also a tendency towards higher extreme precipitation events. All seasons analysed showed an increasing trend for precipitation maxima with autumn being the most pronounced (depicted in Figure 32). An

analysis of the upper percentile (i.e. the 99 % percentile) confirms this assumption which is in line with the state of the art research summarised in the *Background* chapter.

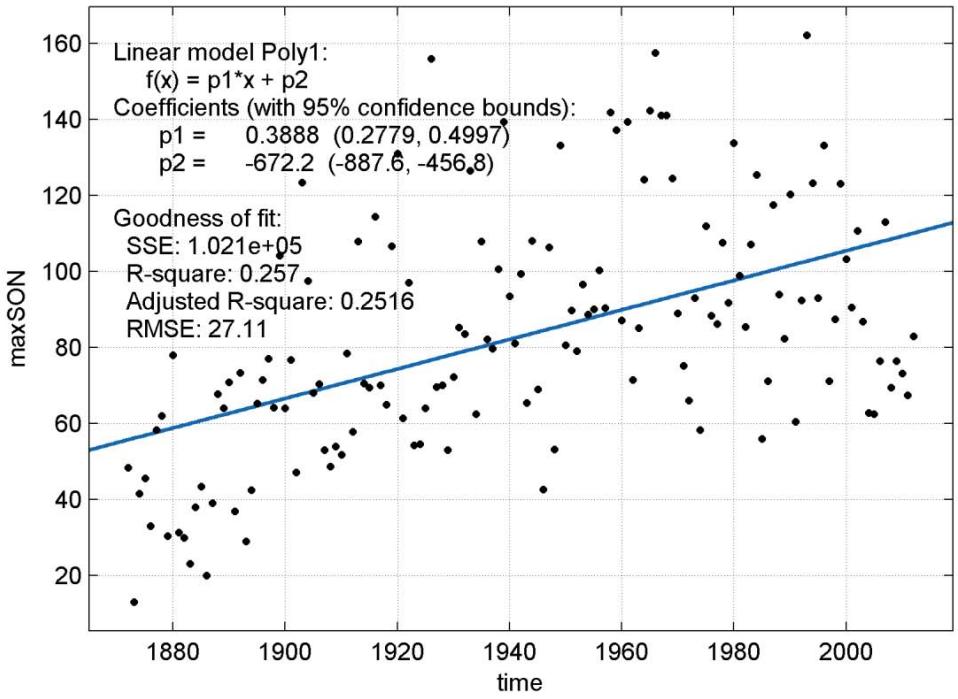

Figure 32: Autumn (SON) precipitation maxima.

Also the other seasons show a similar trend (cf. *Appendix 1 – Evaluation of climatic parameters*) although is it not as pronounced as the autumn precipitation maxima, where the slope of the regression curve is 0.388.

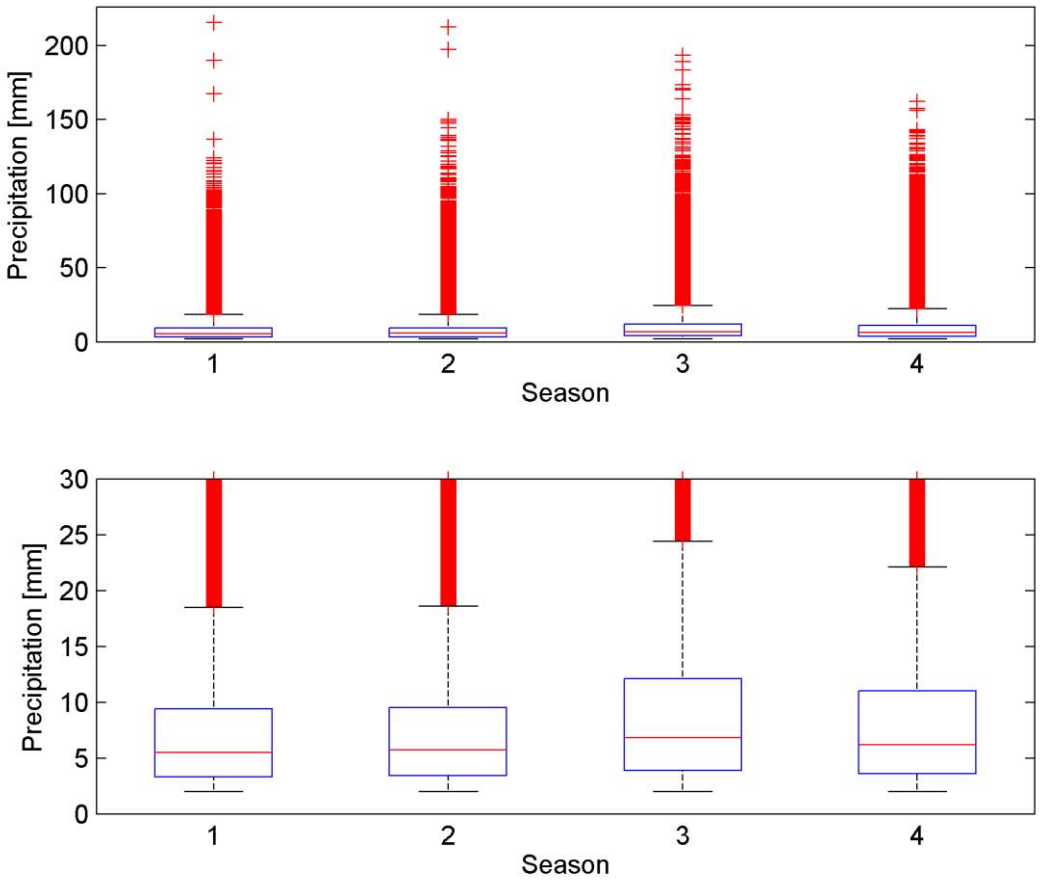

Figure 33: Seasonal analysis of precipitation on different scale; box plots (1=DJF, 2=MAM, 3=JJA, 4=SON).

The box plots in Figure 33 show, that a meaningful statement for whole of Austria is difficult. There is no clear seasonal signal in precipitation variability visible. Due to the large and heterogeneous area it is hard to determine seasonal patterns for precipitation. While there is no clear signal for precipitation maxima, mean precipitation is clearly declining for all seasons, as depicted in box plots (cf. Figure 34) for 30 year intervals of [1916-1946]; [1947-1977]; and [1978-2008].

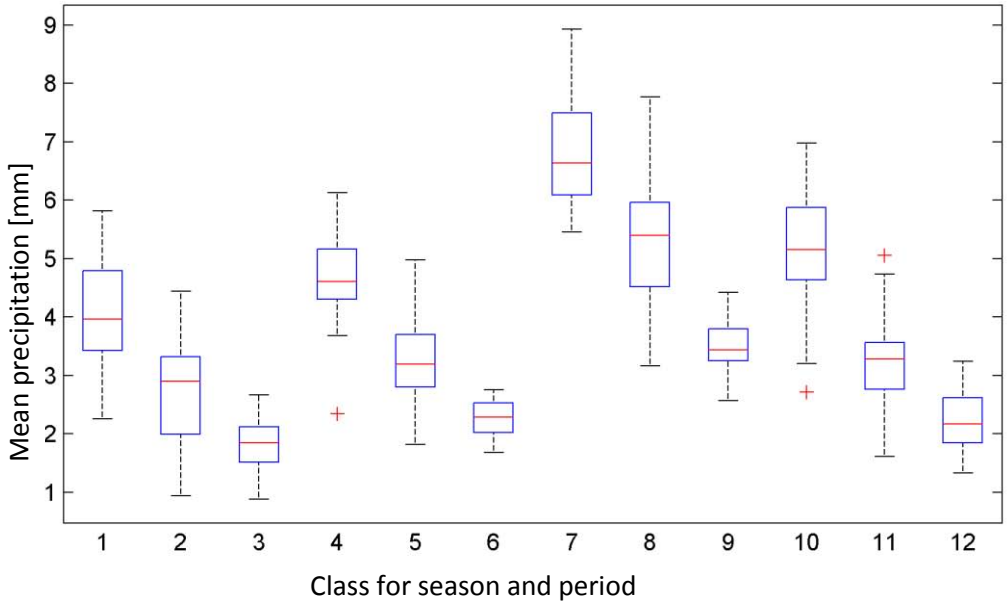

Figure 34: Distribution of mean precipitation (1=DJF 1916-1946, 2=DJF 1947-1977, 3=DJF=1978-2008, 4=MAM 1916-1946, 5=MAM 1947-1977, 6=MAM 1978-2008, … 7-9 JJA, 10-12 SON).

5.1.3 Analysis of Temperature

A similar analysis has been done for temperature data, but the figure below (cf. Figure 35, max temperatures and 95 % quantiles of temperature[9]) shows unusually high temperatures at the beginning of the century. This is due to the fact, that there were fewer precipitation stations at the beginning of the century and because they were likely to be insufficiently sheltered from direct sunlight creating a warm bias in summer and a cold bias in winter, whereas newer stations accounted for this problem already through better standardised procedures. After correcting this data we can see an overall warming trend as well as an increase in extreme temperatures at the right tail of the data, which is also supported by previous research for the Alps (Böhm, 2012; Gobiet et al., 2013) as well as for Austria (Nemec et al., 2013).

[9] Temperature data was not homogenised, which means that the warm bias in early instrumentation is included. However it is not as dramatic for extreme temperatures as for means, for example. The problem was described in Böhm et al. (2009).

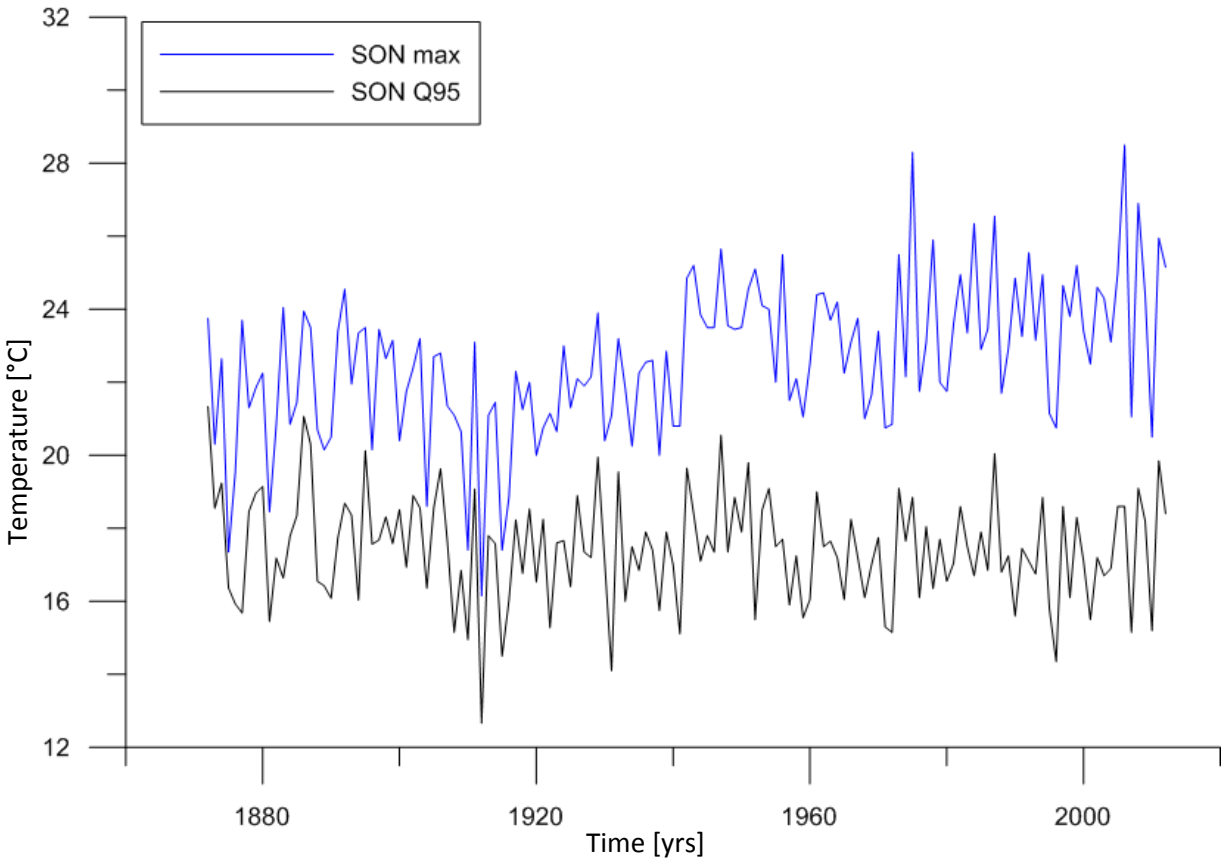

Figure 35: Maximum annual SON temperatures and 95% quantiles for the time period from 1872 to 2012 from the whole dataset.

A box plot of seasonal data for 30 year intervals of [1916-1946]; [1947-1977]; and [1978-2008] shows, that temperature maxima are clearly increasing for each season over time (Figure 36). Although this is an unambiguous indicator a general warming trend, it is important to mention that shifts in temperature are strongly affected by topography, particularly by the orography in Austria. Therefore deductions from overall statements cannot be easily made for regional or even small-scale predictions before it has been downscaled appropriately (Beuchat et al., 2011), which can be also done with the aid of general circulation models (GCM; Groppelli et al., 2011a).

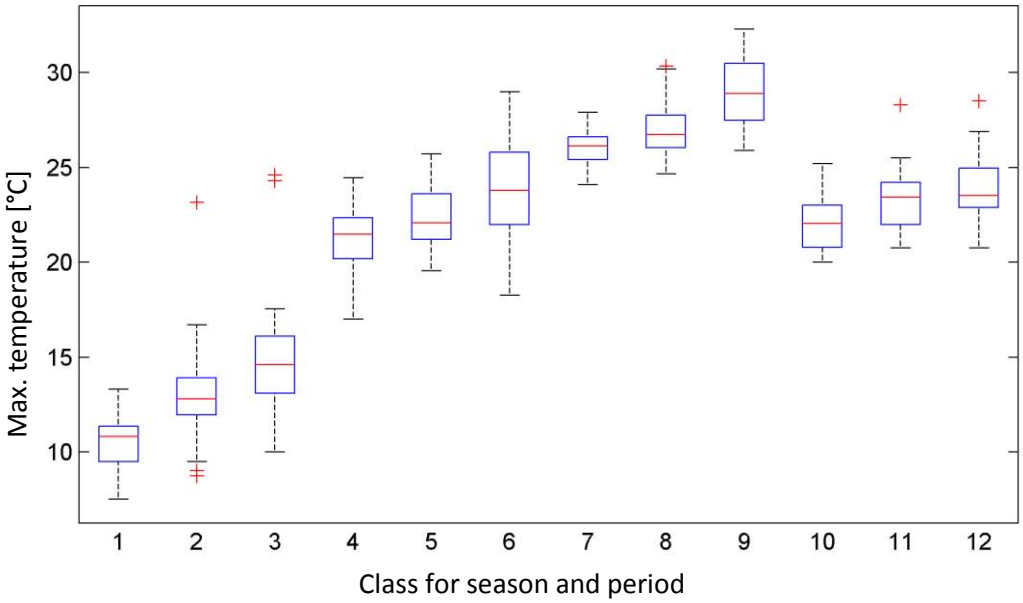

Figure 36: Shifts in the distribution of annual temperature maxima (1=DJF 1916-1946, 2=DJF 1947-1977, 3=DJF=1978-2008, 4=MAM 1916-1946, 5=MAM 1947-1977, 6=MAM 1978-2008, … 7-9 JJA, 10-12 SON).

5.1.4 Analysis of combined indicators

Because previous studies of single climate variables (Beniston, 2007; Klein Tank and Können, 2003) showed rather mixed results, additionally an investigation looking at the combined tails of probability density functions was applied . This method is described in detail in (Beniston and Goyette, 2007; Storch and Zwiers, 1999).

An analysis over all seasons showed a significant increase of warm and wet days[10] for the whole dataset of Austria. The most pronounced and at the same time most significant increases occur in the summer and autumn months which means that the combined mode of the 90th percentile for temperature and the 90th percentile for moisture (warm and moist) are the most pronounced, while the combined mode for the 90th percentile for temperature and the 10th percentile for moisture (warm and dry) has also increased significantly during the last decades. Depending on the season the cool-wet mode and the cool dry mode either don't show a significant trend or are decreasing.

[10] Warm and wet days are determined by examining precipitation and temperature anomalies at a specific percentile. Warm and wet days is the number of days above the warmest decile of temperature and the wettest decile of precipitation (Horton et al., 2001; details in: IPCC, 2007 Ch. 2.8.2.2. Jones et al., 1999)

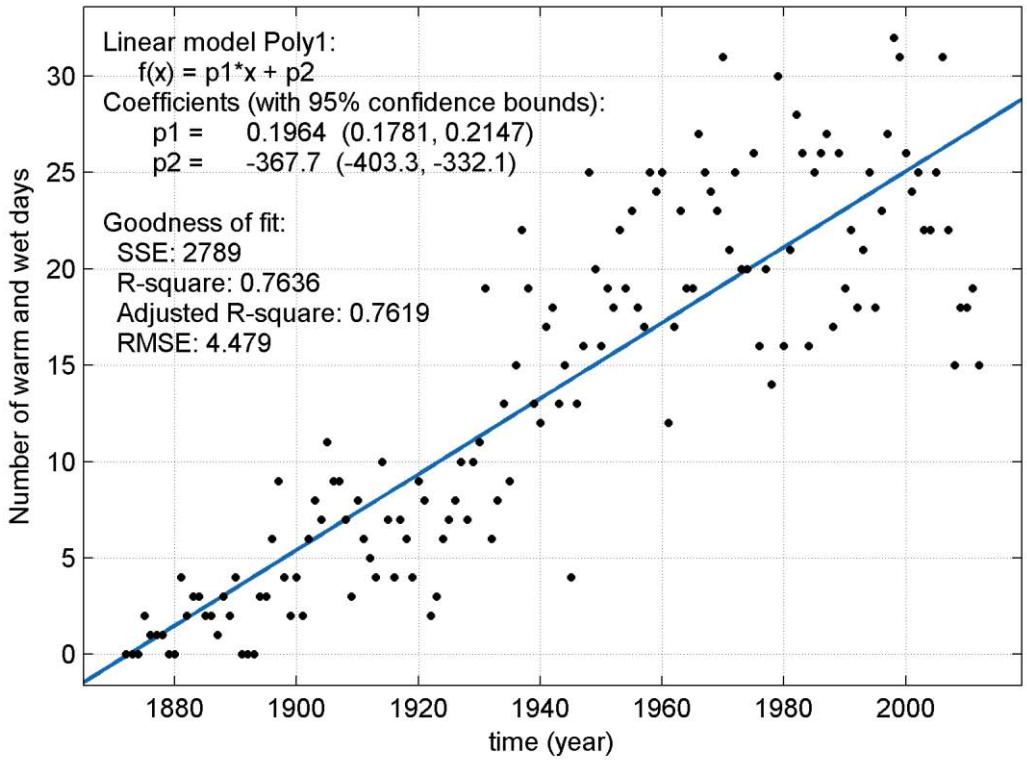

Figure 37: Analysis of annual data for combined warm and wet days. Figures for seasonal analysis can be found in Appendix 1.

If a composite index is built from data, where climate signal is clear, it is possible to use this data for subsequent analysis of the influence of potential climatic shifts and debris flow initiation. To have a starting point the 10% and 90%-percentiles for max Temperature and mean Precipitation respectively were elicited and are documented in the table below:

	DJF 1916-1946	DJF 1947-1977	DJF 1978-2008	MAM 1916-1946	MAM 1947-1977	MAM 1978-2008	JJA 1916-1946	JJA 1947-1977	JJA 1978-2008	SON 1916-1946	SON 1947-1977	SON 1978-2008
Mean precipitation [mm]												
10% perc.	2.69	1.52	1.27	4.02	1.96	1.85	5.61	3.67	2.96	3.51	2.10	1.60
90% perc.	5.48	3.95	2.536	5.44	4.15	2.68	8.13	6.43	4.01	6.07	4.50	3.06
Max temperature [°C]												
10% perc.	8.55	9.55	11.25	19.55	22.23	20.38	2.73	25.13	26.98	20.33	21.03	21.43
90% perc.	12.23	14.75	17.33	23.43	24.03	27.50	27.40	19.45	31.45	23.88	25.30	26.45

Table 14: Percentiles for wet, dry, cold and warm days (perc… percentile)

Table 14 shows the upper and lower deciles from the box plots for precipitation and temperature. This climate data was subsequently used for analysis of potential climatic shifts in debris flow occurrence (cf. Chapter 5.2.2: Analysis of Climatic Shifts, Table 17)

5.1.5 Climate data and DFs

After the general analysis the climatic data with regard to DF initiation was analysed

Triggering Rainfall

Since convective rainfalls per definition consist of high-intensity storm events a good rule of thumb approach is to separate the precipitation ranging from 0-24 hrs from precipitation which lasts longer than 24 hrs. In the dataset at hand this means that daily rainfall could be rather attributed to convective rainfall events and rainfall with duration longer than one day can be considered as advective. Of course this is a rather rough approach, because there could be also several subsequent days of convective precipitation.

Precipitation totals at the respective nearest station of a DF event vary considerably, having a range between 5.2 and 566.9 mm. The data analysis also shows, that small totals of TER can be attributed to small DFs while medium and some of the large DFs are almost exclusively triggered by convective rainstorms (one day rainfall events). For medium DFs the TER totals lie between 5.2 and 87.1 mm. Last but not least many large or extreme DFs were initiated by very-long lasting advective precipitation. Table 15 summarises the information acquired for DFs *magnitude assigned* in the period from 1900 to 2008 with usable data (1756)[11]

Magnitude class	**S**	**M**	**L**	**XL**
Number of events	471	790	372	123
Precipitation type	> 1 day[12]	> 1 day	> 1 day	> 1 day
Precipitation totals (mean) [mm]	79.8	87.1	93.3	104.4
Precipitation totals (minim) [mm]	5.3	5.2	5.3	5.8
Precipitation totals (max) [mm]	566.9	483.6	416.8	344.2
Duration [days] of rainfall events (mean)	9	9	9	9
Seasonality	JJA	JJA	JJA	JA

Table 15: Hydrometeorological conditions during DF events when combining the DF inventory with actually measured precipitation data.

[11] 369 didn't have usable precipitation data.

[12] Since there is now way to resolve precipitation <1 day in the available data, it is not possible to derive the information, if precipitation is advective or convective.

5.2 Analysis of Shifts in DF Occurrence

5.2.1 Analysis of General Shifts

A good overall approach to determine a change in occurrence of hazards is KDE, of which a general overview is given in (Mudelsee et al., 2003). Figure 38 shows the average yearly intensity and occurrence rates as well as a KDE overlay using a Gaussian kernel which was applied to the dataset by using an adapted version of the Gaussian KDE Toolbox (Horová et al., 2012). Another approach with local bandwidth optimisation (Shimazaki and Shinomoto, 2010) was also evaluated, but is not depicted here, since the Gaussian KDE approach is accurate enough and local optimisation focuses on extremes whereas here deviations from the "standard" trend are of interest. From Figure 38 it can be seen, that from the period of around 1950 until the last years, there is a significant peak of DF occurrence in the 1960. After that, DF occurrence rate decreases. The reason for the first observation may be that in the 1960ies there was a series of DFs triggered along whole Austria through strong storms (Eisbacher, 1982; Glade, 2005). Because of an over-reporting of small DFs this can lead to the pronounced peak in KDE. The decreasing trend in the recent years may be connected to the effect of engineering mitigation measures, which started to become effective.

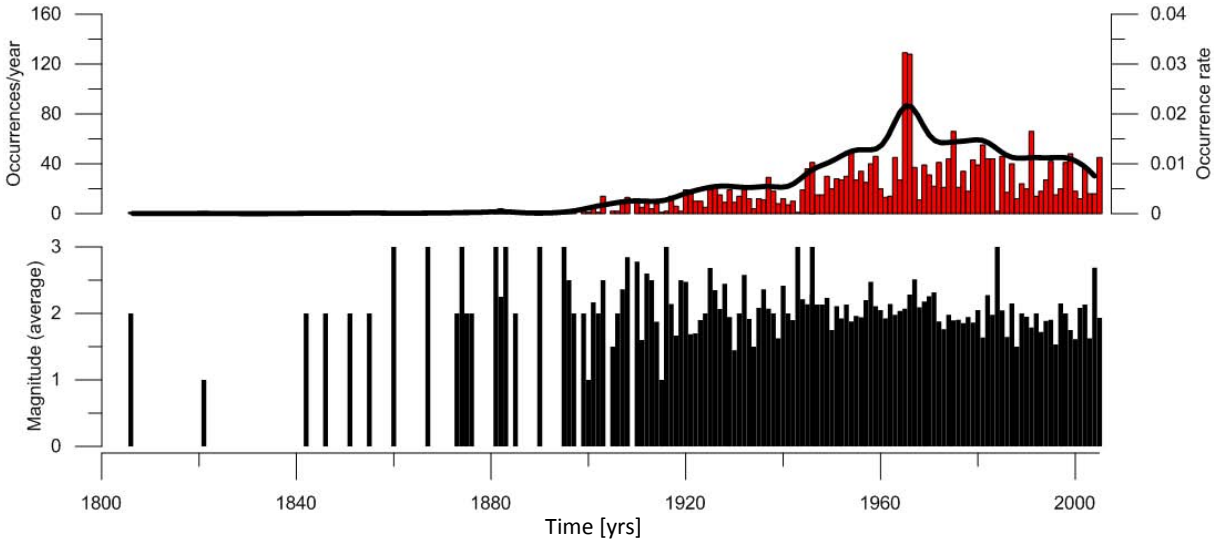

Figure 38: Average yearly magnitude of the investigated dataset (black bars), occurrences per year (red bars and left upper axis) as well as kernel density rate (black solid line).

As already mentioned by previous authors there is a problem with data before 1950 because of data thinning. This means that standardised and routine monitoring was not developed yet and reporting mainly focused on damaging DFs with a focus on large-scale hazardous events. This lead to a significant bias towards higher-magnitude events before this time. As in other Alpine European countries consistent reporting was established in the 1960s by the Austrian torrent and avalanche control. Overall, the analysis shows no upward trends in DF occurrence and a consistent seasonal signal is not detectable in the available dataset.

Additionally, shifts in seasonal occurrence were investigated by calculating the decadal relative percentage of occurrence for each season and by counting the mean Julian day of annual occurrence (as proposed by Stoffel et al., 2011). This analysis showed no significant shift in the season of occurrence, where the main season in Austria is summer throughout the whole analysis (cf. Figure 39) except the first decade under consideration, where a bias due to the lack of events cannot be ruled out. As the numbers below "Events" show there were only 43 events recorded for the decade from 1910-1919 where about 60 % of the DFs occurred in summer.

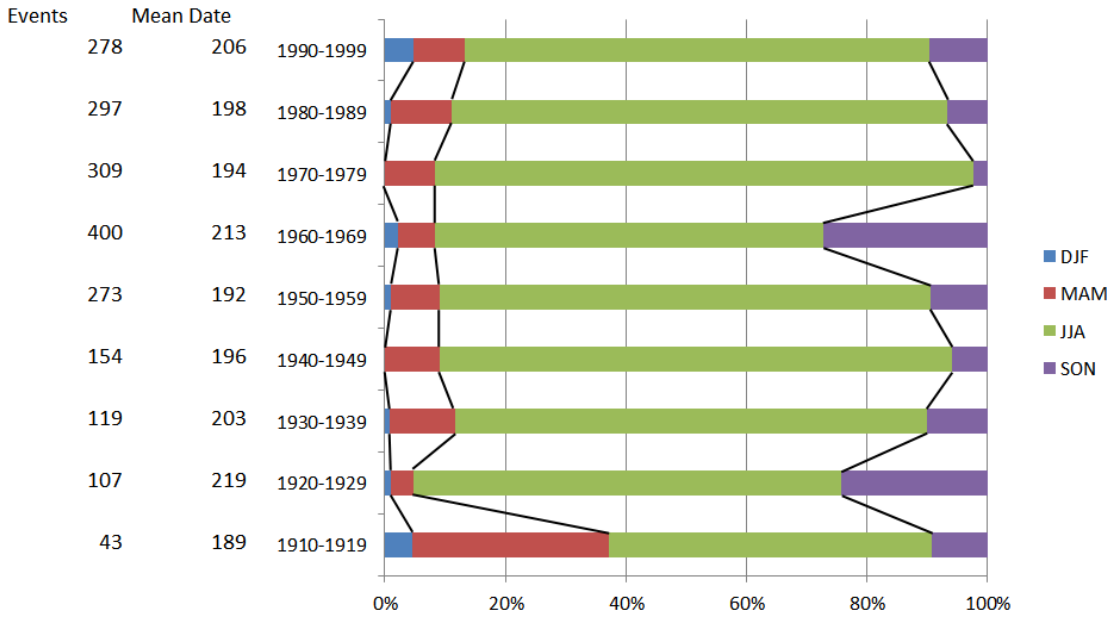

Figure 39: Relative seasonal occurrence rate of DFs per decade (the number of DF is higher in this Figure, because there were also DFs included which don't have an exact day assigned).

5.2.2 Analysis of Climatic Shifts

The data obtained for general shifts as illustrated in Figure 39 was used to further analyse information about precipitation and precipitation duration, which was compiled in Table 16. The table shows information about all 1756 DF events which had *magnitude assigned,* as well as a date and precipitation information of the nearest station.

Magnitude class	S	M	L	XL
1888-1907				
Number of events	4	8	8	3
Precipitation totals (10%, 90%)	17.6, 62.6	31.6, 162.1	28.0, 228.5	8.2, 171.9
Duration of rainfall events (mean)	4	7	7	4
Seasonality	JJ	AS	S	S
1908-1927				
Number of events	20	49	33	15
Precipitation totals (10%, 90%)	8.7, 159.9	11.2, 207.6	15.6, 270.2	11.2, 140.5
Duration of rainfall events (mean)	5	8	8	5
Seasonality	JAS	JAS	JAS	JAS
1928-1947				
Number of events	55	87	53	20
Precipitation totals (10%, 90%)	25.0, 166.2	17.9, 182.5	22.1, 188.2	66.5, 256.3
Duration of rainfall events (mean)	8	8	9	10
Seasonality	JJA	JJA	JJA	JJA
1948-1967				
Number of events	137	242	120	44
Precipitation totals (10%, 90%)	20., 233.4	20.4, 257.1	20.4, 257.4	26.9, 281.0
Duration of rainfall events (mean)	10	9	9	9
Seasonality	JJAS	JJAS	JJAS	JAS
1968-1987				
Number of events	129	246	89	27
Precipitation totals (10%, 90%)	10.0, 170.2	11.0, 164.0	8.4, 157.2	10.3, 120.8
Duration of rainfall events (mean)	7	6	7	6
Seasonality	JJA	JJA	JJA	JAS
1988-2007				
Number of events	126	159	69	14
Precipitation totals (10%, 90%)	8.1, 128.4	10.3, 183.8	17.0, 112.5	9.1, 95.7
Duration of rainfall events (mean)	6	7	6	5
Seasonality	JJA	JJA	JJA	JA

Table 16: Analysis of different event magnitudes in periods of 20 years since 1888 and 1907.

No clear shifts could be determined (Table 16). For all DF-magnitudes occurrence is prevailing in the summer months. The pattern of occurrence of DFs is generally corresponding to the KDE, but can be mainly attributed to "*general shifts*" which is probably over-reporting as mentioned previously.

Another analysis was conducted regarding the potential influence of pronounced climatic shifts on DFs. Here the number of DF for each season was analysed in 30-year steps again [1916-1946, 1947-1977, 1978-2008] and the number of debris flows on warm/wet, warm/dry, cold/wet, and col/dry days was analysed.

Finally, the events from EDB were also considered in the same 30-year steps as before for ID-analysis

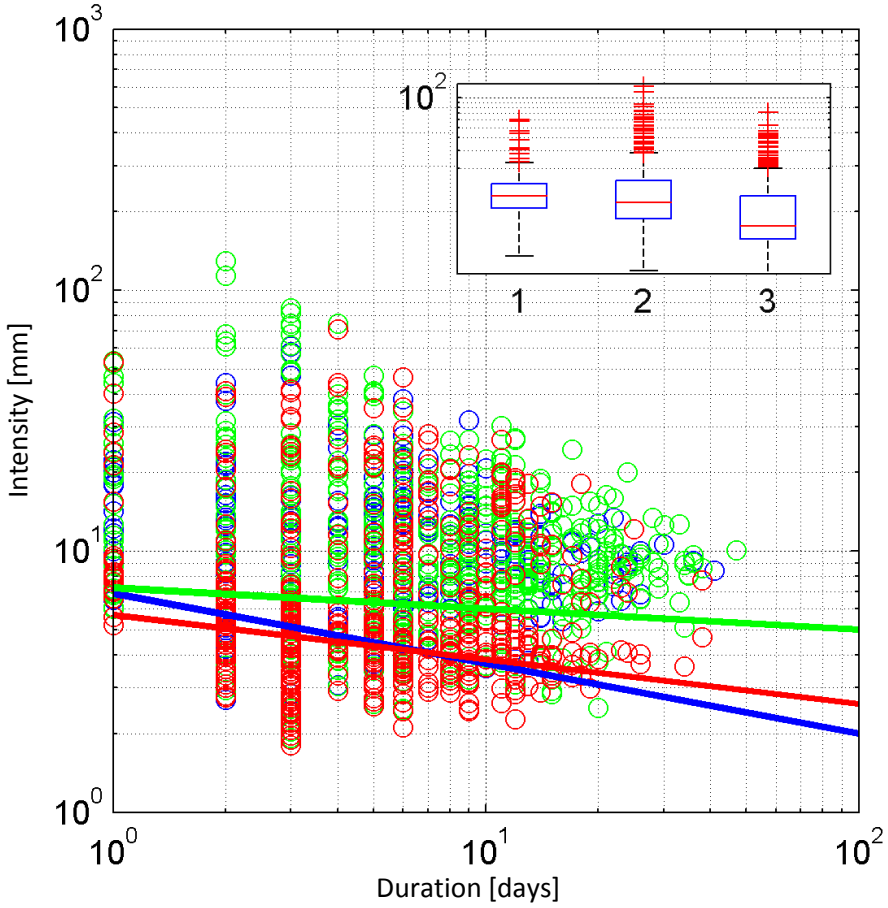

Figure 40: Overview of lower 10%-percentile threshold for the period 1916-1946 (blue, n=321), 1947-1977 (green, n=929), 1978-2008 (red, n=726). In the nested element the numbers on the x-axis correspond to 1:blue, 2:green, 3:red. The higher threshold in green is due to the wider distribution.

Figure 40 shows ID-thresholds for the three 30-year periods. The lower 10%-percentile was computed for 1-day rainfall and 10-day rainfall and then extrapolated. The difference in the green threshold (2) is partly due to the distribution and partly due more outliers compared to distributions 1 and 3.

Period	Index	Count	Percentage[13]
DJF			
1947-1977	Cool/dry	3	27.27 %
1978-2008	Cool/dry	8	72.73 %
MAM			
1916-1946	Cool/wet	1	1.72 %
	Cool/dry	2	3.45 %
1947-1977	Cool/wet	26	44.83 %
	Cool/dry	4	6.90 %
1978-2008	Cool/wet	19	32.76 %
	Cool/dry	6	10.34 %
JJA			
1947-1977	Warm/wet	83	14.36 %
	Warm/dry	11	1.90 %
	Cool/wet	129	22.32 %
	Cool/dry	64	11.07 %
1978-2008	Cool/wet	216	37.37 %
	Cool/dry	75	12.98 %
SON			
1916-1946	Cool/wet	6	6.90 %
	Cool/dry	2	2.30 %
1947-1977	Cool/wet	48	55.17 %
	Cool/dry	4	4.60 %
1978-2008	Cool/wet	22	25.29 %
	Cool/dry	5	5.75 %

Table 17: Summary of a composite analysis of 10% and 90%-percentiles.

The statistical analysis shows that during DJF all DFs are likely to be caused rain-on-snow events, since temperatures were around thawing temperature (Table 17). In 9 out of 11 cases it was raining for ≥ 5 days, with an average daily precipitation around 20 mm/day. In the period from 1978-2008 the average temperature for these events was mostly higher than in the period from 1947-1977.

Table 17 also shows that initiation of DFs under more extreme climate variables is dominated by the cool/wet-index. When looking into this index in more detail, it is visible that summer DFs are increasing at the expense of cool/wet MAM and JJA DFs. It has to be considered that this table only represents combinations of upper/lower percentiles (n=764 DFs), and that other DFs are probably not subject to climatic shifts. Nevertheless, this number is a considerable part of the DFs selected for analysis. About 89 % of the DFs used for analysis of rainfall intensity are subject to one combination of the outer 20 % boundary of all the climatic data which could be obtained for Austria.

[13] Percentages show the proportion of an index-period combination amongst the quantity of DFs occurring in a season.

5.3 Bayesian Analysis

Additionally to climatic shifts, climatic parameters can also be included for DF hazard estimation through the application of Bayesian theory (Bras, 1990). For a reliable analysis the key factors of precipitation were identified and analysed in 1D and 2D approaches.

5.3.1 Definition of Triggering Events

Because there is no standardised approach on how a "typical" rainfall event looks like, it had to be defined beforehand to be of use for the Bayesian analysis. Therefore the cumulative precipitation of the nearest station of each event was plotted, assessed manually and subsequently divided in well-defined rainfall events or uncertain rainfall events. In this context well-defined TER is an event where a steep precipitation curve before the occurrence of an event is clearly visible. Usually the end of this event is defined as the day of DF initiation. The beginning of an event is a moment in time before which no or no significant rainfall occurred and after which a steep and constant increase in cumulative precipitation is clearly visible. Such procedure of defining start and end dates of cumulative precipitation events has then been conducted for *all events* with date and precipitation data assigned (2412-378) to get a set of "typical" TER for the triggering of DFs. Because this procedure is prone to subjective biases, but is unomittable for the analysis in mind, the evaluation of diagrams was performed by the author of the thesis at hand and repeated independently twice by two students, which were previously schooled by example datasets and simplified parts from previous research performed by (Berti et al., 2012). From these assessments the ones with the highest deviation from standardised event precipitation were re-examined and corrected where deemed implausible. Subsequently, the TER and the rainfall duration for each event were averaged. This result then provided a training dataset to feed into a heuristic which looked through all measuring stations in the whole dataset to find similar TER which fit to the training set.

If we look for patterns we need to define a certain threshold for the dataset under examination which has the smallest error compared to the training dataset. To accomplish this the rainfall detection algorithm provided by Berti (*pers. comm.*[14]) was adapted to the MatLab routines developed for answering the questions stated in the Introduction and all possibilities of a TER between 0 and 10 mm (in 1 mm steps) and 1 to 10 days (in 1-day steps) were compared and the relative RMSEP (root mean square error of prediction) was computed for each combination.

[14] Matteo Berti provided a very helpful example by e-mail (24.11.2013) of a learning-based approach to train an algorithm for automated detection of TER explaining methodological aspects of his research published in Berti et al. (Berti et al., 2012)

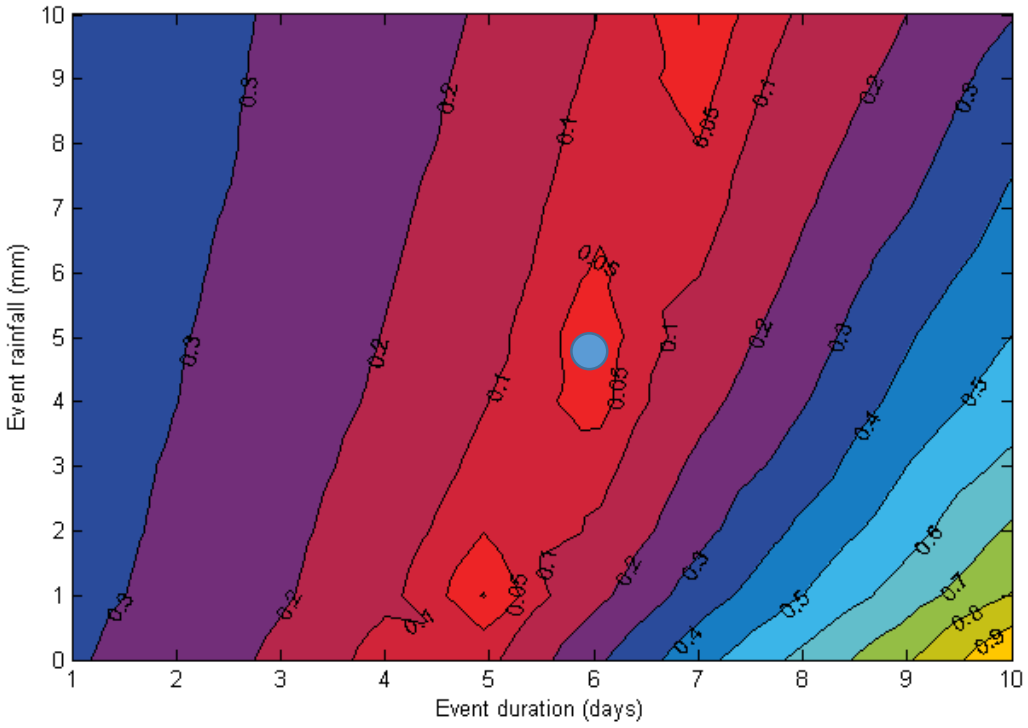

Figure 41: Contour plot of RMSEP calculation showing the results of the rainfall detection algorithm for different combinations of event rainfall and rainfall duration compared to the training dataset (i.e. the reference dataset). The blue indicates on what values the algorithm should be trained (6 days, 5 mm; as described in the text)

The analysis resulted in a training rainfall of 5 mm and a duration of 6 days. This means, that a rainfall event starts when the cumulative rainfall exceeds 5 mm in 1, 2, 3, 4, 5, or 6 days (i.e. if 5 mm are exceeded on the first day, the rainfall starts at day 1. The end of the rainfall is defined when it doesn't rain above 5 mm for at least 6 days (or if a debris flow is triggered). This pattern is the most representative for all events which could be evaluated. Figure 41 shows a contour plot of the relative RMSEP for the event rainfall and the event duration between manually evaluated DF TER and the all the possibilities between an event rainfall of 0 to 9 mm and 1 to 10 days. The blue circle represents the calibrated value for event rainfall and event duration associated with the minimum RMSEP.

5.3.2 One-Dimensional Analysis

Because no significant shifts could be detected, the whole dataset was analysed to detect the significant parameters with regard to precipitation and DFs.

For all 2,412 events the cumulative precipitation was plotted and the start and end of the rainfall was defined. With this data, the rainfall detection algorithm (Berti et al., 2012) could be trained to find typical TER in the whole precipitation dataset.

This helped to acquire substantiated values for the total amount of TER-events within the considered time frame. By classification of potential TER, actual TER and threshold classes, Bayes' theorem (Bras, 1990) could be applied.

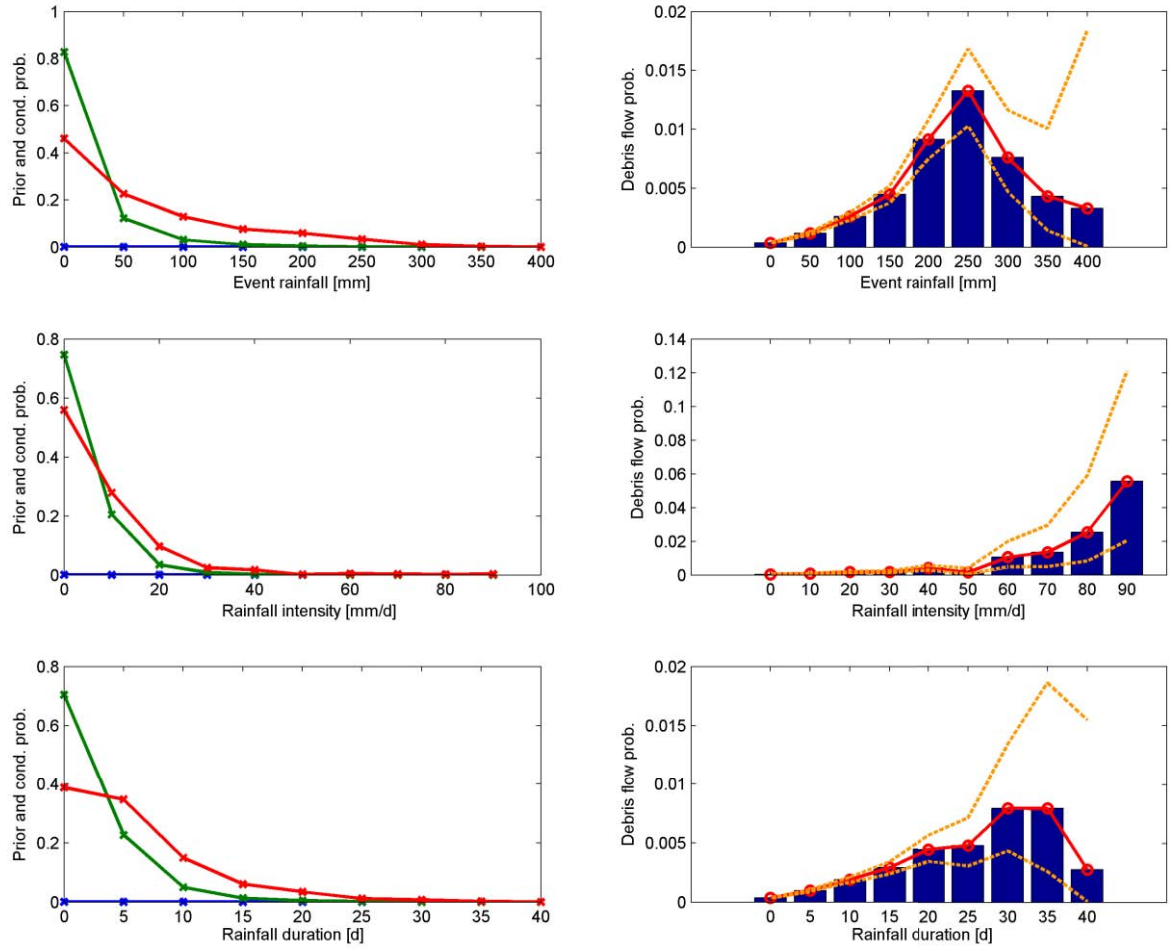

Figure 42: 1D Bayesian analysis for the parameters: event rainfall, rainfall intensity, and rainfall duration. Column (a) shows prior DF probability P(A) in blue, marginal probability P(B) in red, and likelihood P(B|A) in green; column (b) shows the posterior probability P(A|B) and the confidence interval as dashed lines.

Bayesian analysis was applied for five parameters, the event rainfall, rainfall intensity, rainfall duration, and two different lengths of antecedent rainfall. Event rainfall is the amount of rain that accumulates before the initiation of a DF. Because there is no standardised rule for what defines a typical rainfall event, it was defined as in section 5.3.1.

In Figure 42 and Figure 43 we see, that event rainfall has the highest posterior probability and is thus the most significant parameter in our analysis. While the left illustration show the prior probability, the marginal probability, and the conditional probability (likelihood). The right diagrams show the conditional landslide (or posterior) probability

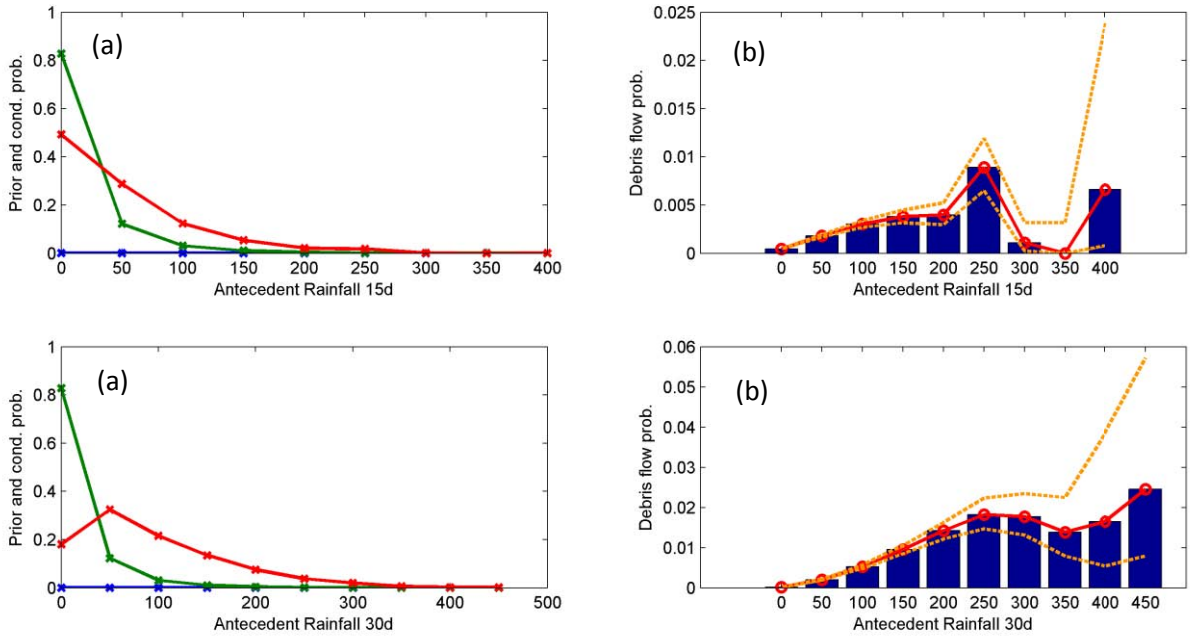

Figure 43: 1D Bayesian analysis for two lengths of antecedent rainfall. (a) show prior DF probability P(A) in blue, marginal probability P(B) in red, and likelihood P(B|A) in green; (b) shows the posterior probability P(A|B) and the confidence interval as dashed lines.

Figure 43 shows the antecedent rainfall in hours. Also the antecedent rainfall shows some relation with DF initiation. In both plots there is a peak at around 11 days (250 hrs) which shows that this aspect of precipitation plays a role in long-term advective rainfall. Above about 400 hrs uncertainties get to high to draw a reliable conclusion from this aspect of precipitation. As already noted by Guzzetti (2008) there are too many potential secondary factors when investigating very short or very long periods of time, since at short durations it is hard to attribute slope failures to rain alone and for long time scales it is hard to adequately prove the causal relationship.

5.3.3 Two-Dimensional Analysis

After the 1D analysis a 2D analysis was conducted as described in the methods section. Here, the duration of event triggering rainfall was compared with all of the parameters including event magnitude to find if a pattern exists for any of these combinations.

In our case this is the conditional probability of a DF occurring when rainfall intensity $i = \log_{10} I$ [mm], with

$$i_i \leq i < i_{i+1} \text{ with } i_{1:n} = \{0: 0.2: 1.2\}$$

and when duration $d = \log_{10} D$ [days] with

$$d_d \leq d < d_{d+1} \text{ with } d_{1:n} = \{0:, 0.2: 1.8\}$$

and with $i, d \in A$.

If different DF magnitudes are computed separately, the results on the right are even more pronounced.

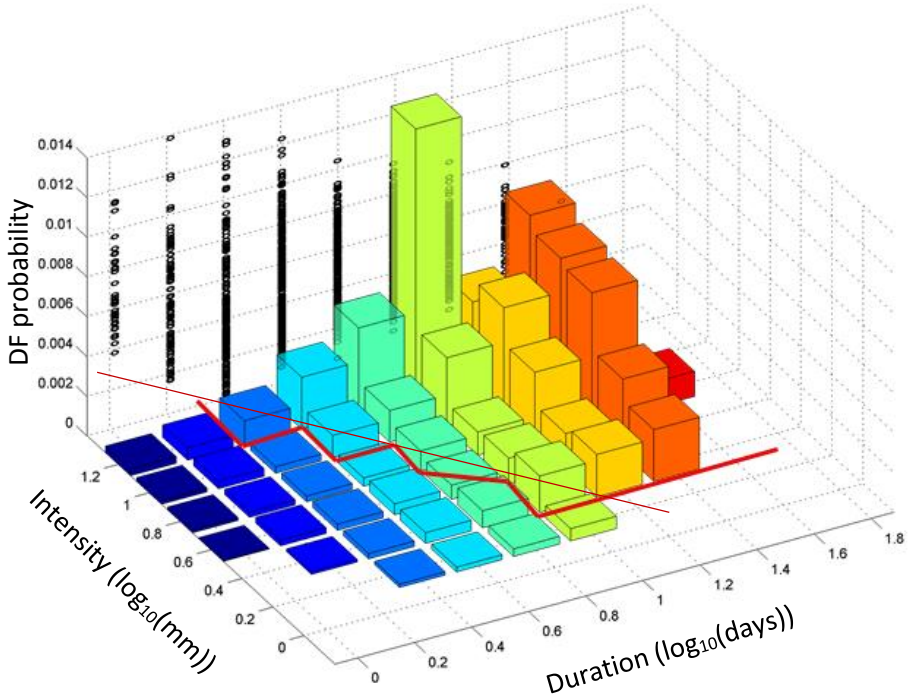

Figure 44: 2D analysis of precipitation (intensity vs. duration). The red line separates marginal areas of probability from more significant ones (visual estimation) and approximation (thin red line)

Figure 44 shows the decadal logarithm coloured graph for different event rainfall classes (x-Axis) versus different classes of precipitation intensities (y-Axis). As a result the posterior probabilities, i.e. DF probabilities are depicted (z-Axis). Illustratively an ID-diagram was fitted for the event rainfall length (on the y-z-Plane for visualisation, the x-y-Dimensions correspond to Figure 30). As can be seen from the plot, rather large durations of 10-16 days [axis: 10^{1}-$10^{1.2}$ days] show the highest probability for DF initiation, which is about 1.4 % for the duration and an intensity class of 16-25 mm [axis: $10^{1.2}$-$10^{1.4}$ mm]/10-16 days [axis: 10^{1}-$10^{1.2}$ days]. That means that the highest probabilities of a DF occurring are in this bandwidth of long-duration, high-intensity rainfall. The selected probabilities for different ID-classes allow to derive an ID-threshold (Figure 44, red line).

When visually separating clusters of occurrences from aggregates with negligible activity (cf. red line in Figure 44) a power law could be formulated to describe thresholds between $<10^{0.4}$ days and $<10^{1.2}$ days. From 15 days on there is not enough data available and causality questionable, but one way to approach this is to keep the threshold constant here. With shorter rainfall durations a formulation of a power law makes sense. Thus, the information available can be extrapolates for shorter TERs.

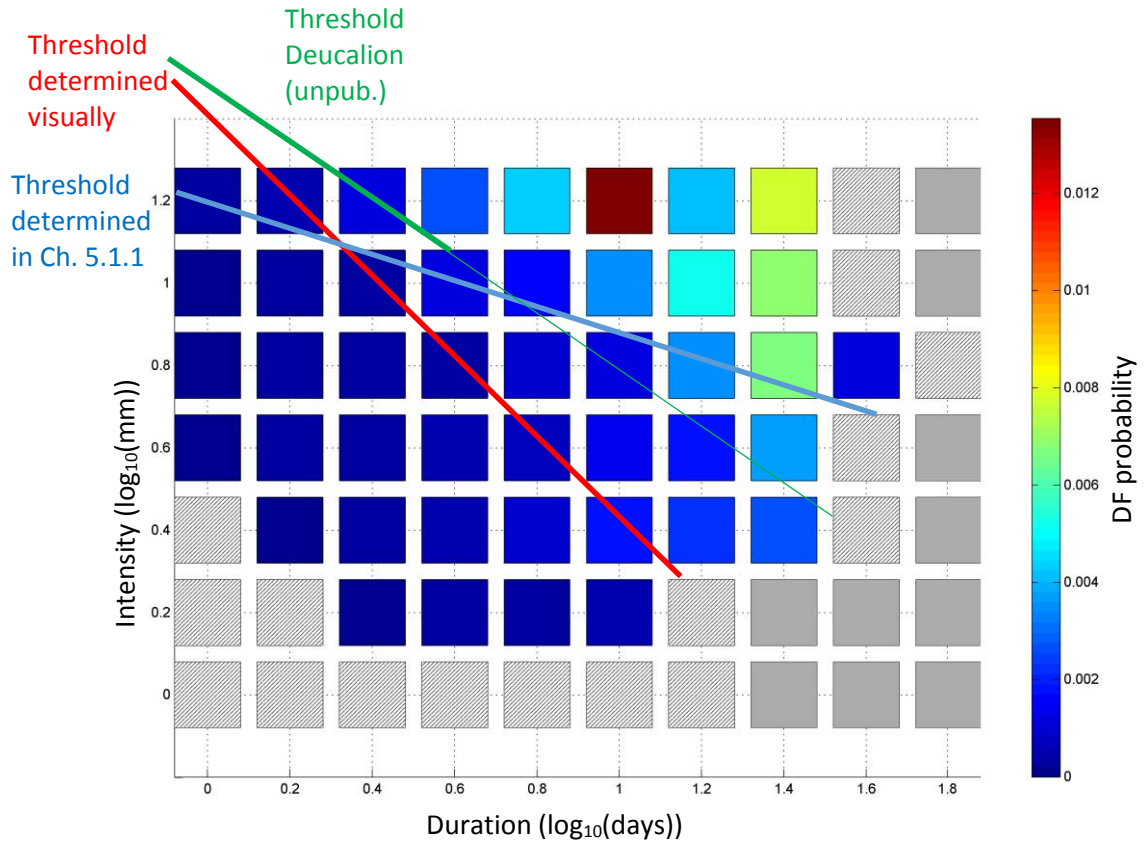

Figure 45: 2D Bayesian analysis visualising the whole usable dataset (all events that with an active station. Threshold derived from combined information is indicated in red (derived from the thin red line in Figure 44).

Because of the large amount of precipitation data one the one hand, but the comparably few inventoried DF events on the other hand, the detected probabilities are very small. From Figure 45 it is clearly visible that long-term advective rainfall is well resolved in the analysis. For the whole dataset the highest DF probability is shown by the dark red square in the picture. This means that for the duration interval between 1 and 1.2 (10 to 16 days) and the intensity between 1.2 and 1.4 (about 16 to 25 mm/day) have the highest conditional probability for DF occurrence of about 1.2 %. The hatched squares mean that there were no rainfall events are existent in the dataset, while the white squares mean, that no DFs were observed in this interval classes.

From this result is becomes obvious that sub-daily rainfall data is missing and the computations do not resolve the influence of high intensity precipitation. If high-resolution precipitation data would be available, the author would expect a second peak in landslide probability on the beginning of the x-Axis (sub-daily) for high-intensity convective precipitation, based on a broad literature review.

This analysis including all data was also applied to investigate precipitation data for each of the four magnitude classes defined in the EDB. Because not all DFs had a magnitude assigned the conditional probabilities for each class are naturally considerably smaller. All classes have in common that long-term wet conditions are positively correlated with DF initiation. Even though the conditional probability is increasing due to the smaller number of events occurring it is visible that there is a strong

tendency for DFs occurring at a TER-duration of >0.6 (> 4 days) and that virtually no extreme DFs occur below that class (keeping in mind that sub-daily rainfall is not being resolved).

Because no clear differentiation between DF magnitudes could be found, the ID-plot described before was overlain with TER for different magnitudes. However, also these plots don't show any clear signal that for whole Austria the DF magnitude would dependent on rainfall intensity or duration. To further elaborate conclusions for the data at hand it would be necessary to obtain more information about site conditions and to divide the data into homogenous precipitation regions (or climatic regions).

Based on the information collected in the whole Bayesian analysis it is feasible to define a threshold separating negligible probabilities from significant ones. With the aid of Figure 45 and the plots provided in the appendix the threshold depicted as red line accounts for most of the DFs. For comparison there is a blue threshold line added, which represents the consideration of the upper 90%-percentiles of precipitation above the threshold from previous analysis in Chapter 5.1.1. For comparison a bold green line from the project Deucalion[15] (Kaitna et al., n.d.*a*, n.d.*b*) for up to 5 days was added and extrapolated as thin green line.

[15] Deucalion was a project for the 2nd call of the Austrian Climate Research Programme.

5.3.4 Sensitivity Analysis and Robustness Check

These above analyses included all nearest stations found. Since the distance of the measuring station is a critical parameter, the dataset of nearest stations was furthermore reduced to a maximum distance of 10 km, 20 km, and 30 km for comparison. All other data were discarded in the respective data sets.

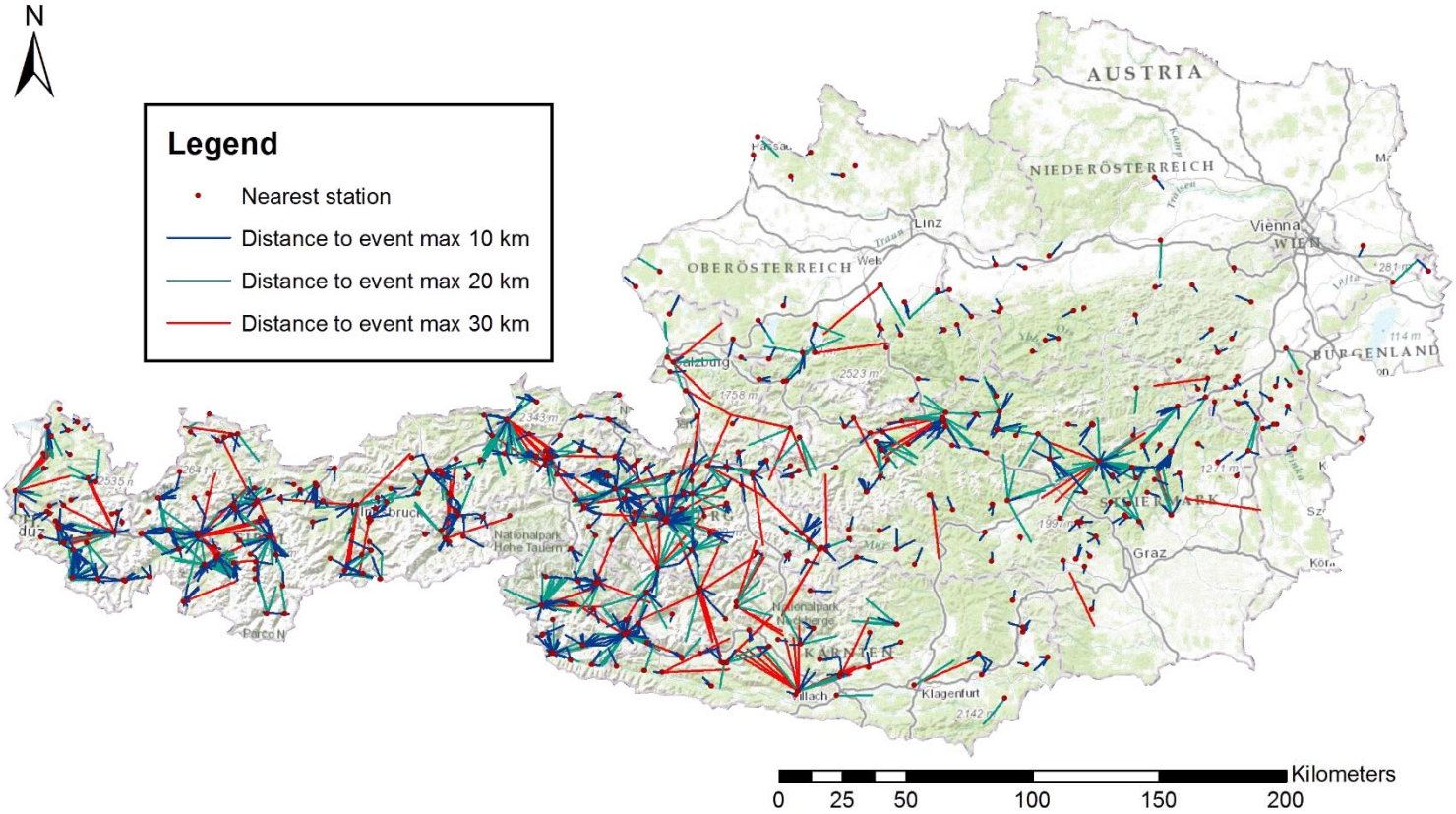

Figure 46: Overview of stations considered for events which are not farther away from a rain gauge than 10 km (green), 20 km (green), and 30 km. Some events can't be included anymore if the maximum distance is limited further

To check for differences results of 2D Bayesian analysis the whole computation procedure was repeated and computed for the two distances mentioned above.

After a reduction to a maximum distance of 30 km, the resulting number of rain gauges considered was reduced to 452. At maximum distance of 20 km, there is further reduction to 431 stations, while at max. 10 km this number was further reduced to 405 stations. As visible in Figure 46 one station can be used for different DFs at different times.

Max. distance	Number of stations	Number of events
No limitation	452 (100 %)	2,034 (100 %)
30 km	436 (96.4 %)	862 (42.4 %)
20 km	431 (95.4 %)	769 (37.8 %)
10 km	405 (89.6 %)	541 (22.4 %)

Table 18: Overview of stations utilisable from the whole dataset *according to limiting the maximum distance of a station from the event.*

Subsequently, the relative differences were calculated for the following combinations: Bayesian analysis for max. 20 km distance and max 10 km distance; 30 km distance and 10 km distance; and nearest station irrespective of distance and 10 km. The relative deviation was calculated as follows:

Equation 11

$$deviation = \frac{Bayes_{Large} - Bayes_{Small}}{Bayes_{Large}}$$

With $Bayes_{Large}$ denoting probabilities based on the bigger distance and $Bayes_{Small}$ based on the smaller one.

All pairs show an increasing importance of high-intensity short-term rainfall when moving towards lower distances. As we can see in Figure 47 (comparing the difference between conditional probability of all nearest stations (irrespective of distance) versus stations, which are not farther than 10 km), the relative differences indicate generally a positive dependency of rainfall towards lower distances which means that DFs are more dependent of rainfall occurring nearer to site. However, it also shows higher positive deviations towards the upper left of the illustration, which means that for smaller distances, shorter and more intense precipitation gets more important. In other words: The reliability of estimates increases with shorter distance from the rain gauge to the event, but the availability of data decreases.

It has to be kept in mind, that the black dots represent the deviation in probability for the respective class and thus the interpolation sometimes leads to artefacts. In all three Figures we can see the influence of very long term rainfall too. In most cases these were TER with very long duration and one short, intense rainfall event leading to high precipitation intensity (y-axis).

To make data more visible, deviations of 100 % were removed for special cases. This can happen if there is data available for a DF in the larger-distance dataset but the DF was excluded in the smaller-distance dataset because of missing data which means zero (no observed DF for this duration/intensity class). These 100 %-values were replaced by NaN (not a number), because they are not defined in this context.

A priori NaN were also excluded. They occur, if there is no precipitation data available in the whole dataset for a specific combination of duration/intensity classes and are thus also excluded.

Additionally extreme singular results were taken out a posteriori to ensure correct grading (otherwise one extreme value would get a colour assignment, while the other ones are assigned to one pool). These out-takes are indicates separately next to the respective data point (black dot).

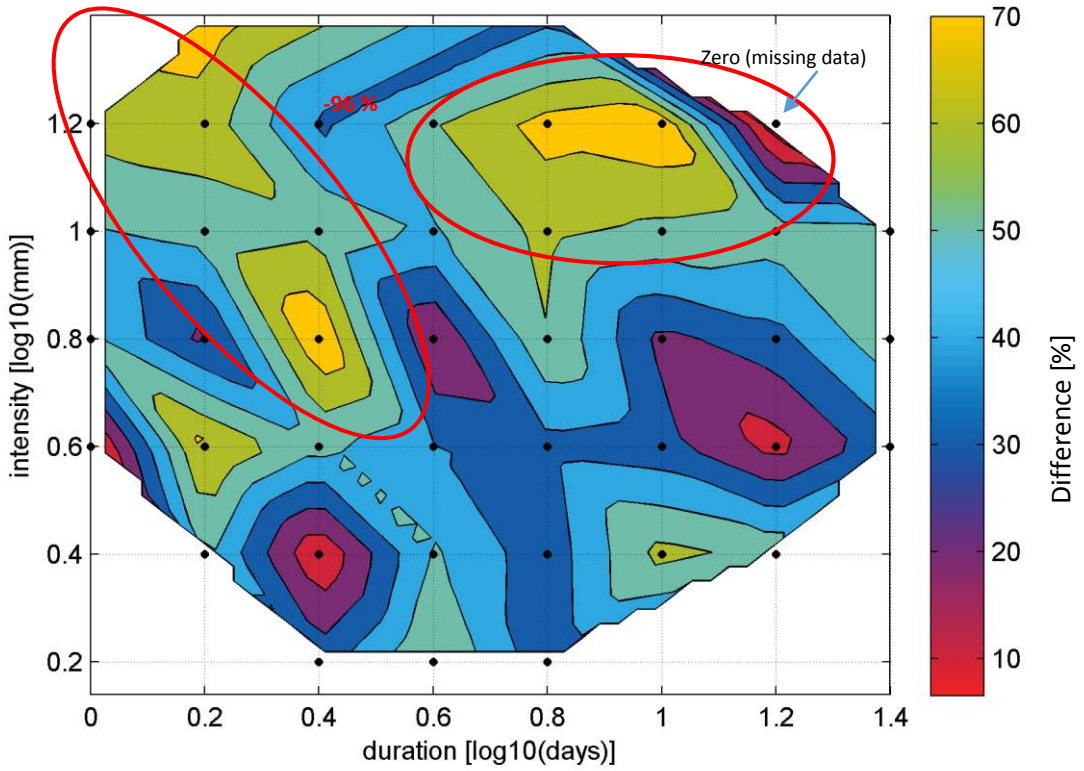

Figure 47: Difference between conditional probability of all nearest stations (irrespective of distance) versus stations, which are not farther than 10 km.

While Figure 47 does not show a clear overall clear pattern, it can be summarised, that all deviations are positive. This means that for each point the conditional probability of a DF occurring depends on duration and intensity increase with decreasing distance, i.e. an inverse relationship of rainfall parameters and probability.

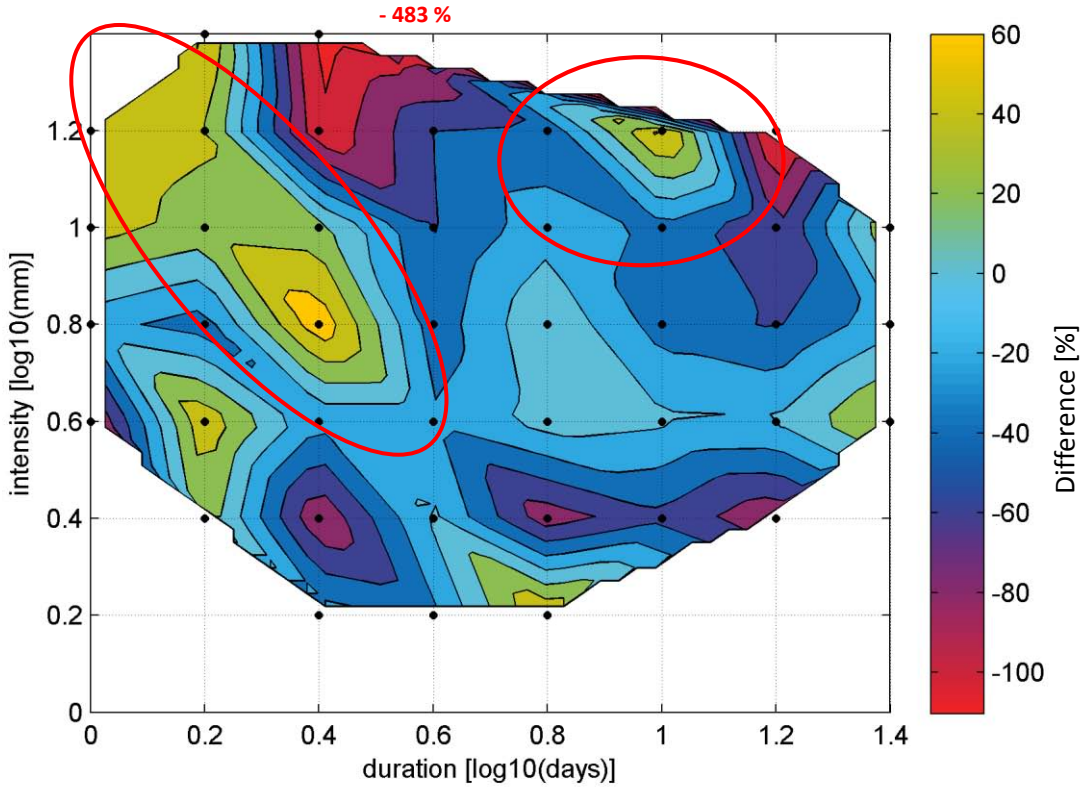

Figure 48: Relative difference of conditional probabilities between 30 km and 10 km.

Also Figure 48 shows a clear trend towards an increasing importance of increasing precipitation intensity and decreasing duration. There is still a prominent peak at a duration of 10 days and an intensity of 15 days, but an increasing separation between rainfall lasting several days and shorter-duration TER is clearly visible showing that there is an increasing importance of these two patterns, the nearer the precipitation gauge is from the actual event.

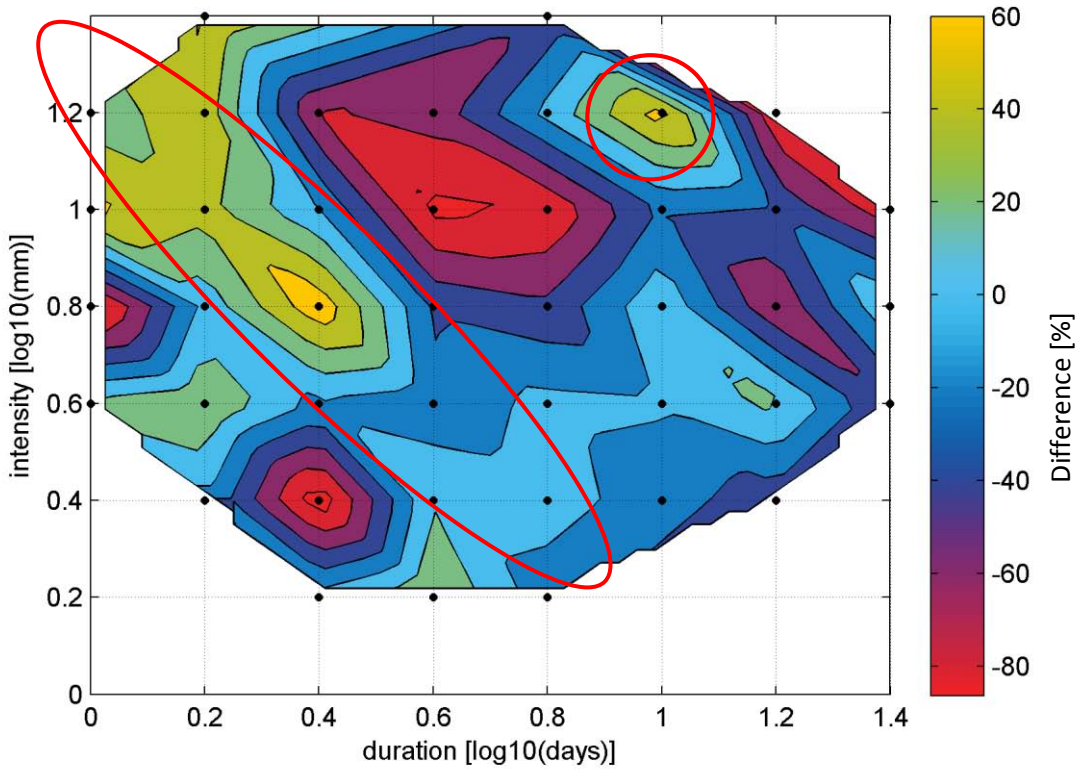

Figure 49: Relative differences between 20 km and 10 km.

Figure 49 shows the relative difference of conditional probability between precipitation data for stations which were at a maximum distance of 20 km and such which were not located at a greater distance than 10 km. This figure furthermore illustrates well the declining importance of long term rainfall (except for very long TER events of 10 days with an intensity of about 16 mm). Whereas for the long-term component there is only one class (duration [1,1.2], intensity [1,1.2]) supporting the assumption, this deviation is visible throughout all dataset indicating a pattern worth further investigation.

Basically, this sensitivity analysis shows that although including stations farther away is not wrong in particular, an increasing distance smoothens out noteworthy distinctive features, making it more difficult to assess the role of short-term TER

The main drawback in the presented analysis is, that temperature and precipitation data resolved only on a daily basis, which renders an analysis of the effects of short-term intensive precipitation impossible.

A further disadvantage is that there is no rule for the selection of triggering precipitation. That means that it is not possible to determine, whether TER was the main trigger of a DF or not. All DFs which showed an increase in cumulative precipitation were included in the analysis.

Another approach could be to exclude DFs with a TER below a certain threshold. This is only expected to make sense if there is higher-resolution precipitation data available. Otherwise it will certainly distort results even more.

The advantage of the presented approach is the possibility to visually assess DF probability and thus acquire valuable information for establishing new ID-thresholds. The contour plots of the differences in distance provide valuable information on how to evaluate rainfall data. In a next step, probabilities from DFs farther away from a precipitation gauge could be normalised to probabilities from closer DFs.

6 Discussion

The analysis shows that no distinct climatic shifts could be found for DF initiation mechanisms, although there are clear shifts evident for climatic parameters such as heavy rainfall and temperature extremes throughout the last 100 yrs. The ID-thresholds for 30-year periods since 1916 (in Chapter 5.2.2.), don't show changes in ID-thresholds. The occurrence of different event magnitudes does not change significantly, and only the amount of DF occurring on cool/wet days show a significant increase (Table 17) irrespectively of the season. It also is shown that 89 % of DFs used for analysis in Chapter 5.2.2. are occurring under a combination of extreme temperature/precipitation deciles.

Furthermore my results are in line with other research with respect to the frequency of occurrence of hydrological hazards (Mudelsee et al., 2003). The KDE showed one prominent peak, but no clear trend could be deduced from this. This particular peak in the 1960s can be attributed to over reporting in that decade. Although the Austrian torrent and avalanche control has provided the public with considerable hazard mitigation efforts before, a systematic approaches to inventorisation hand in hand with extensive protection efforts with respect to hydrologic and gravitational mass movements has not started before 1960. Interestingly this period of over reporting even overshadows the preeminent "years of hazard" in 1987 and 2009 (mainly ring-on-snow events after the "avalanche winter")

In particular my investigation shows two important aspects of precipitation: when combining intensity and duration with the Bayes theorem we can see that there is a pattern in nearly all investigations for very-short (assumed as convective) to short term (assumed as adjective) precipitation. While the short-term advective precipitation is expected to be well represented in the 2D-Bayesian Histograms, the convective part is not depicted due to the lack of data. Nevertheless there is a trend towards a strong convective effect represented well through the contour plots of relative deviations with regard to event-distance to the precipitation gauge. The long term component is also represented in all analyses as potential bias due to distance. It can be excluded, since the conditional probability increases with decreasing distance. This short-duration pattern is prominent up to 2.5 days. Conditional probability is high for very short events with very high intensities, whereas it can be lower for increasing durations (cf. Contour plots). There is a very distinctive peak for Bayesian analysis as well as for distance relationships for the duration class between about 2.5 and 4 days [0.4, 0.6] for higher precipitation, indicating that this duration-intensity class was rather frequently triggering hazards in our dataset.

The second noteworthy feature is very long precipitation lasting roughly between 6.3 and 20 days [1.0, 1.4]. Here the highest probability is already evident at about 16mm [1.4], but there were also events being triggered at lower intensities for this duration.

Answering our first research question we can tell that significant seasonal shifts could not be found for DFs, which could be affected by data thinning. Nevertheless it was possible to assess the evolution and the occurrence rates of DFs for the last 100 yrs.

Answering the second research question it can be stated that there are clear seasonal shifts in precipitation and temperatures whereas the distinction between convective and adjective cannot be made due to temporal resolution issues. Our analysis furthermore shows that it is possible to determine clear conditional probabilities for different precipitation-intensity classes, as well as to quantify frequencies and ID-thresholds, although in a very general way.

The 2D-Bayes-aproach and the contour plots are an ideal way to quantitatively describe the relationship between magnitude, frequency and probability, while seasonality didn't have a significant effect. When comparing the overall results with data from Guzzetti (2008), Aleotti (2004) and the Deucalion project (n.d., n.d.) it is possible to make a comparison, which is shown in Figure 50.

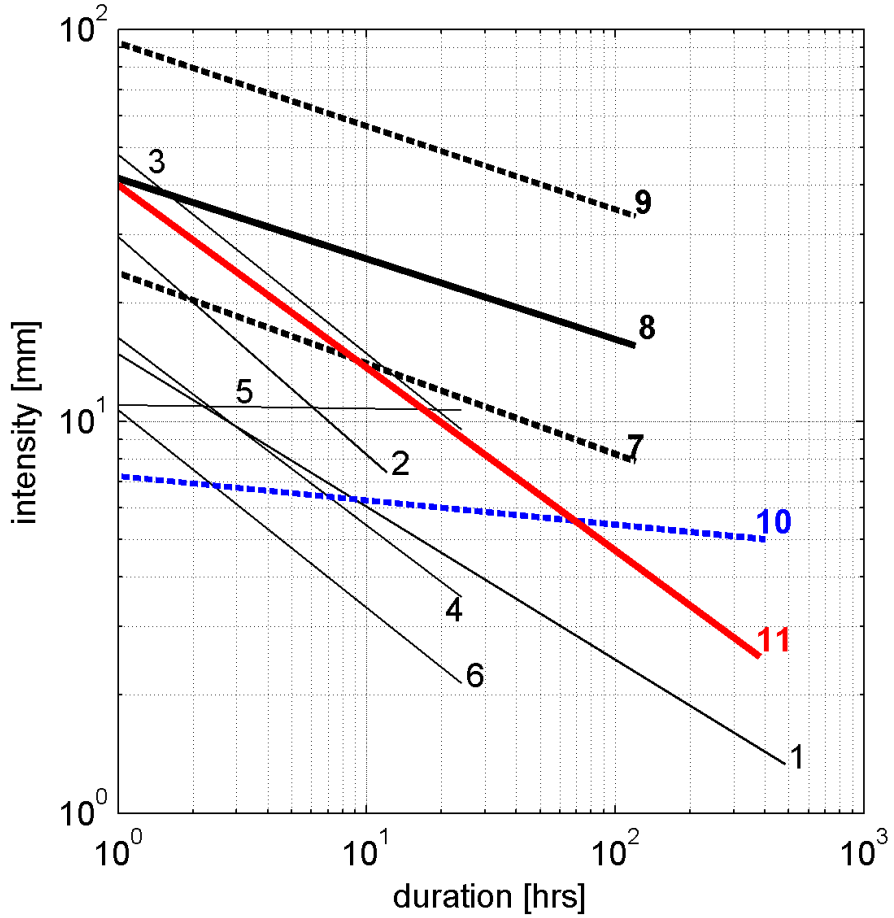

Figure 50: Comparison of selected ID-tresholds for DFs from other studies: 1. Caine (1980)*, 2. Jibson (1989), 3. Paronuzzi et al. (1998), 4. to 6. Bolley and Olliaro (1999); 1. to 6 are cited in Guzzetti (2007b), 7. to 9. Deucalion project (bold lines; with dashed upper being max. threshold, dashed lower min. threshold, bold drawn-through line mean threshold), 10. extrapolated ID-threshold from Chapter 5.1.1, 11. extrapolated ID-threshold from Bayesian analysis (Figure 45 under consideration of ID-plots for magnitude stated in the Appendix)*

From the non-standardised data analysed in Chapter 5.1.1., the ID-thresholds are rather low which I assume is due to the large data-set at hand, where the nearest stations of some DFs didn't measure significant amounts of precipitation before DF initiation. This can occur either through missing data from the precipitation gauge, where the cumulative sum of precipitation does not increase significantly. Another possibility is that some nearest-neighbour gauges are more than 30 km away and thus include the possibility of distortion of precipitation data. Bearing these effects in mind the analysis points to the influence of convective, strongly localised precipitation (visible e.g. in the ID-threshold curves in the *Results* section). When analysing ID-data from Bayesian analysis this problem can be partly visually accounted for through looking at Bayesian DF probabilities. Here it was tried to consider also extreme and large hazards which then results in a steeper ID-threshold, because large DFs are tried to be included into the threshold.

When extrapolated, the red line in Figure 50 is in accordance with Deucalion data for short-term TER, while the long-term TER is considerably lower because of a stronger inclusion of extreme DFs. The author thinks that this is a viable ways to adequately account for DF initiation, alleviating the problem of a quantile-approach, where short-term thresholds would be too low and long-term thresholds wouldn't account for extreme hazards.

While the probabilities presented in the Bayesian analysis seem very small, it has to be considered that the number of potential TERs was very high, while the sample data-set was rather small. This shows that while rainfall is quite well represented, the whole sample of debris flows seems vastly underrepresented.

The author is aware that this work omits several aspects of this topic, but hopes to make a contribution to an overall picture for CC impacts on DF processes. When such subsequent studies would be extended to all relevant types of gravitational mass movements it can provide valuable insights to the effects of CC on such type of hazard.

7 Conclusion

Temporal resolution

Although the results show first interesting trends in how DFs are initiated; they also show some limitations which were discovered using Bayesian analysis. All results indicate that there is a short-term component missing when analysing rainfall events. This component is lost, because the highest available resolution for the whole dataset was one day.

To account for this component sub daily resolutions are needed, which could be derived by e.g. using ultra high resolution radar datasets of up to 15 min. With complementing the current dataset by this component it would be possible to downscale all available precipitation patterns and to create subduing Bayesian classes. However, this would result in another problem: Ultra-high resolution data for Austria are only available since 2002 which would render analysis of climatic shifts completely impossible.

In this case, there are two further possibilities: either trying to project shifts on a daily scale at a minimum onto shorter durations with theoretical methods or empirical approaches from studies already made or to use downscaled GCM-data to utilise projections for possible future shifts which was also part of core research throughout the project Deucalion (Kaitna et al., n.d., n.d.).

Spatial resolution

A difficulty adding to the uncertainties induced by temporal resolution is the vastly discussed heterogeneity of precipitation throughout Austria, which introduces distortions and biases when going towards a whole-country approach. Here the solution could be to define homogenous precipitation regions – an approach which has been already carried out by Matulla et al. (2003) – from the meteorological perspective. Even without temporal downscaling this would lead to clearer results, where regionally validated ID-curves could be aggregated to a curve for the whole country. Additionally this would provide the advantage of being able to see the impact of topographic differences on such an approach.

Generally spoken, this study provides a methodological toolbox and a rough estimate for a rather big and diverse area. To better assess rainfall effects on DFs, but still be able to conduct investigations in a quantitatively viable way, an important step for future work is to define regions of homogenous precipitation. Since it is probable that very-short, high-intensity rainfall events are neglected in the study at hand, it is advisable to conduct downscaling experiments with recent data and use the information gathered to perform precipitation downscaling for all the historical daily precipitation data

at hand similar to other smaller-scale studies (e.g. Jomelli et al., 2009). Robust and suitable methods have been developed and tested during the last years to address this issue (Beuchat et al., 2011).

The conducted investigation of precipitation threshold provides a fundament for a more thorough investigation. As van Asch (after Crozier, 2010) has concluded, interpretations with regard to a shift in landslide occurrence has to be carried out for the same type of landslide material within the same geomorphological framework. It is difficult to use overall frequency data to reconstruct CC effect in the past. This is also true for the assessment of future shifts, especially for DFs.

Implications for DFs in a changing climate

Already previous studies have tried to assess the likelihood of DF occurrence for future CC (Belaya, 2003; Dehn and Buma, 1999; Schmidt and Glade, 2003). These studies all have in common that they illustrate the uncertainty associated with predictions by using secondary models which derive information from climate models. Nevertheless they provide scientifically a first hint of what could happen in the future. As mentioned above, CC will cause different responses with regard to the surface and subsurface hydrology of catchments in the temporal as well as in the spatial domain. From my study I can derive that there are influences mainly by rainfall intensity, but also interactions with TER and antecedent conditions. This means that further investigations about the future climate will have to take into account possible shifts, but also uncertainties for each variable of interest.

This means that future investigations of climatic effects on DF activity any shifts of TER are needed to be taken into account, as well as variations in storm frequency and variations in storm intensity. Another important task is to relate general catchment information to the EDB to investigate relationships of TER with respect to geological conditions, catchment size, catchment morphology and other parameters.

As a summary for the whole thesis the table below discusses obtained results in comparison to the research questions stated in a kind of check list.

No.	Question	Description	Answered
1	How did the temporal occurrence of DFs evolve in Austria?	KDE shows that there are no significant shifts for DF in the last 100 years except a peak in the 1960s which is likely due to over reporting	Yes, there is a hint of a downward trend in from 1980, but data from 2008-2014 would be needed to substantiate an assumed downward trend
1a	Are there seasonal shifts occurring in events triggered?	Our extensive analysis showed no seasonal, shifts over time. There are uncertainties regarding the DF inventory, short-term precipitation and rain-on-snow events (not investigated)	Yes
1b	Is it possible to assess the development of occurrence rates and magnitudes for the last 100 years?	Yes, but there is no significant pattern for occurrence rates and magnitudes. However, the analysis sheds more light on magnitude-frequency relationships	Yes, but other potential parameters which could affect the occurrence of DF of a certain magnitude should be investigated. Magnitude classes are too general for thorough assessment
2	What can the examination of rainfall data tell us with regard to triggering mechanisms of DFs?	Rainfall intensity and duration have the biggest influence on conditional probability. Also the cumulated sum of a TER and antecedent rainfall play a role	Yes. An investigation on rain-on-snow events is necessary to reduce uncertainties
2a	What is the percentage of events triggered by precipitation?	The current approach is not suitable to analyse DF which are not triggered by precipitation. This could have led to "false positives" (very low precipitation is attributed to rainfall induced triggering)	No. It is difficult to approach this task with current analysis. It would be necessary to define how much TER is attributed to "rainfall induced"
2b	Can seasonal shifts be determined with regard to this systems?	No	Yes. With current data and literature seasonal shifts are likely not to be the primary driver for changes in DF occurrence. It is very likely that they can be a secondary driver
2c	Which patterns exist between magnitude, frequency, triggering precipitation and seasonality over time?	The rather complex results for this questions are described in the results section and partly illustrated in *Appendix 1*	Yes, partly (analysis in 30-year intervals)

Table 19: Overview of research questions dealt with in the thesis.

Table 19 summarises information to what extent it is possible to answer the research questions with all the available data, which could be acquired for the investigation of potential climatic effects on hydrometeorological triggers of DFs.

An important next step would be to conduct more pilot studies for selected areas to have control catchments, where every occurring DF can be registered (ideally with high resolution precipitation data and additional parameters). When focusing on a smaller temporal and spatial window with well-observed parameters more robust estimates for Bayesian probability can be made. Several catchments representative for designated climatic and geomorphologic regions would give valuable insights on how future debris flows can possibly change under a changing climate.

Literature

Aleotti, P., 2004. A warning system for rainfall-induced shallow failures. Eng. Geol. 73, 247–265.

Ambaum, M., Hoskins, B., Stephenson, D., 2001. Arctic oscillation or North Atlantic oscillation? J. Clim. 14, 3495–3507.

Andrecs, P., Hagen, K., 2010. Analyse der Sicherheit und Genauigkeit von Bemessungswerten bei gravitativen alpinen Naturgefahren und Ableitung von Anpassungsstrategien an den Klimawandel. Endbericht des BFW im Auftrag des BMLFUW. Wien.

APCC, 2014. Österreichischer Sachstandsbericht Klimawandel 2014. Verlag der Österreichischen Akademie der Wissenschaften, Vienna.

Arctic Monitoring and Assessment Programm (AMAP), 2011. Snow, Water, Ice and Permafrost in the Arctic (SWIPA): Climate Change and the Cryosphere. Arctic Monitoring and Assessment Programme (AMAP), Oslo.

Aulitzky, H., 1980. Preliminary two-fold classification of torrents. In: Internationales Symposion Interpraevent. Bad Ischl, September 8-12. pp. 285–309.

Bardou, E., Delaloye, R., 2004. Effects of ground freezing and snow avalanche deposits on debris flows in alpine environments. Nat. Hazards Earth Syst. Sci. 4, 519–530.

Bardou, E., Niggli, M., Musy, A., 2003. The Role of Snow in the Generation of Debris Flow in small Watersheds of European Alps. In: EGS - AGU - EUG Joint Assembly, Abstracts from the Meeting Held in Nice, France, 6-11 April 2003. p. s.p.

Barry, R.G., 2008. Mountain Weather and Climate. Cambridge Univ. Press, New York.

Bates, B., Kundzewicz, Z., Wi, S., Palutikof, J., 2008. Climate change and water. IPCC Technical Paper VI.

Belaya, N., 2003. Distribution model for periods of debris-flow danger. In: Rickenmann, D., Chen, C.-L. (Eds.), Debris-Flow Hazards Mitigation: Mechanics, Prediction, and Assessment: Proceedings of the 3rd International Conference, Davos, Switzerland, September 10-12. Millpress, Rotterdam, pp. 59–70.

Beniston, M., 2007. Entering into the “greenhouse century”: Recent record temperatures in Switzerland are comparable to the upper temperature quantiles in a greenhouse climate. Geophys. Res. Lett. 34, 1–5.

Beniston, M., Goyette, S., 2007. Changes in variability and persistence of climate in Switzerland: Exploring 20th century observations and 21st century simulations. Glob. Planet. Change 57, 1–20.

Bergmeister, K., Suda, J., Hübl, J., Rudolf-Miklau, F., 2009. Schutzbauwerke gegen Wildbachgefahren. Ernst & Sohn, Berlin.

Berti, M., Martina, M.L. V., Franceschini, S., Pignone, S., Simoni, a., Pizziolo, M., 2012. Probabilistic rainfall thresholds for landslide occurrence using a Bayesian approach. J. Geophys. Res. 117, F04006.

Bertrand, M., Liébault, F., Piégay, H., 2013. Debris-flow susceptibility of upland catchments. Nat. Hazards 67, 497–511.

Beuchat, X., Schaefli, B., Soutter, M., Mermoud, a., 2011. Toward a robust method for subdaily rainfall downscaling from daily data. Water Resour. Res. 47, 1–18.

Blodgett, J., Poeschel, K., Osterkamp, W., 1996. Characteristics of debris flows of noneruptive origin on Mount Shasta, northern California. USGS Open-File Report.

Böhm, R., 2012. Changes of regional climate variability in central Europe during the past 250 years. Eur. Phys. J. Plus 127, 54.

Böhm, R., Jones, P.D., Hiebl, J., Frank, D., Brunetti, M., Maugeri, M., 2009. The early instrumental warm-bias: a solution for long central European temperature series 1760–2007. Clim. Change 101, 41–67.

Bollschweiler, M., Stoffel, M., 2010. Changes and trends in debris-flow frequency since AD 1850: Results from the Swiss Alps. The Holocene 20, 907–916.

Bras, R., 1990. Hydrology. An introduction to hydrologic science. Addison-Wesley, Reading, MA.

Bronstert, A., Niehoff, D., Bürger, G., 2002. Effects of climate and land-use change on storm runoff generation: present knowledge and modelling capabilities. Hydrol. Process. 16, 509–529.

Caine, N., 1980. The rainfall intensity-duration control of shallow land- slides and debris flows. Geogr. Ann. Ser. A, Phys. Geogr. 62, 23–27.

Campbell, R., 1974. Debris flow originating from soil slip during rainstorm in southern California. Q. J. Eng. Geol. Hydrogeol. 7, 339–349.

Campbell, R., 1975. Soil slips, debris flows, and rainstorms in the santa monica mountains and vicinity, southern california. USGS Prof. Pap. 851, 1–51.

Carson, R., 2002. Take the a-frame: debris flow during 1996 rain-on-snow event, Blue Mountains. In: Proceedings of the Geological Society of America Cordilleran Section 98th Annual Meeting, May 13-15. p. Abstract.

Coppola, D., 2011. Introduction to international disaster management, 2nd ed. Elsevier, Burlington.

Costa, J., 1984. Physical Geomorphology of Debris Flows. In: Costa, J., Fleisher, P. (Eds.), Developments and Applications of Geomorpholofy. Springer, Berlin, Heidelberg, p. 374.

CRED, 2009. EM-DAT. The International Disaster Database [WWW Document]. URL http://www.emdat.be/ (accessed 6.3.14).

Crosta, G., 1998. Regionalization of rainfall thresholds: an aid to landslide hazard evaluation. Environ. Geol. 35, 131–145.

Crozier, M.J., 2010. Deciphering the effect of climate change on landslide activity: A review. Geomorphology 124, 260–267.

Crozier, M.J., Glade, T., 1999. Frequency and magnitude of landsliding: Fundamental research issues. Zeitschrift für Geomorphol. Neue Folge 15, 141–155.

D'Agostino, V., Cerato, M., Coali, R., 1996. Sediment transport of extreme events in torrents of eastern Trentino. In: Int. Symp. Interpraevent, Villach, Austria, Vol. 2. pp. 377–386.

D'Agostino, V., Marchi, L., 2001. Debris flow magnitude in the Eastern Italian Alps: data collection and analysis. Phys. Chem. Earth - Part C 26, 657–663.

Davies, A., Fearn, T., 2006. Back to basics: calibration statistics. Spectrosc. Eur. 18, 31–32.

De Blasio, F.V., 2011. Introduction to the Physics of Landslides. Lecture Notes on the Dynamics of Mass Wasting. Springer, Dordrecht, Heidelberg.

De Perez, E.C., Monasso, F., van Aalst, M., Suarez, P., 2014. Science to prevent disasters. Nat. Geosci. 7, 78–79.

Dehn, M., Buma, J., 1999. Modelling future landslide activity based on general circulation models. Geomorphology 30, 175–187.

Deser, C., 2000. On the teleconnectivity of the "Arctic Oscillation". Geophys. Res. Lett. 27, 779–782.

DIS-ALP, 2007. Disaster Information System of Alpine Regions. DIS-ALP Report.

Dobler, C., Stötter, J., Schöberl, F., 2010. Assessment of climate change impacts on the hydrology of the Lech Valley in northern Alps. J. Water Clim. Chang. 1, 207.

Dramis, F., Govi, M., Guglielmin, M., Mortara, G., 1995. Mountain permafrost and slope instability in the Italian Alps: The Val Pola Landslide. Permafr. Periglac. Process. 6, 73–81.

Eckhart, T., 2012. Estimation of climate change impact on the runoff from a small alpine watershed in Austria. Univ. of Nat.l Res. and Life Sci.

EEA, 2012. Climate change, impacts and vulnerability in Europe 2012.

Eisbacher, G., 1982. Mountain torrents and debris flows. Episodes 4, 12–17.

Embleton-Hamann, C., 2007. Geomorphological hazards in Austria. In: Kellerer-Pirklbauer, A., Keiler, M., Embleton-Hamann, C., Stötter, J. (Eds.), Geomorphology for the Future. Joint Meeting of the Commission on Geomorphology of the Austrian Geographical Society and the IAG Working Group on Geomorphology and Global Environmental Change. Obergurgl, Austria, September 2-7. Innsbruck Univ. Press, Innsbruck, pp. 33–56.

Fischer, L., Kääb, a., Huggel, C., Noetzli, J., 2006. Geology, glacier retreat and permafrost degradation as controlling factors of slope instabilities in a high-mountain rock wall: the Monte Rosa east face. Nat. Hazards Earth Syst. Sci. 6, 761–772.

Fuchs, S., Birkmann, J., Glade, T., 2012. Vulnerability assessment in natural hazard and risk analysis: current approaches and future challenges. Nat. Hazards.

Fuchs, S., Keiler, M., 2006. Natural hazard risk depending on the variability of damage potential. WIT Trans. Ecol. Environ. 91, 13–22.

Fuchs, S., Keiler, M., Sokratov, S., Shnyparkov, A., 2013. Spatiotemporal dynamics: the need for an innovative approach in mountain hazard risk management. Nat. Hazards 68, 1217–1241.

Glade, T., 2005. Linking debris-flow hazard assessments with geomorphology. Geomorphology 66, 189–213.

Gobiet, A., Kotlarski, S., Beniston, M., Heinrich, G., Rajczak, J., Stoffel, M., 2013. 21st century climate change in the European Alps-A review. Sci. Total Environ.

Groppelli, B., Bocchiola, D., Rosso, R., 2011a. Spatial downscaling of precipitation from GCMs for climate change projections using random cascades: A case study in Italy. Water Resour. Res. 47, 1–18.

Groppelli, B., Soncini, a., Bocchiola, D., Rosso, R., 2011b. Evaluation of future hydrological cycle under climate change scenarios in a mesoscale Alpine watershed of Italy. Nat. Hazards Earth Syst. Sci. 11, 1769–1785.

Guha-Sapir, D., Vos, F., Below, R., Ponserre, S., 2011. Annual Disaster Statistical Review 2010. The Numbers and Trends. Brussels.

Guzzetti, F., Peruccacci, S., Rossi, M., Stark, C.P., 2007. Rainfall thresholds for the initiation of landslides in central and southern Europe. Meteorol. Atmos. Phys. 98, 239–267.

Guzzetti, F., Peruccacci, S., Rossi, M., Stark, C.P., 2008. The rainfall intensity–duration control of shallow landslides and debris flows: an update. Landslides 5, 3–17.

Haeberli, W., 1983. Frequency and characteristics of glacier floods in the Swiss Alps. Ann. Glaciol. 4, 85–90.

Haeberli, W., 1992. Construction, environmental problems and natural hazards in periglacial mountain belts. Permafr. Periglac. Process. 3, 111–124.

Hampel, R., 1977. Geschiebewirtschaft in Wildbächen. Wildbach- und Lawinenverbau 41, 3–34.

Harris, R., Lisle, T., Ziemer, R., 1997. Aftermath of the 1997 flow. In: USDA Forest Service Workshop, April 8-9. p. s.p.

Harris, S., Gustafson, C., 1993. Debris flow characteristics in an area of continuous permafrost, St. Elias Range, Yukon Territory. Zeitschrift für Geomorphol. Neue Folge 37, 41–56.

Horová, I., Koláček, J., Zelinka, J., 2012. Kernel Smoothing in MATLAB: Theory and Practice of Kernel Smoothing. World Scientific, Singapore.

Horton, E., Folland, C., Parker, D., 2001. The changing incidence of extremes in worldwide and central England temperatures to the end of the twentieth century. Clim. Change 50, 267–295.

Horton, P., Schaefli, B., Mezghani, A., Hingray, B., Musy, A., 2006. Assessment of climate-change impacts on alpine discharge regimes with climate model uncertainty. Hydrol. Process. 20, 2091–2109.

Hübl, J., 2006. Vorläufige Erkenntnisse aus 1:1 Murenversuchen: Prozessverständnis und Belasungsannahmen. In: FFIG, Reiser, G. (Eds.), Geotechnik Und Naturgefahren: Balanceakt Zwischen Kostendruck Und Notwendigkeit,. Univ. of Nat. Res. and Life Sci., Wien.

Hübl, J., Fuchs, S., Sitter, F., Totschnig, R., 2011. Towards a frequency-magnitude relationship for torrent events in Austria. In: Genevois, R., Hamilton, D., Prestizini, A. (Eds.), 5th International Conference on Debris-Flow Hazards Mitigation: Mechanics, Prediction and Assessment. Univ. La Sapienza, pp. 895–902.

Hübl, J., Totschnig, R., Sitter, F., Mayer, B., Schneider, A., 2008. Historische Ereignisse - Band 2: Auswertung von Wildbach Schadereignissen in Westösterreich auf Grundlage der Wildbachaufnahmeblätter, IAN Report 111. Vienna.

Huggel, C., Clague, J.J., Korup, O., 2012. Is climate change responsible for changing landslide activity in high mountains? Earth Surf. Process. Landforms 37, 77–91.

Huggel, C., Kääb, a., Haeberli, W., Krummenacher, B., 2003. Regional-scale GIS-models for assessment of hazards from glacier lake outbursts: evaluation and application in the Swiss Alps. Nat. Hazards Earth Syst. Sci. 3, 647–662.

Huggel, C., Kääb, A., Haeberli, W., Teysseire, P., Paul, F., 2002. Remote sensing based assessment of hazards from glacier lake outbursts: a case study in the Swiss Alps. Can. Geotech. J. 39, 316–330.

Huggel, C., Salzmann, N., Allen, S., 2013. High-mountain slope failures and recent and future warm extreme events. In: McGuire, B., Maslin, M. (Eds.), Climate Forcing of Geological Hazards. Wiley-Blackwell, Chichester, p. 323.

Hungr, O., Evans, S., Bovis, M., Hutchinson, N., 2001. A review of the classification of landslides of the flow type. Environ. Eng. Geosci. 7, 221–238.

Hungr, O., McDougall, S., Bovis, B., 2005. Entrainment of material by debris flows. In: Jakob, M., Hungr, O. (Eds.), Debris Flow Hazard and Related Phenomena. Springer, Heidelberg, Berlin, pp. 135–158.

IPCC, 2007. Climate Change 2007: The Physical Science Basis. Contribution of Working group I to the Fourth Assessment Report of the Intergovernmental Panel on Climate Change. Cambridge, Cambridge.

IPCC, 2013. Climate Change 2013: The Physical Science Basis. Contribution of Working Group I to the Fifth Assessment Report of the Intergovernmental Panel on Climate Change. Cambridge Univ. Press, Cambridge.

IPCC, 2014. Climate Change 2014: Impacts, Adaptation, and Vulnerability. Contribution of Working Group II to the Fifth Assessment Report of the Intergovernmental Panel on Climate Change. Cambridge Univ. Press, Cambridge.

Jomelli, V., Brunstein, D., Déqué, M., Vrac, M., Grancher, D., 2009. Impacts of future climatic change (2070–2099) on the potential occurrence of debris flows: a case study in the Massif des Ecrins (French Alps). Clim. Change 97, 171–191.

Jones, J. a., Swanson, F.J., Wemple, B.C., Snyder, K.U., 2000. Effects of Roads on Hydrology, Geomorphology, and Disturbance Patches in Stream Networks. Conserv. Biol. 14, 76–85.

Jones, P., Horton, E., Folland, C., Hulme, M., Parker, D., Basnett, T., 1999. The use of indices to identify changes in climatic extremes. Clim. Change 42, 131–149.

Kaitna, R., Hübl, J., 2013. Silent witnesses for torrential processes. In: Schneuwly-Bollschweiler, M., Stoffel, M. (Eds.), Dating Torrential Processes on Fans and Cones. Methods and Their Application for Hazard and Risk Assessment. Springer, Dordrecht, pp. 111–130.

Kaitna, R., Stoffel, M., Gobiet, A., Sinabell, F., n.d.*a.* Klimawandel und Muren - Das Projekt Deucalion. Zeitschrift für Wildbach-, Lawinen-, Erosions- und Steinschlagschutz.

Kaitna, R., Stoffel, M., Gobiet, A., Sinabell, F., n.d.*b.* Abschätzung der Änderung der Murengefahr im Zuge des Klimawandels. Zeitschrift für Wildbach- und Lawinenverbauung.

Kappas, M., 2009. Klimatologie. Spektrum Akad. Verlag, Heidelberg.

Keiler, M., Knight, J., Harrison, S., 2010. Climate change and geomorphological hazards in the eastern European Alps. Philos. Trans. A. Math. Phys. Eng. Sci. 368, 2461–79.

Kellerer-Pirklbauer, A., Kaufmann, V., 2007. Paraglacial Talus Slope Instability in Recently Deglaciated Cirques (Schober Group, Austria). Grazer Schriften der Geogr. und Raumforsch. 43, 121–130.

Klein Tank, A., Können, G., 2003. Trends in indices of daily temperature and precipitation extremes in Europe, 1946–99. J. Clim. 16, 3665–3680.

Klose, B., 2008. Meteorologie. Eine inderdisziplinäre Einführung in die Physik der Atmosphäre. Springer, Heidelberg, Berlin.

Konagai, K., Johansson, J., Numada, M., 2007. Extracting Necessary Parameters from Real Landslide mass for Mitigating Landslide Disaster. In: Sassa, K., Fukuoka, H., Wang, F., Wang, G. (Eds.), Progress in Landslide Science. Springer, Berlin, Heidelberg, p. 376.

Korvanen, D., Slaymaker, O., 2008. The morphometric and stratigraphic framework for estimates of debris flow incidence in the North Cascades foothills, Washington State. Geomorphology 99, 224–245.

Krainer, K., 2007. Permafrost und Naturgefahren in Österreich. Ländlicher Raum 1–18.

Kronfellner-Kraus, G., 1984. Extreme Feststoffrachten und Grabenbildungen von Wildbächen (extreme sediment loads and erosion of torrents). In: Proc. Int. Symp. Interpraevent, Villach, Austria, Vol. 2. pp. 109–118.

Kronfellner-Kraus, G., 1987. Zur Anwendung der Schätzformel für extreme Wildbach-Feststofffrachten im Süden und Osten Österreichs. Wildbach- und Lawinenverbau 51, 187–200.

Kropp, J., Schellnhuber, H. (Eds.), 2011. In Extremis. Disruptive Events and Trends in Climate and Hydrology. Springer, Heidelberg, Berlin.

Liggins, F., Betts, R., McGuire, B., 2013. Projected future climate changes in the context of geological and geomorphological hazards. In: McGuire, B., Maslin, M. (Eds.), Climate Forcing of Geological Hazards. Wiley-Blackwell, Chichester, p. 323.

Lionello, P., Boldrin, U., Giorgi, F., 2008. Future changes in cyclone climatology over Europe as inferred from a regional climate simulation. Clim. Dyn. 30, 657–671.

Malamud, B.D., Turcotte, D.L., Guzzetti, F., Reichenbach, P., 2004. Landslide inventories and their statistical properties. Earth Surf. Process. Landforms 29, 687–711.

Mao, L., Cavalli, M., Comiti, F., Marchi, L., Lenzi, M., Arattano, M., 2009. Sediment transfer processes in two Alpine catchments of contrasting morphological settings. J. Hydrol. 1-2, 88–98.

Matulla, C., Penlap, E., Haas, P., Formayer, H., 2003. Detection of homogeneous precipitation regions in Austria during the 20th century.

Mazzorana, B., Comiti, F., Scherer, C., Fuchs, S., 2012. Developing consistent scenarios to assess flood hazards in mountain streams. J. Environ. Manage. 94, 112–24.

Melton, M., 1957. An Analysis of the Relation Among Elements of Climate, Surface Properties and Geomorphology. Office of Naval Research Project NR389-042, Technical Report 11. New York.

Montgomery, D., Dietrich, W., 1994. A physically-based model for the topographic control on shallow landsliding. Water Resour. Res. 30, 1153–1171.

Mudelsee, M., Börngen, M., Tetzlaff, G., Grünewald, U., 2003. No upward trends in the occurrence of extreme floods in central Europe. Nature 425, 166–9.

Nakamura, F., 2000. Disturbance regimes of stream and riparian systemsÐa disturbance cascade perspective. Hydrol. Process. 2860, 2849–2860.

Naylor, M., Greenhough, J., McCloskey, J., Bell, a. F., Main, I.G., 2009. Statistical evaluation of characteristic earthquakes in the frequency-magnitude distributions of Sumatra and other subduction zone regions. Geophys. Res. Lett. 36, L20303.

Nemec, J., Gruber, C., Chimani, B., Auer, I., 2013. Trends in extreme temperature indices in Austria based on a new homogenised dataset. Int. J. Climatol. 33, 1538–1550.

Phillips, J., 2003. Sources of nonlinearity and complexity in geomorphic systems. Prog. Phys. Geogr. 27, 1–23.

Rebetez, M., Lugon, R., Baeriswyl, P.-A., 1997. Climatic change and debris flows in high mountain regions: The case study of the ritigraben torrent (Swiss Alps). Clim. Change 36, 371–389.

Reichenbach, P., Cardinali, M., De Vita, P., Guzzetti, F., 1998. Regional hydrological thresholds for landslides and floods in the Tiber River Basin (central Italy). Environ. Geol. 35, 146–159.

Rickenmann, D., 1995. Beurteilung von Murgängen. Scbweizer Ing. und Archit. 48, 1104–1108.

Rickenmann, D., 1999. Empirical relationships for debris flows. Nat. hazards 19, 47–77.

Rickenmann, D., 2009. Channel processes (floods, sediment transport, debris flows). Lecture held by R. Kaitna at Univ. of Nat. Res. and Life Sci. Vienna.

Rickenmann, D., Zimmermann, N., 1993. The 1987 debris flows in Switzerland: Documentation and analysis. Geomorphology 8, 175–189.

Rodda, J., 1967. The rainfall measurement problem. In: Proceedings of the Bern Assembly of IAHS. pp. 215–231.

Sauer, P., Seifert, P., Wessely, G., Piller, W., Kleemann, E., Fodor, L., Hofmann, T., Mandl, G., Lobitzer, H., 1992. Guidebook to Excursions in the Vienna Basin and the adjacient Alpine-Carpathian thrustbelt in Austria. Mitteilungen der österreichischen Geogr. Gesellschaft 85, 1–264.

Schmidt, M., Glade, T., 2003. Linking global circulation model outputs to regional geomorphic models: A case study of landslide activity in New Zealand (Case studies from New Zealand). Clim. Res. 25, 135–150.

Sene, K., 2010. Hydrometeorology. Forecasting and Applications. Springer, Dordrecht.

Shimazaki, H., Shinomoto, S., 2010. Kernel bandwidth optimization in spike rate estimation. J. Comput. Neurosci. 29, 171–82.

Sillmann, J., Roeckner, E., 2007. Indices for extreme events in projections of anthropogenic climate change. Clim. Change 86, 83–104.

Sitter, F., 2010. Historische Ereignisdokumentation. Auswertung von Schadereignissen in Österreich auf Grundlage der Wildbach- und Lawinenaufnahmeblätter.

Slaymaker, O., 2010. Mountain Hazards. In: Alcántara-Ayala, I., Goudie, A. (Eds.), Geomorphological Hazards and Disaster Prevention. Cambridge Univ. Press, Cambridge, p. 291.

Steijn, H. van, 1996. Debris-flow magnitude—frequency relationships for mountainous regions of Central and Northwest Europe. Geomorphology 15, 259–273.

Stoffel, M., 2010. Magnitude–frequency relationships of debris flows — A case study based on field surveys and tree-ring records. Geomorphology 116, 67–76.

Stoffel, M., Bollschweiler, M., Beniston, M., 2011. Rainfall characteristics for periglacial debris flows in the Swiss Alps: past incidences–potential future evolutions. Clim. Change 105, 263–280.

Stoffel, M., Huggel, C., 2012. Effects of climate change on mass movements in mountain environments. Prog. Phys. Geogr. 36, 421–439.

Storch, H. Von, Zwiers, F.W., 1999. Statistical Analysis in Climate Research. Cambridge Univ. Press, Cambridge.

Tablebi, A., Nafarzadegan, A., Malekinezhad, H., 2010. A Review on Empirical and Physically Based Modelling of Rainfall Triggered Landslides. Phys. Geogr. Res. Quaterly 70, 8–10.

Takahashi, T., 2007. Progress in Debris Flow Modeling. In: Sassa, K., Fukuoka, H., Wang, F., Wang, G. (Eds.), Progress in Landslide Science. Springer, Berlin, Heidelberg, p. 376.

Takei, A., 1980. Interdependence of sediment budget between individual torrents and a river-system. In: Int. Symp. Interpraevent, Villach, Austria, Vol. 2. pp. 35–48.

Tebaldi, C., Mearns, L., Nychka, D., Smith, R., 2004. Regional probabilities of precipitation change: a Bayesian analysis of multimodel simulations. Geophys. Res. Lett. 31, L24213.

Tebaldi, C., Smith, R., Nychka, D., Mearns, L., 2005. Quantifying uncertainty in projections of regional climate change: a Bayesian approach to the analysis of multi-model ensembles. J. Clim. 18, 1524–1540.

Teegavarapu, R., 2012. Floods in a Changing Climate. Extreme Precipitation. Cambridge Univ. Press, Cambridge.

Terlien, M., 1998. The determination of statistical and determin- istic hydrological landslide-triggering thresholds. Environ. Geol. 2-3, 124–130.

The World Bank, 2005. Natural Disaster Hotspots. A Global Risk Analysis. The World Bank, Washington DC.

Trenberth, K., Dai, A., 2014. Global warming and changes in drought. Nat. Clim. Chang. 4, 3–8.

United Nations, 1992. Internationally agreed glossary of basic terms related to disaster management (DNA/93/36).

Weinmeister, H.W., 1994. Skriptum Wildbachkunde (lecture notes). Univ. of Nat. Res. and Life Sci. Vienna.

Wentz, F.J., Ricciardulli, L., Hilburn, K., Mears, C., 2007. How much more rain will global warming bring? Science 317, 233–5.

Whittow, J., 2000. Dictionary of Physical Geography, 2nd ed. Penguin, London.

Wieczorek, G., Glade, T., 2005. Climatic factors influencing occurrence of debris flows. In: Jakob, M., Hungr, O. (Eds.), Debris-Flow Hazards and Related Phenomena. Springer, Berlin, Heidelberg, p. 795.

Wilson, R., Wieczorek, G., 1995. Rainfall thresholds for the initiation of debris flow at La Honda, California. Environ. Eng. Geosci. 1, 11–27.

Zechmeister-Boltenstern, S., 2014. Ökosystemdynamik und ihre Austwirkung auf Treibhausgase. Lecture by S. Zechmeister-Boltenstern. Univ. of Nat. Res. and Life Sci. Vienna.

Zeller, J., 1985. Feststoffmessung in kleinen Gebirgseinzugsgebieten. Wasser, Energie, Luft 77, 246–251.

List of Figures

List of Tables

Acronyms and Abbreviations

1D	One-Dimensional, used for Bayesian analysis with one factor (resulting in two-dimensional graphs)
2D	Two-Dimensional, used for Bayesian analysis with two factors (resulting in either three-dimensional graphs or two-dimensional graphs with additional colour scaling)
AMAP	Arctic Monitoring and Assessment Programme
AO	Arctic Oscillation
BFW	Austrian Research Centre for Forests [Bundesforschungszentrum für Wald]
BMN	Austrian federal reporting network [Österreichisches Bundesmeldenetz], projection grid based on Mercator projection and divided in three strips: M28, M31, M34
CC	Climate Change
CGCM	Coupled Global Climate Model
CRED	Centre for Research on the Epidemiology of Disasters
CSV	Comma Separated Values
DF	debris flow
DIS-ALP	Disaster Information System of Alpine Regions
DJF	Winter Season (December, January, February)
EDB	Event-Database [Ereignisdatenbank] of IAN
EEA	European Environment Agency
eHYD	Hydrographic database of the Austrian Federal Ministry of Agriculture, Forestry and Water Management
EM-DAT	Emergency Events Database of CRED
ETRS89	European Terrestrial Reference System 1989, an Earth-centred, Earth-fixed geodetic Cartesian reference frame
GCM	General Circulation Model
GHG	Greenhouse Gases
GIS	Geographic Information System
GLOF	Glacier Lake Outburst Flow
hrs	hours
IAN	Institute of Mountain Risk Engineering [Institut für Alpine Naturgefahren], University of Natural Resources and Life Sciences, Vienna
iD	Identification (sequence number; identification code)
ID	Intensity-Duration
IPCC	Intergovernmental Panel on Climate Change
JJA	Summer season (June, July, August)
KDE	Kernel Density Estimation
LULUCF	Land Use, Land Use Change, and Forestry
MAM	Spring season (March, April, May)
MatLab	Matrix Laboratory (numerical computing environment)
min	minutes
minim	minimum
NaN	Not a Number, used for undefined or unrepresented values (Institute of Electrical and Electronics Engineers 754 standard)
NAO	North Atlantic Oscillation
RCM	Regional Climate Model
RMSEP	Root Mean Square Error of Prediction
SON	Autumn season (September, October, November)
TER	Triggering Event Rainfall
WLV	Austrian Service for Torrent and Avalanche Control [Wildbach und Lawinenverbauung]
WMO	World Meteorological Organization
ZAMG	Central Institution for Meteorology and Geodynamics

Appendix 1 – Evaluation of climatic parameters

Precipitation

Mean annual DJF precipitation

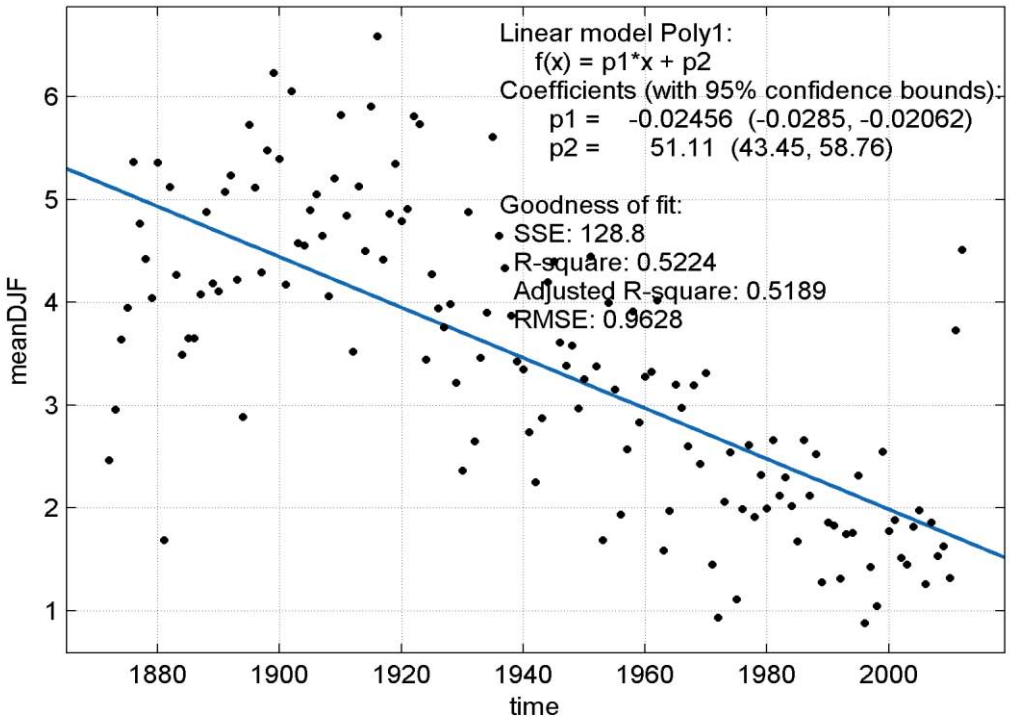

Mean annual MAM precipitation

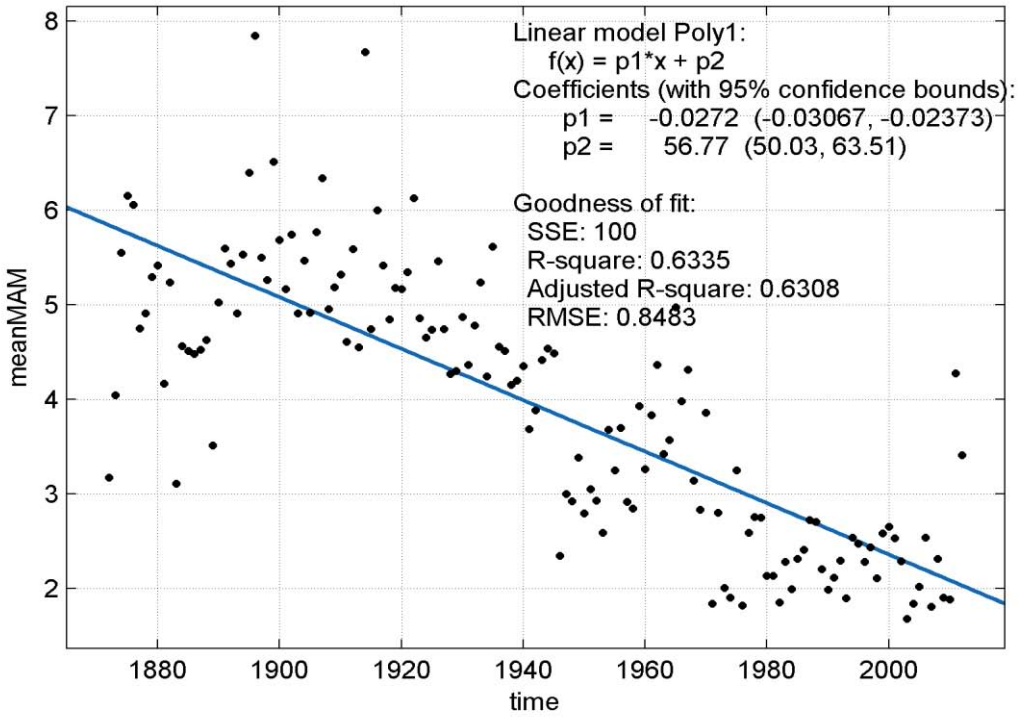

Mean annual JJA precipitation

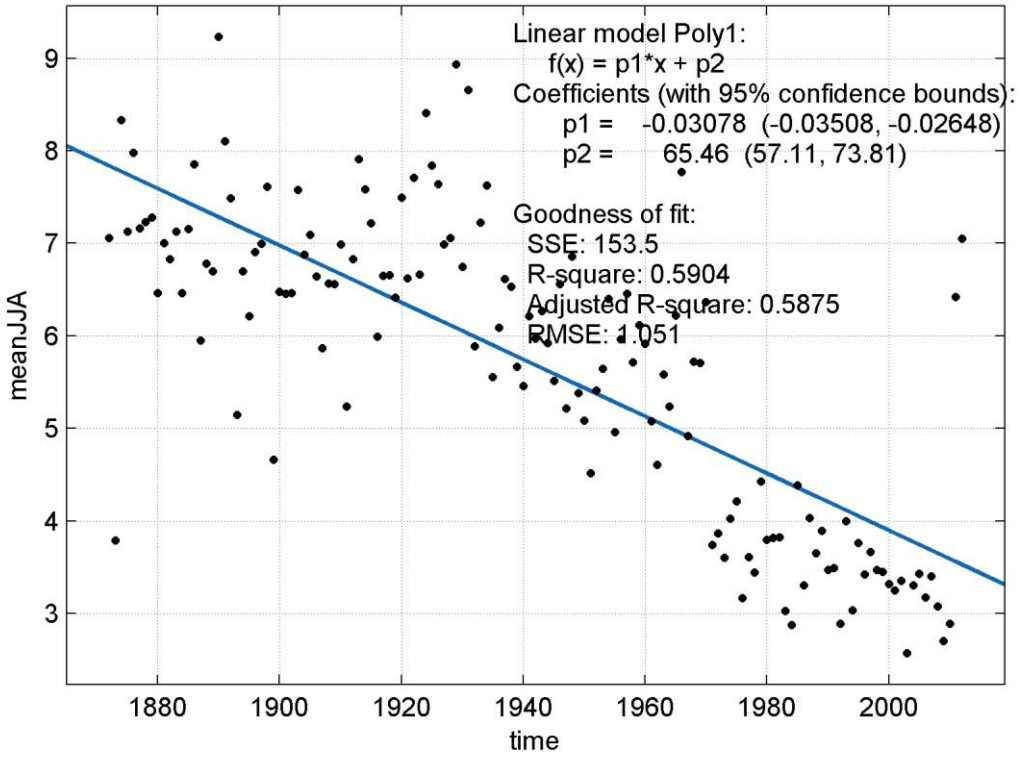

Mean annual SON precipitation

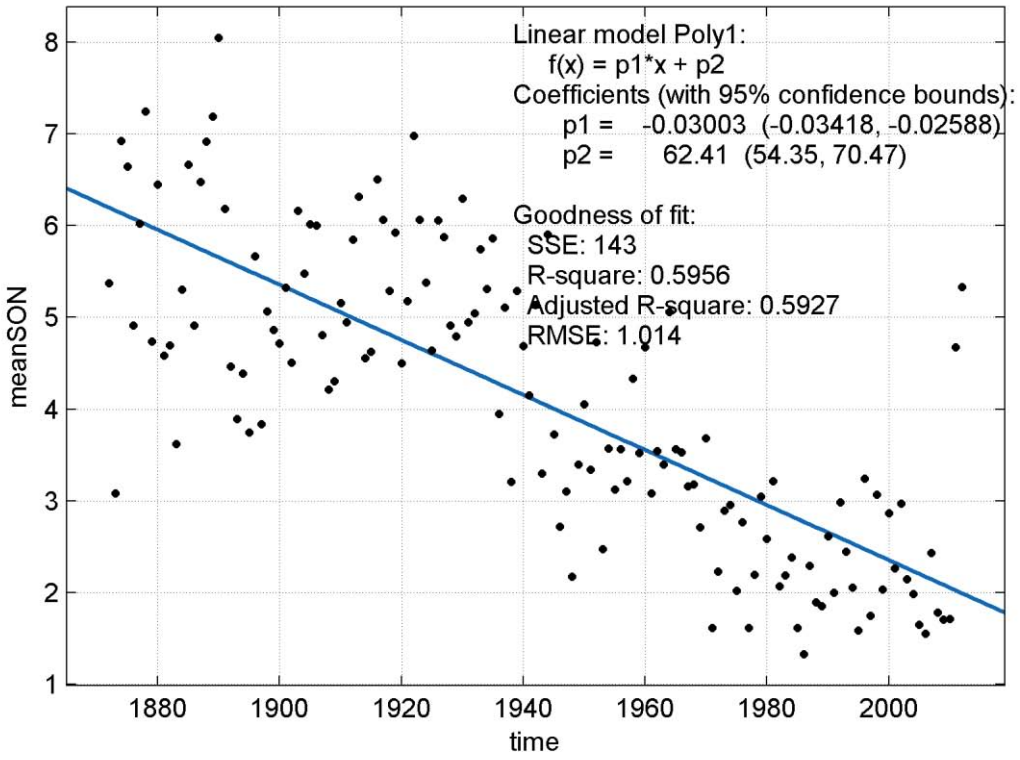

Maximum annual DJF precipitation

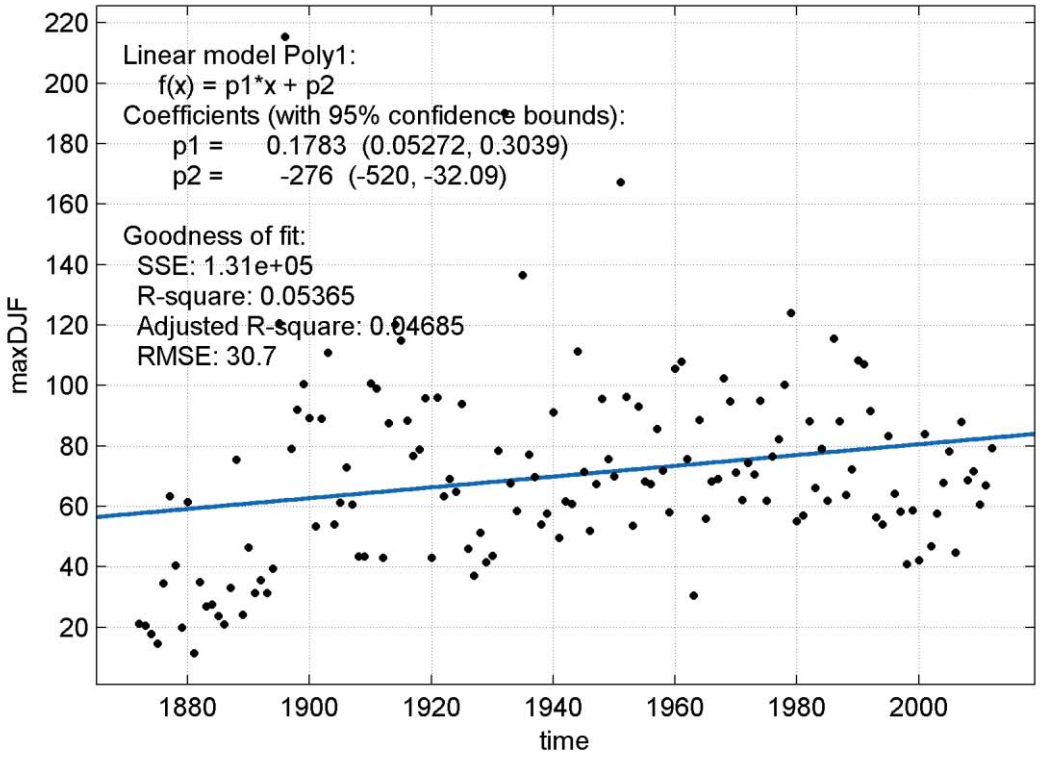

Maximum annual MAM precipitation

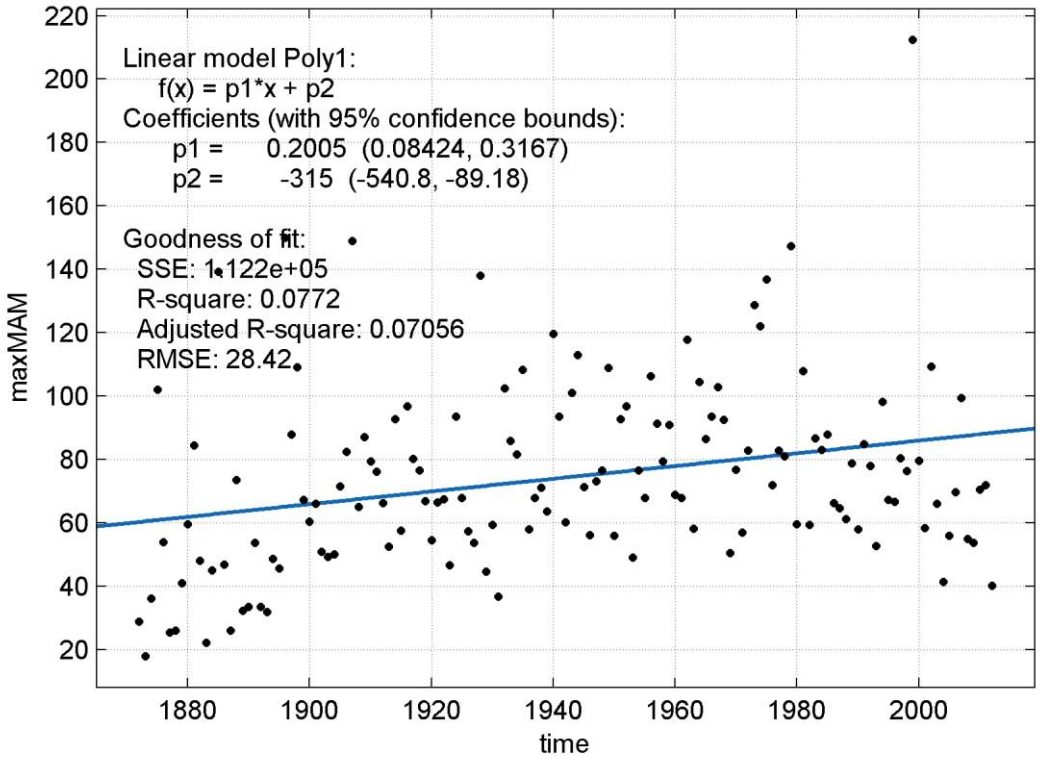

Maximum annual JJA precipitation

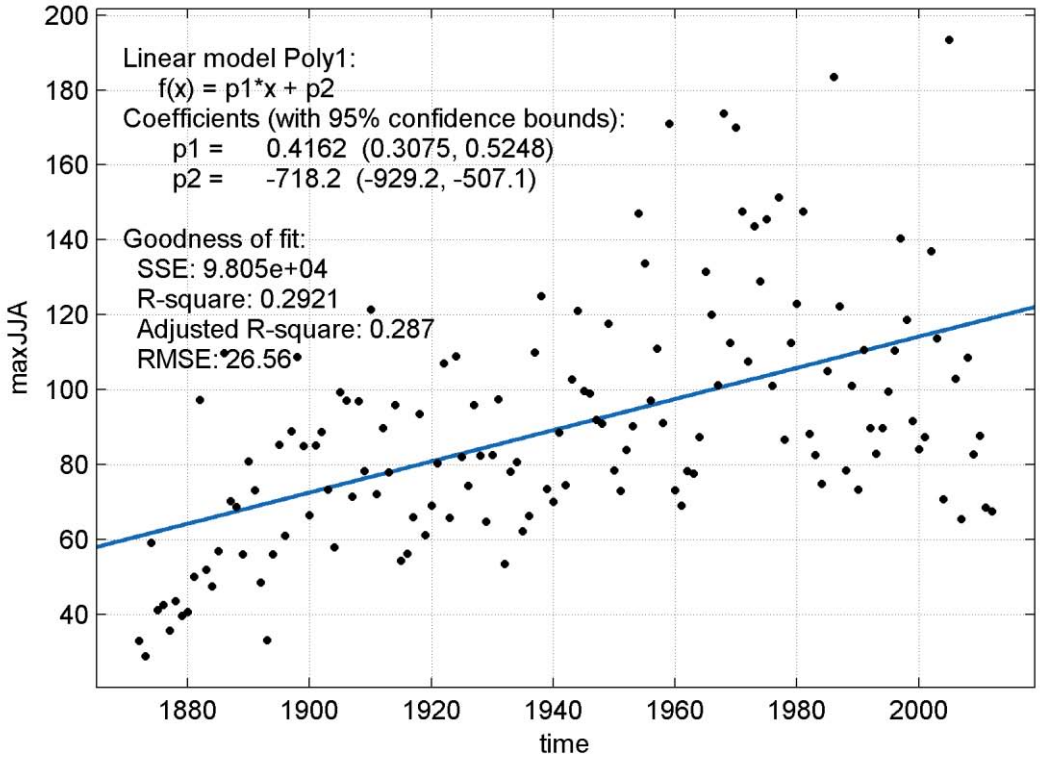

Maximum annual SON precipitation

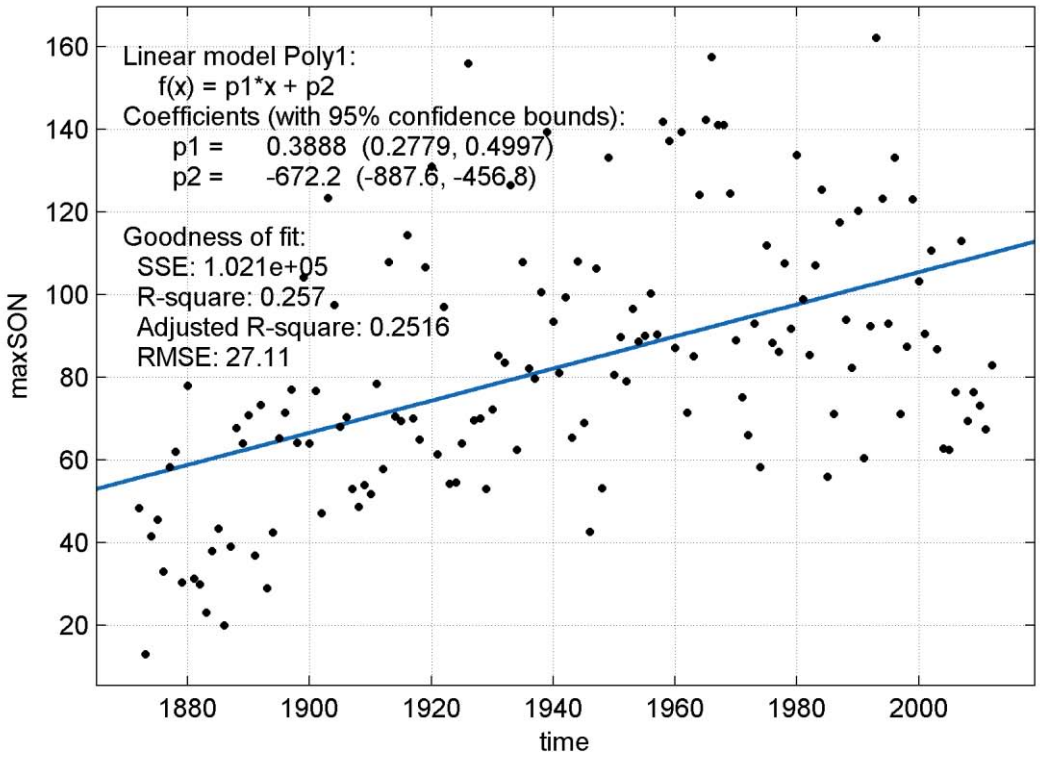

Temperature

Changes in DJF temperature from 1872 to 2012 (T_{max} and 95% quantiles)

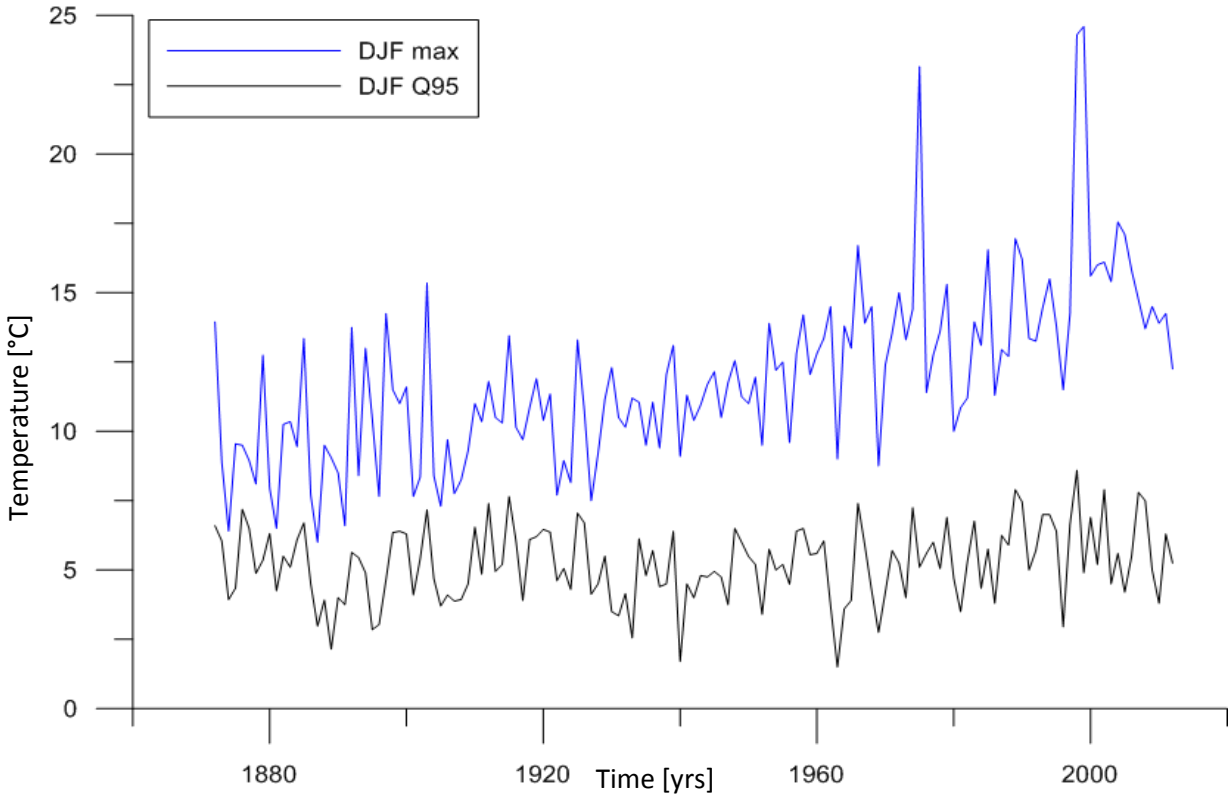

Changes in MAM temperature from 1872 to 2012 (T_{max} and 95% quantiles)

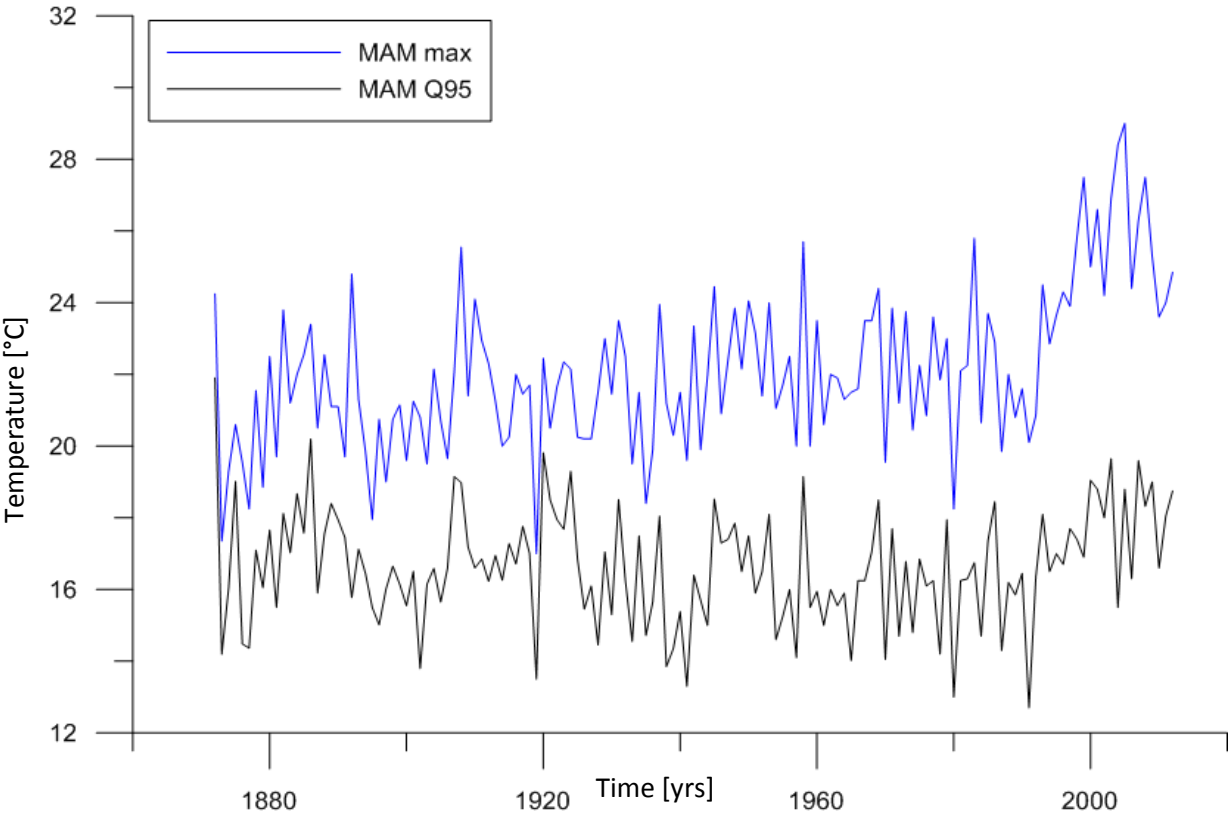

Changes in JJA temperature from 1872 to 2012 (T_{max} and 95% quantiles)

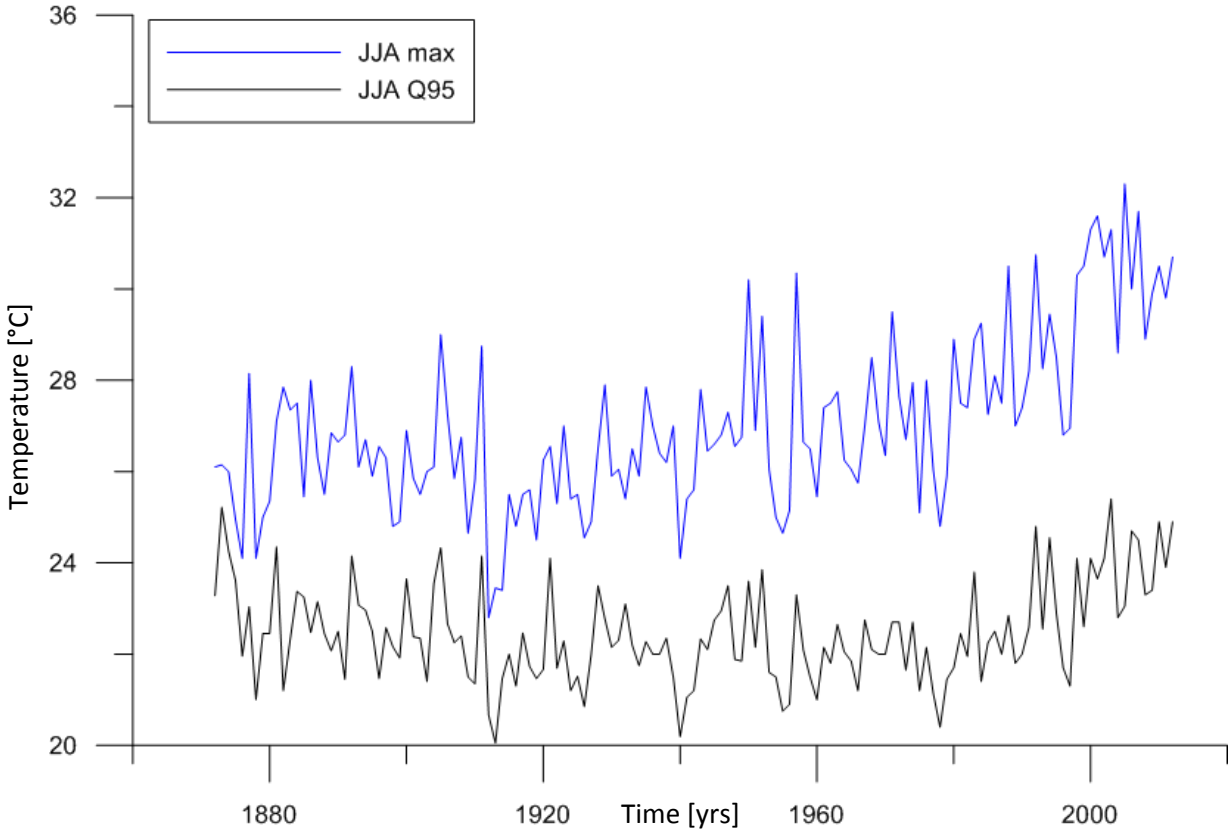

Changes in SON temperature from 1872 to 2012 (T_{max} and 95% quantiles)

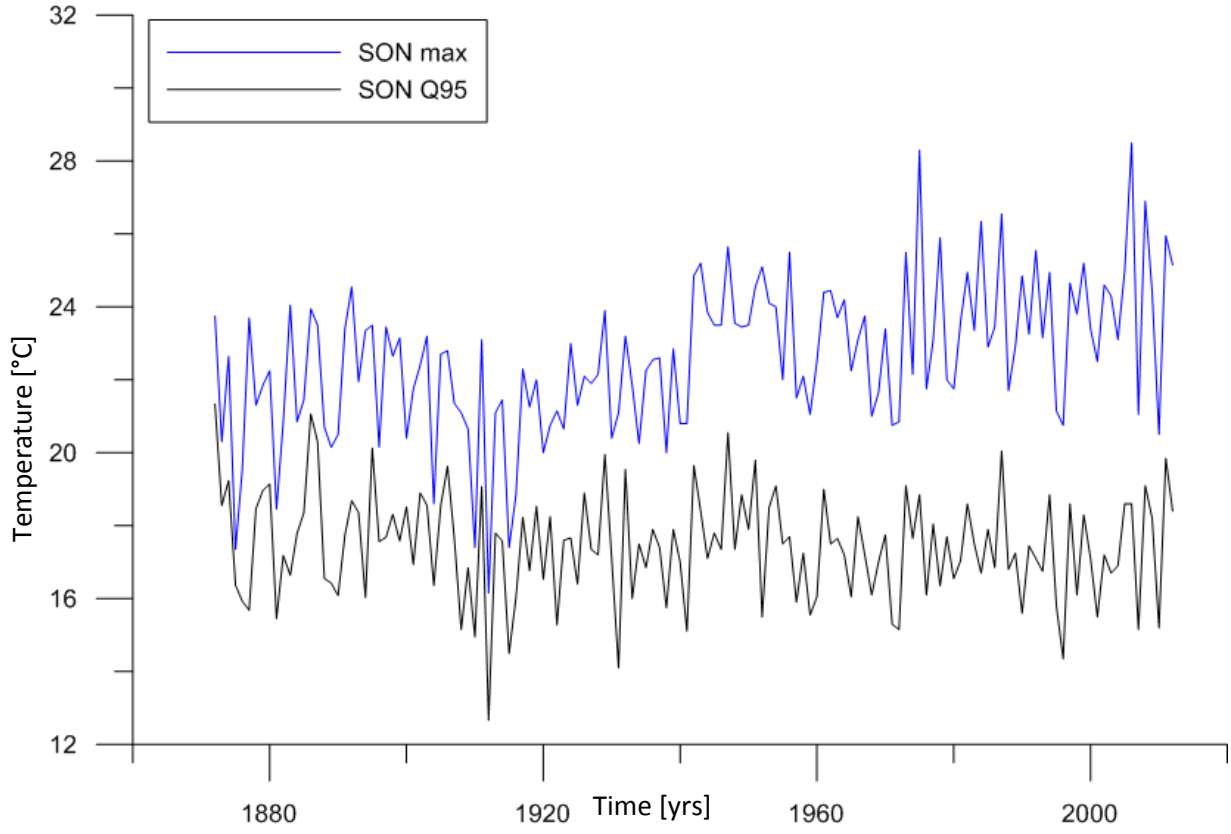

Analysis of joint quantiles

Cold/Dry and Cold/Wet Days – Annually; compared to 10/10 and 10/90 percentile

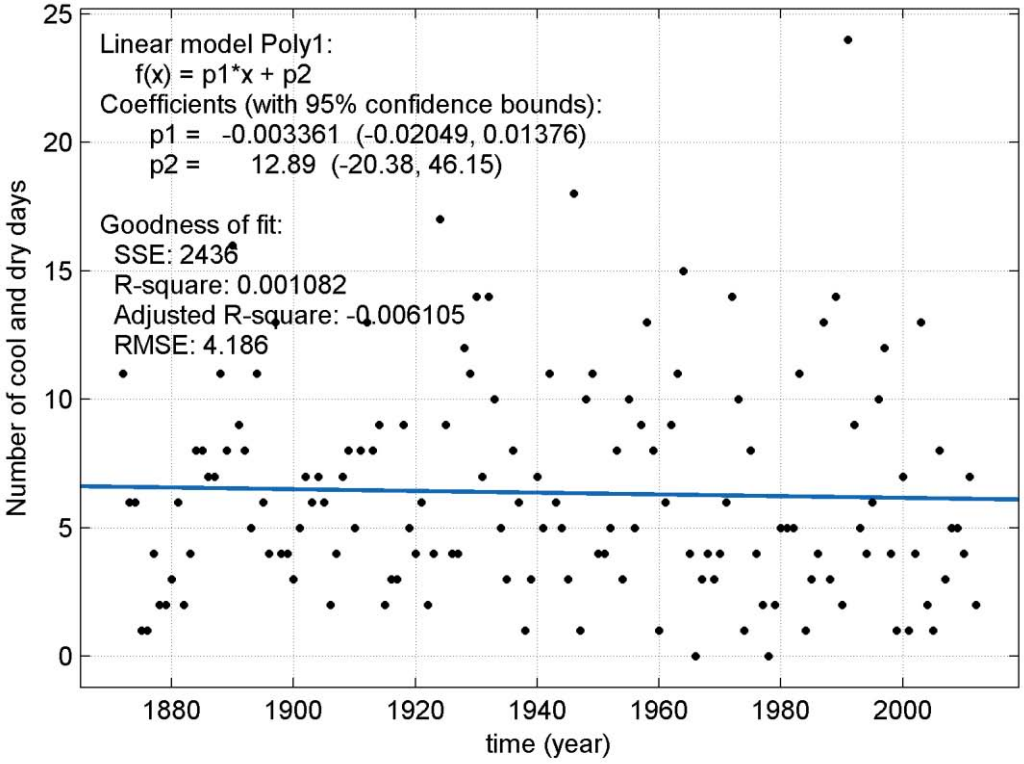

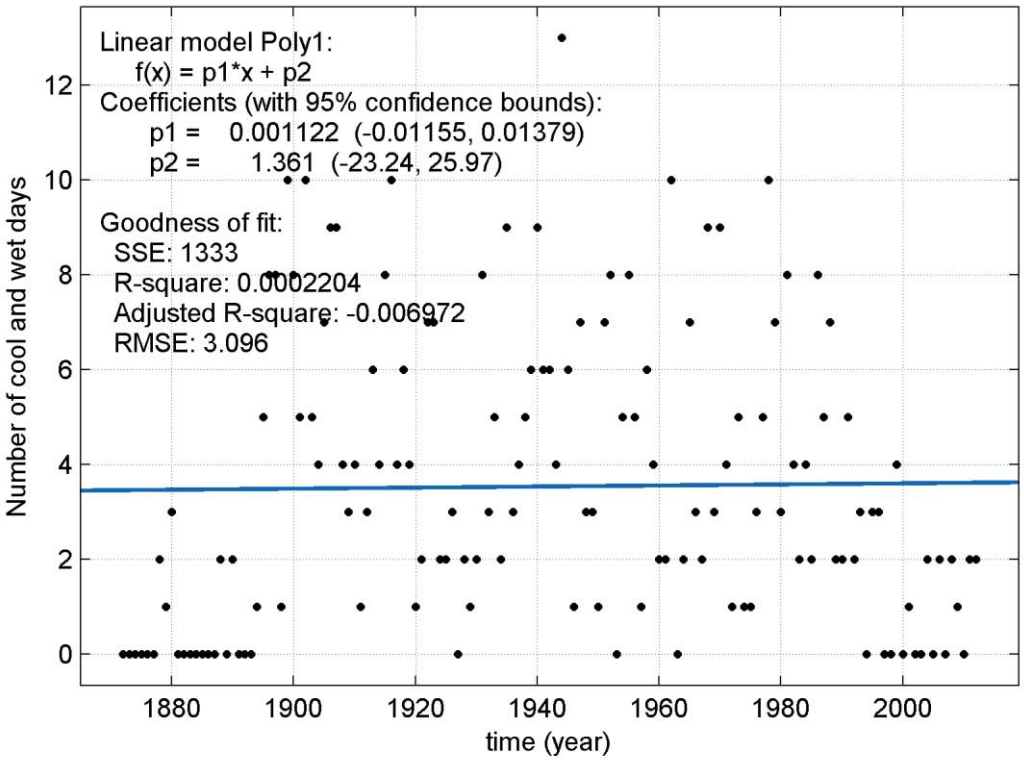

Warm/Dry and Warm/Wet Days – Annually; compared to 90/10 and 90/90 percentile

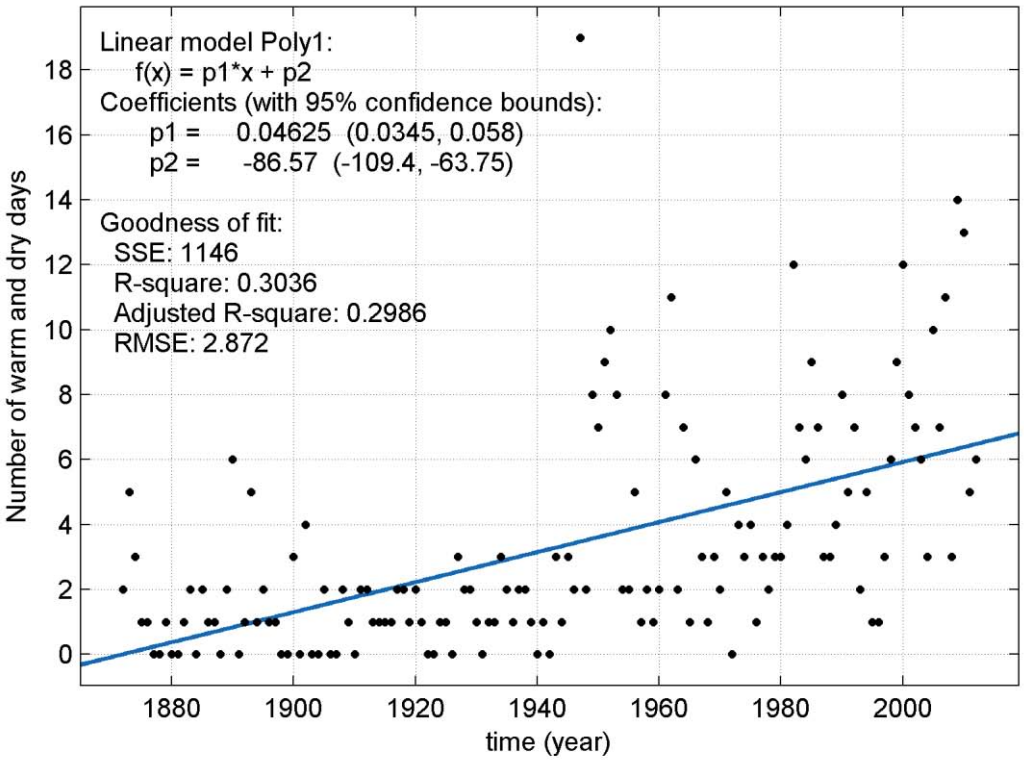

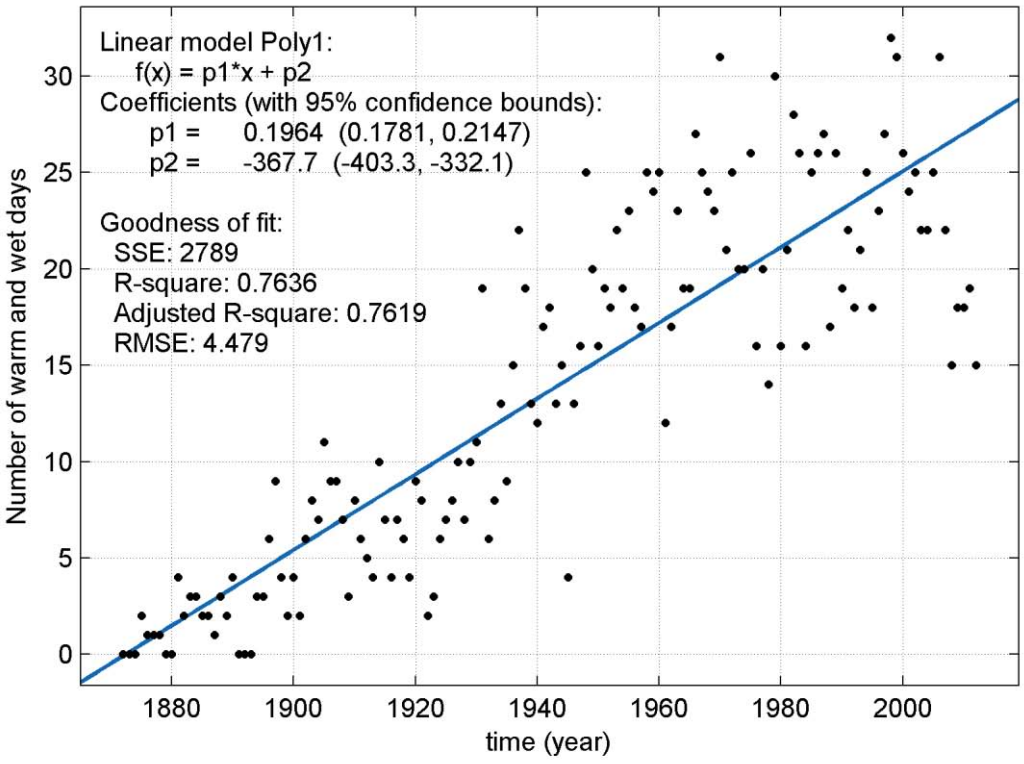

Cold/Dry and Cold/Wet Days – DJF; compared to 10/10 and 10/90 percentile

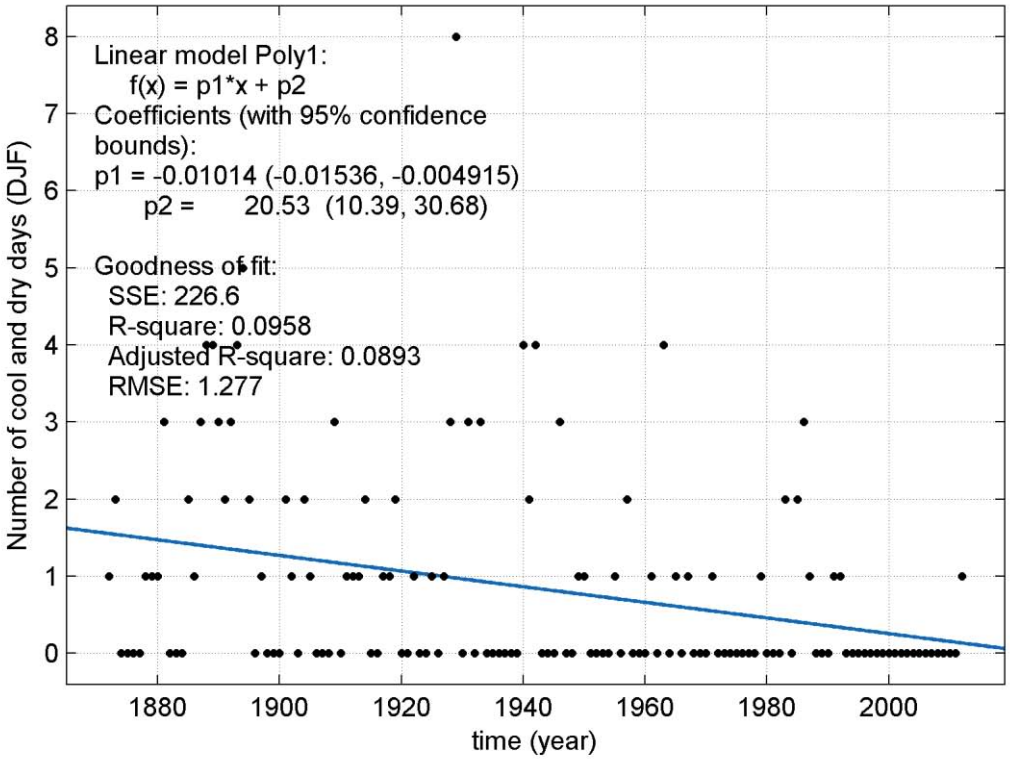

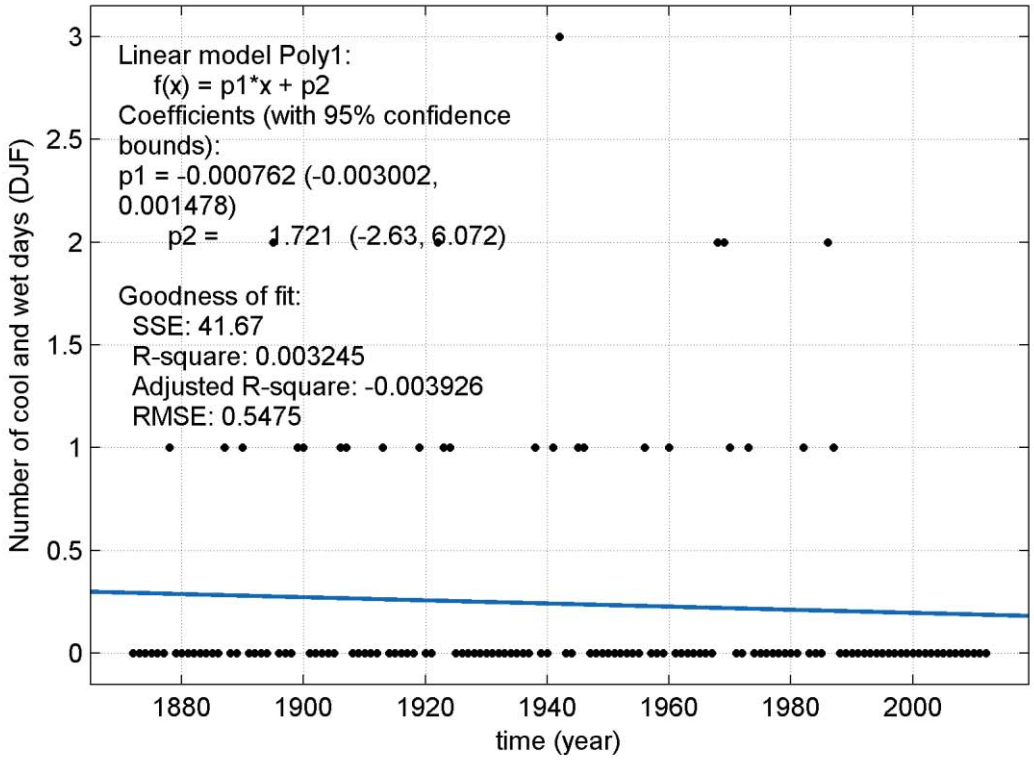

Warm/Dry and Warm/Wet Days – DJF; compared to 90/10 and 90/90 percentile

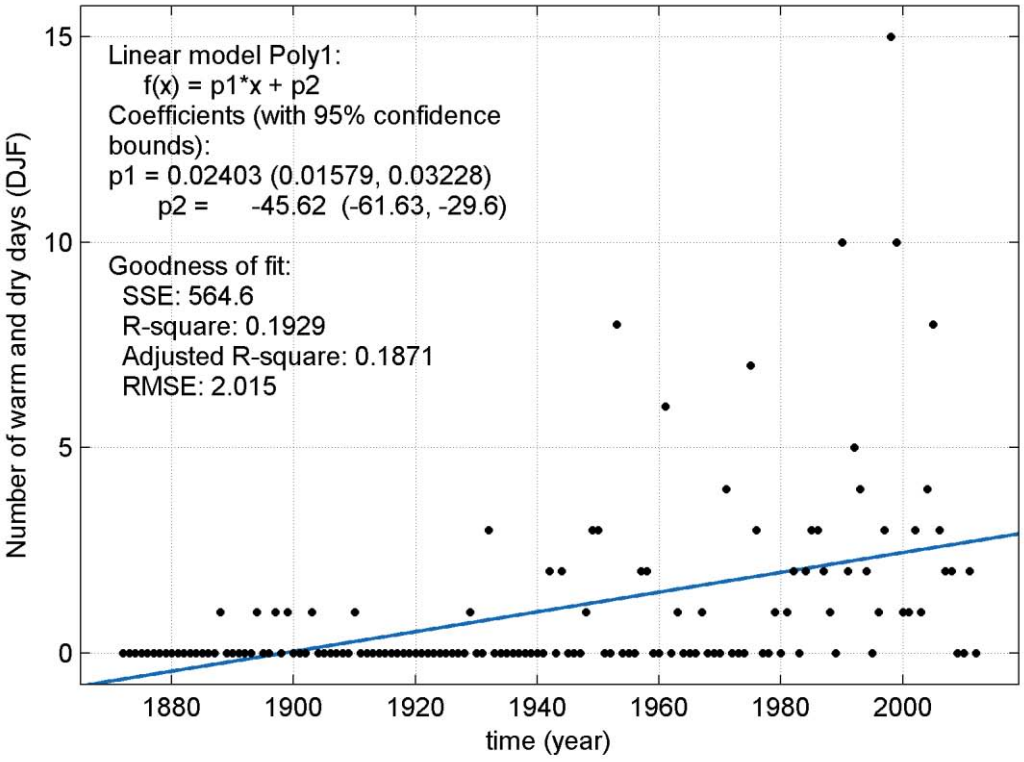

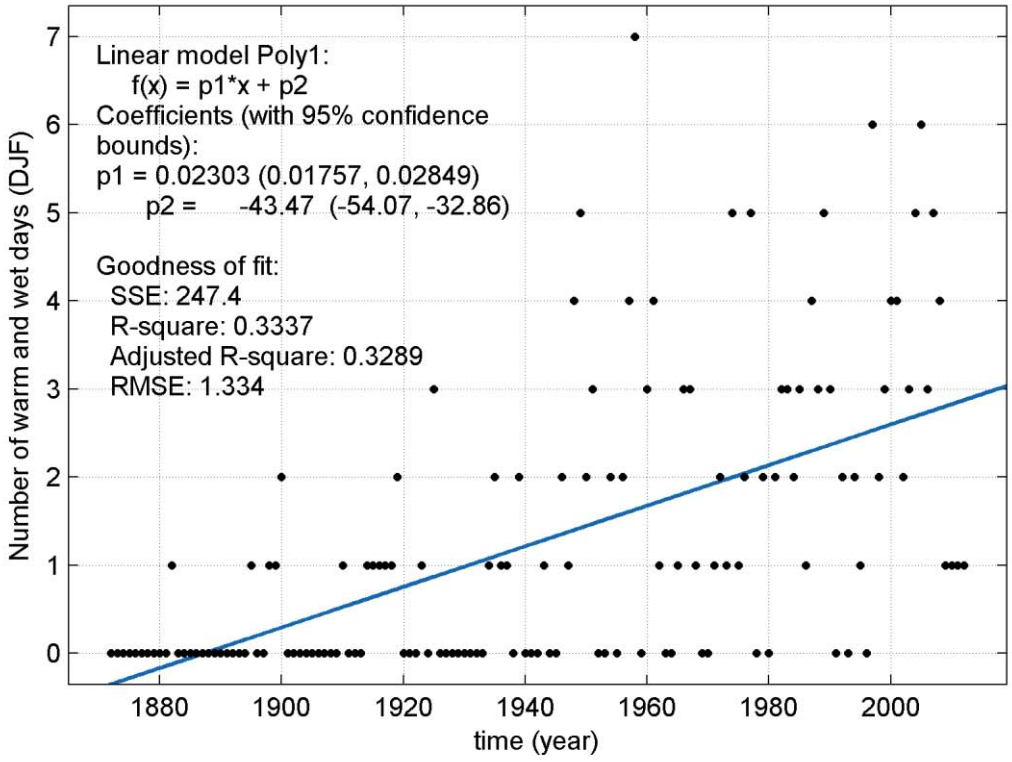

Cold/Dry and Cold/Wet Days – MAM; compared to 10/10 and 10/90 percentile

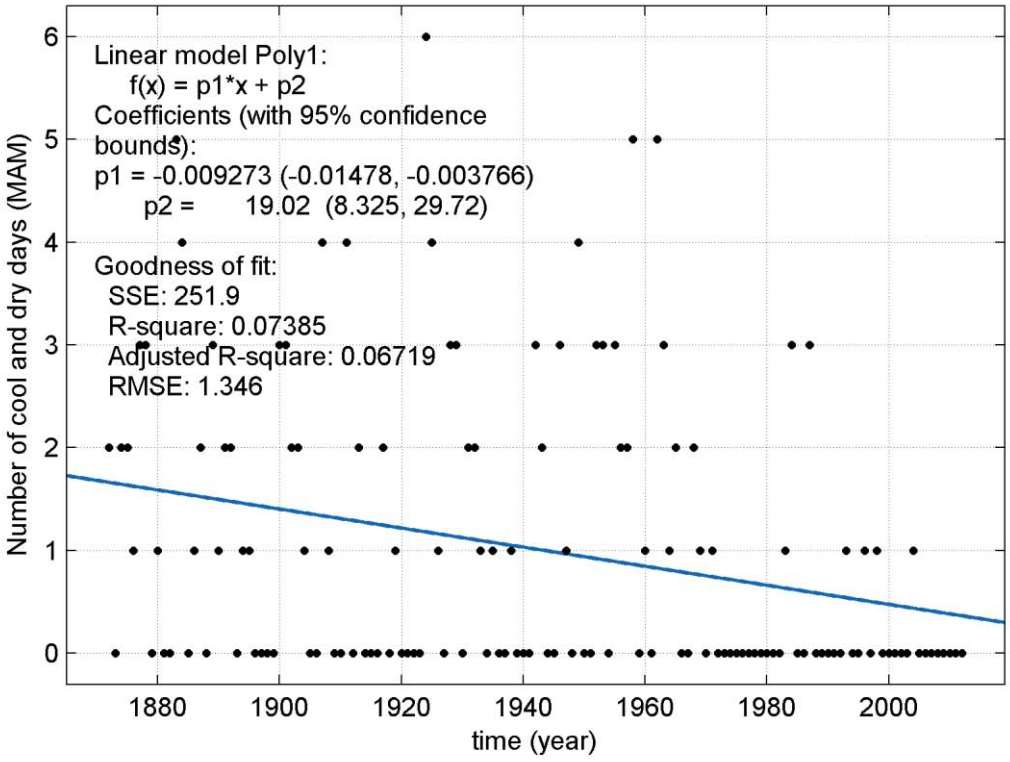

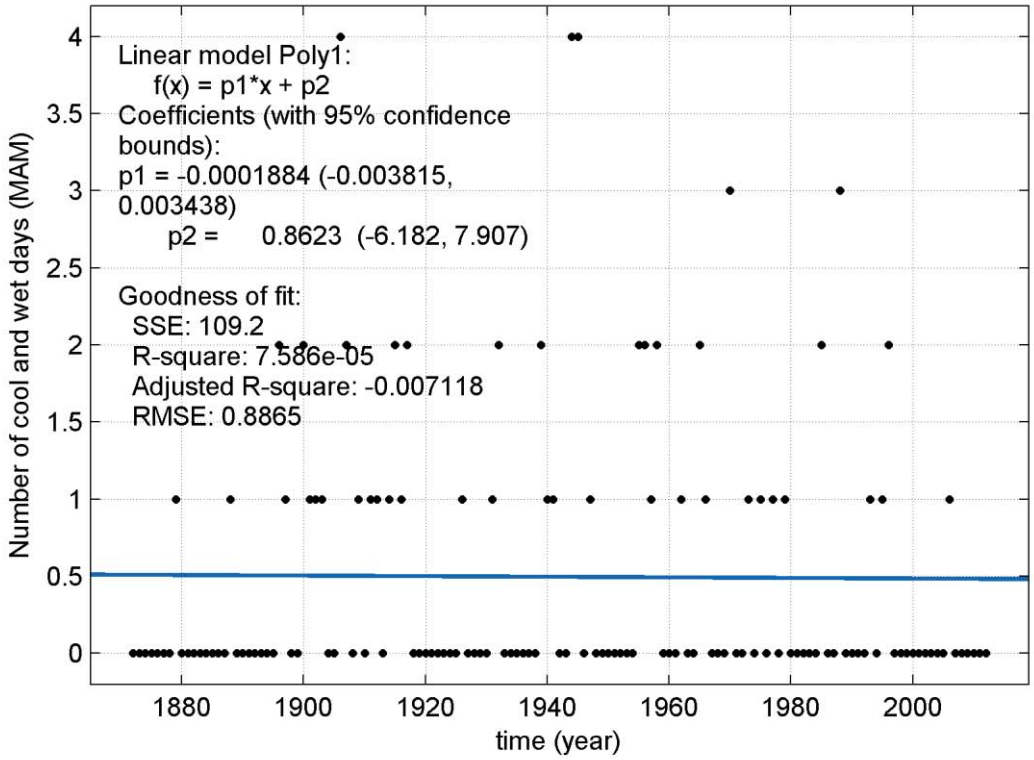

Warm/Dry and Warm/Wet Days – MAM; compared to 90/10 and 90/90 percentile

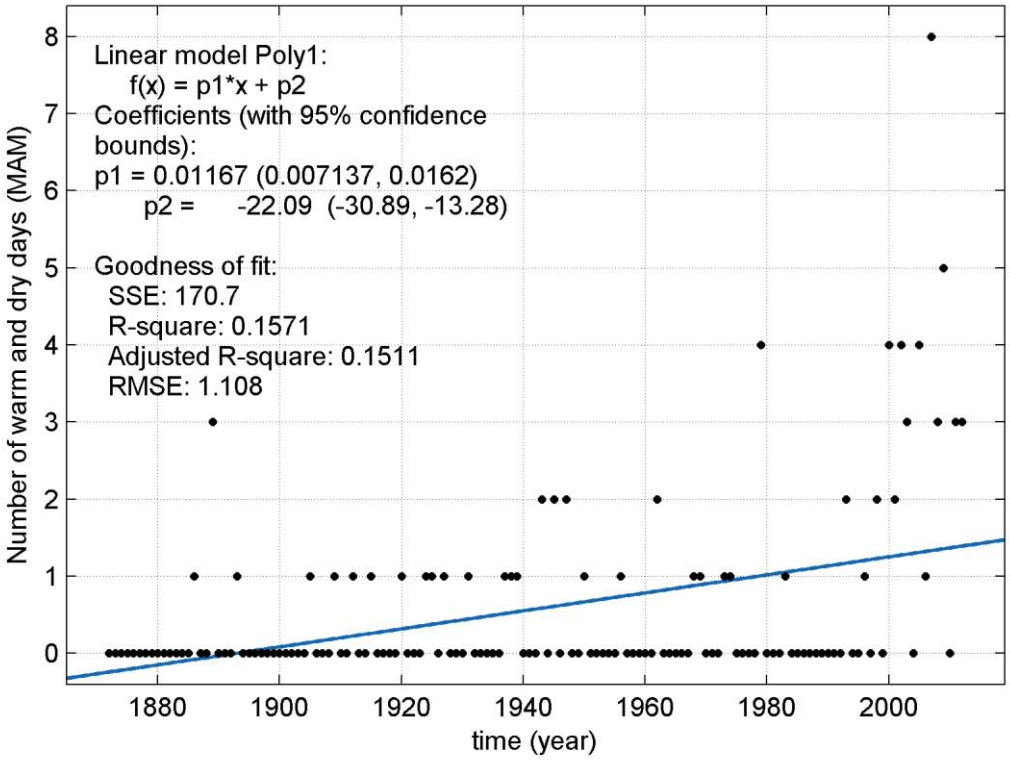

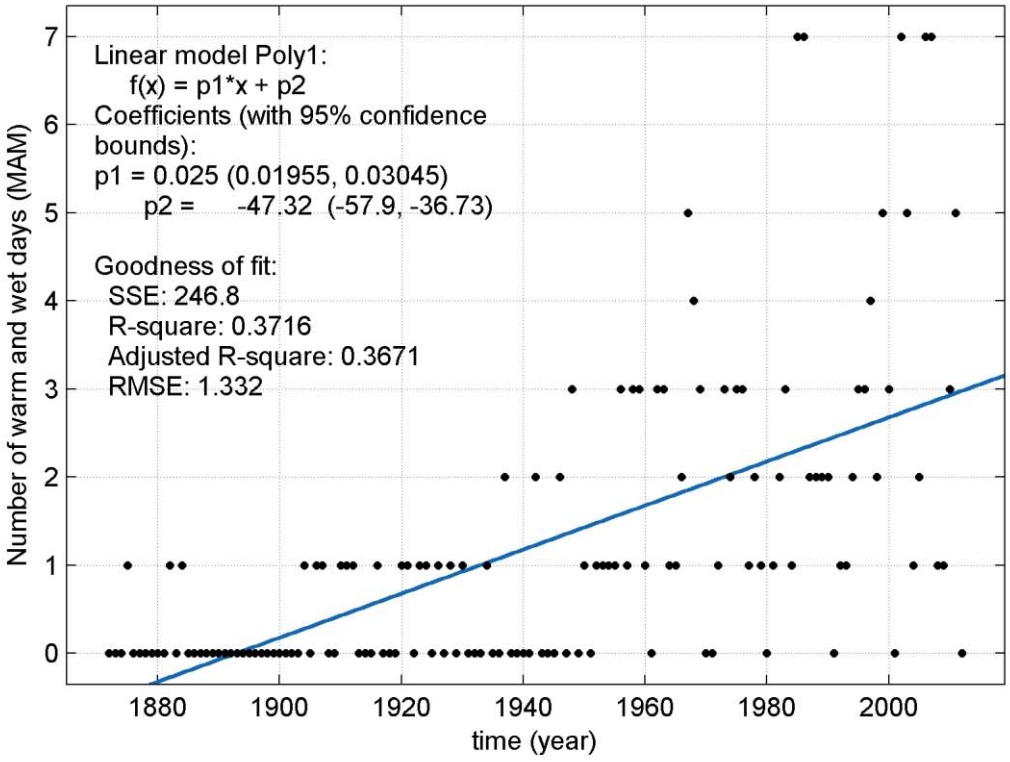

Cold/Dry and Cold/Wet Days – JJA; compared to 10/10 and 10/90 percentile

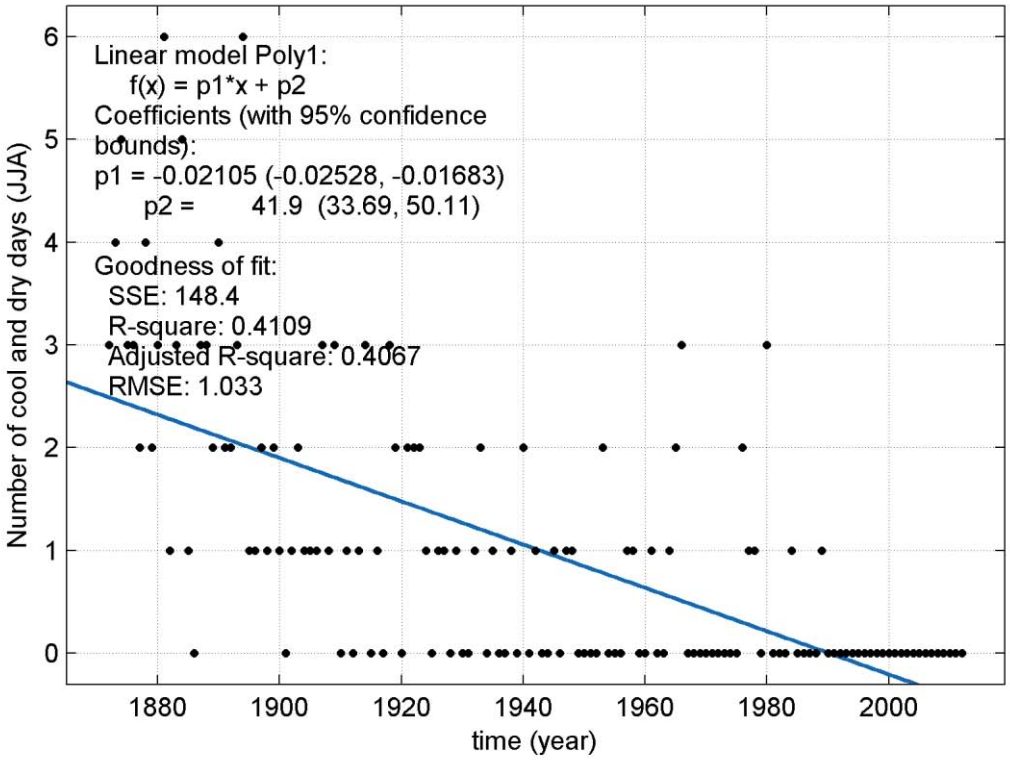

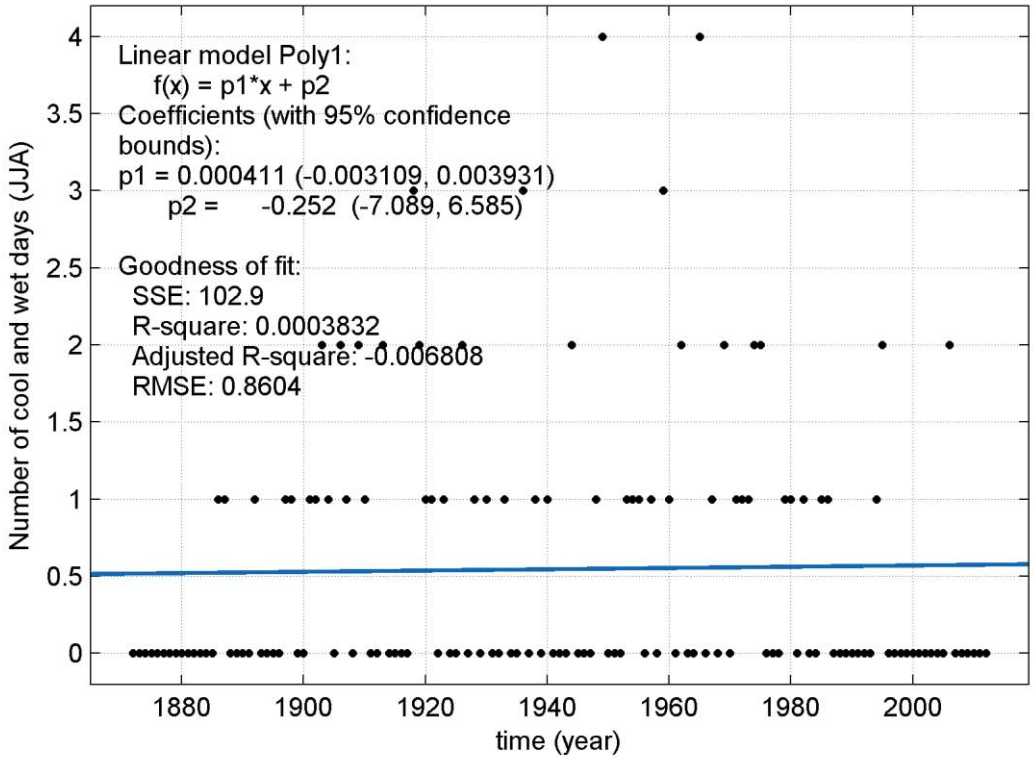

Warm/Dry and Warm/Wet Days – JJA; compared to 90/10 and 90/90 percentile

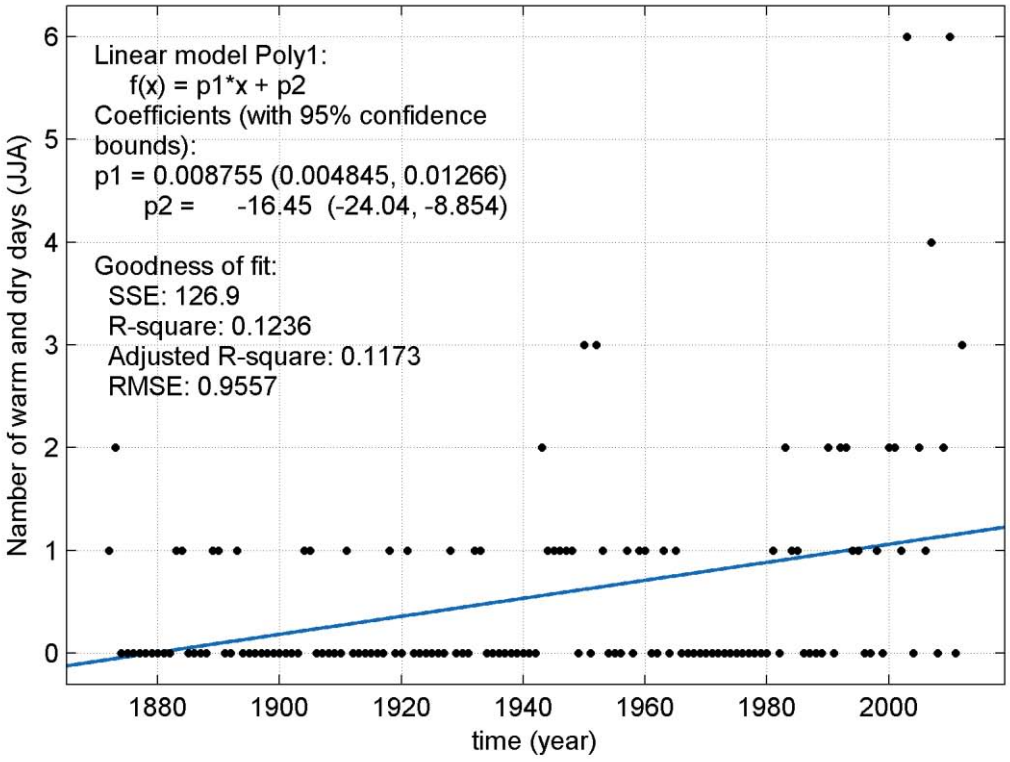

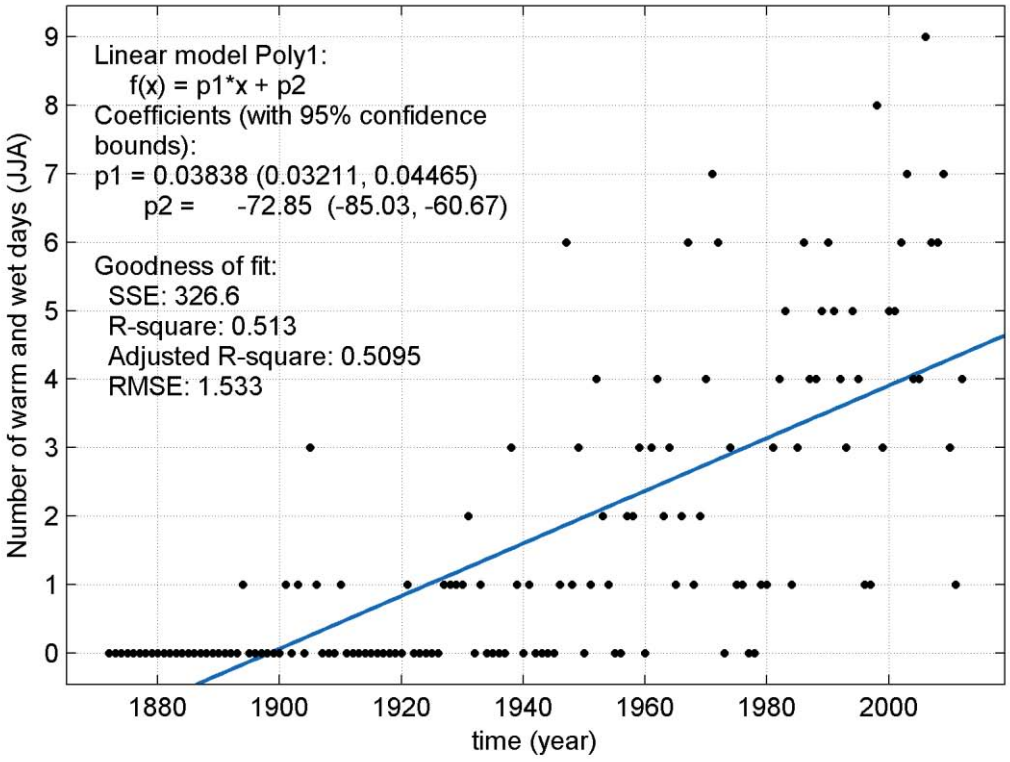

Cold/Dry and Cold/Wet Days – SON; compared to 10/10 and 10/90 percentile

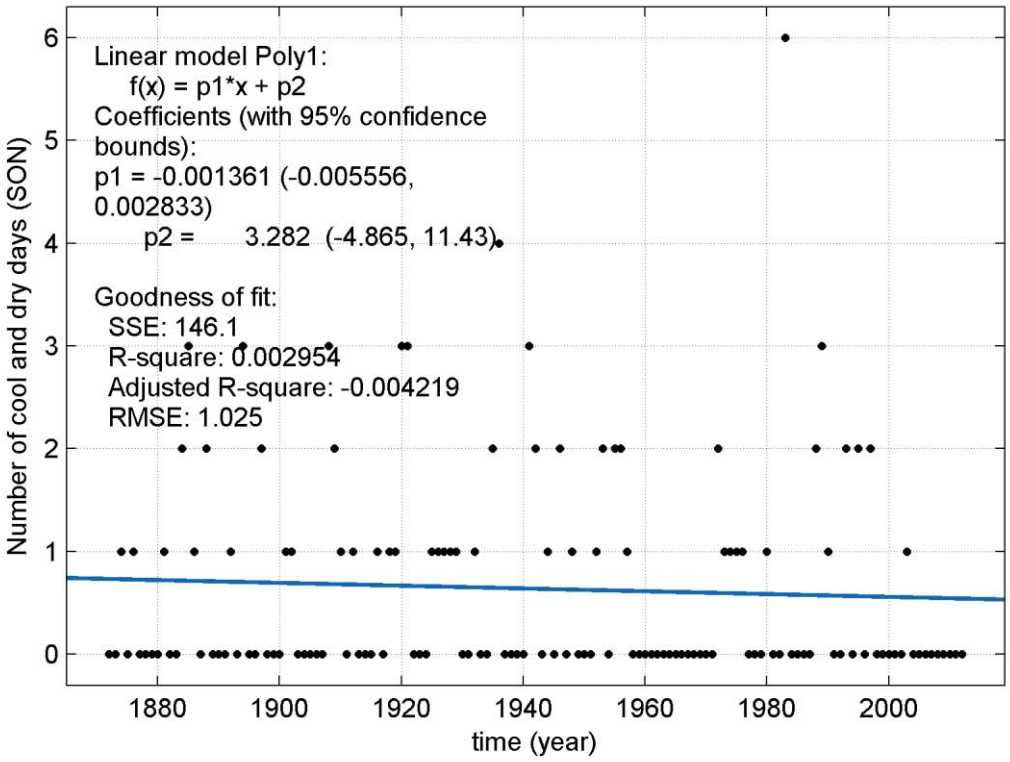

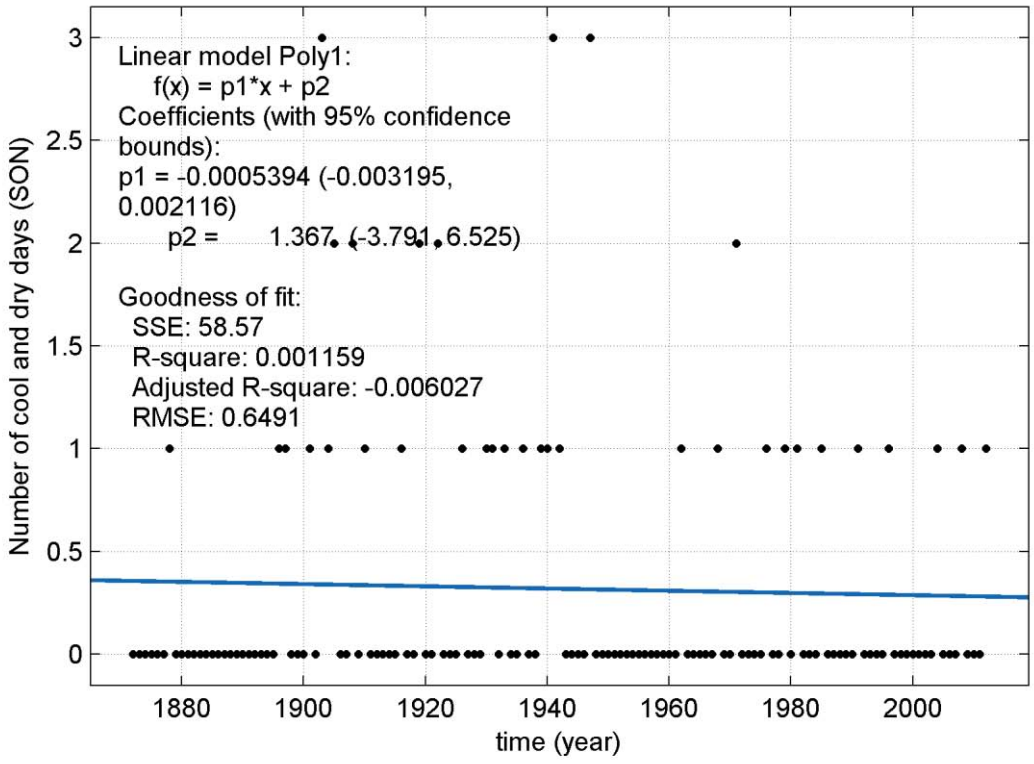

Warm/Dry and Warm/Wet Days – SON; compared to 90/10 and 90/90 percentile

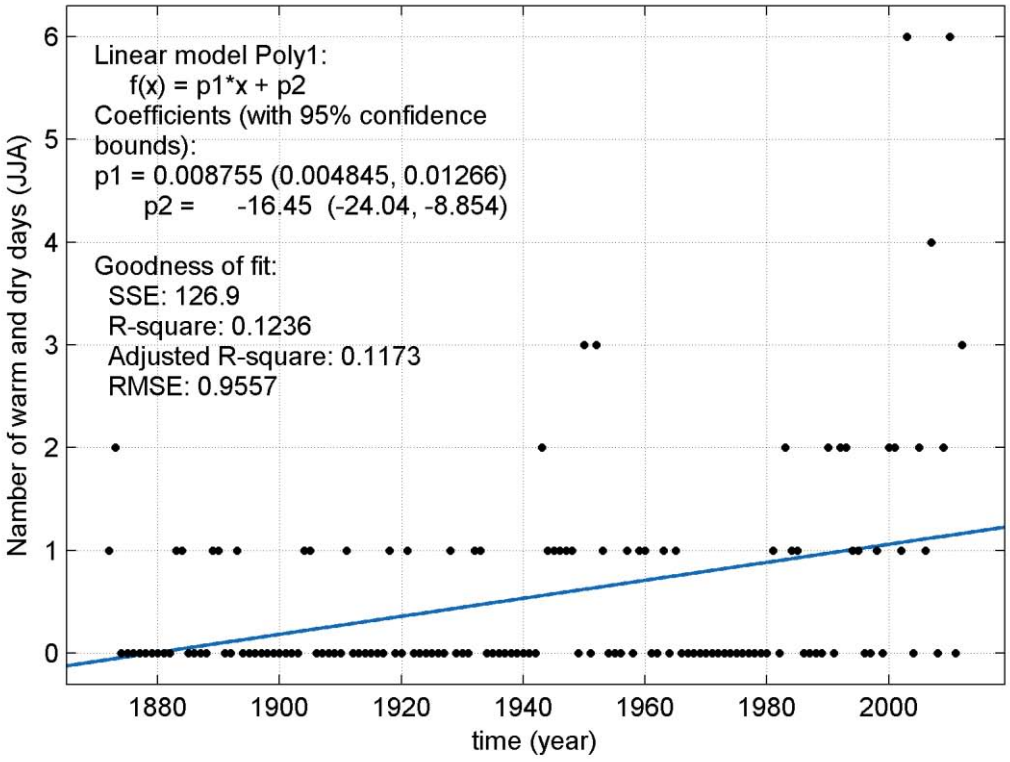

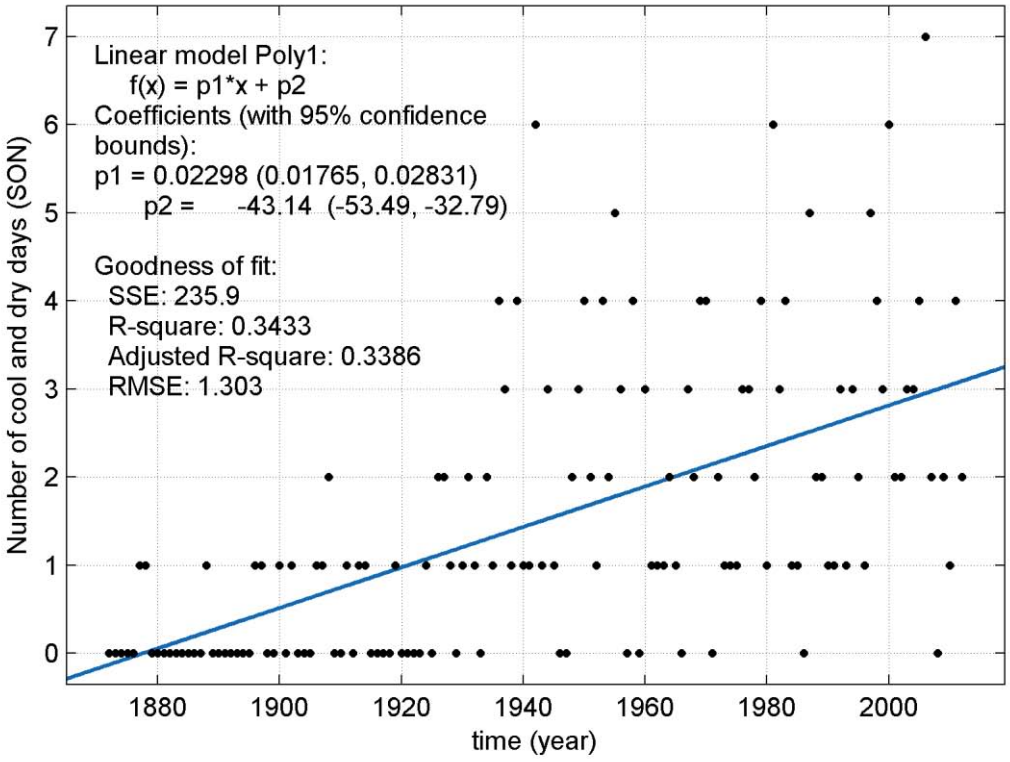

Intensity-Duration relationships

Intensity-duration diagram for TER (black) and for TER of DFs of magnitude=1

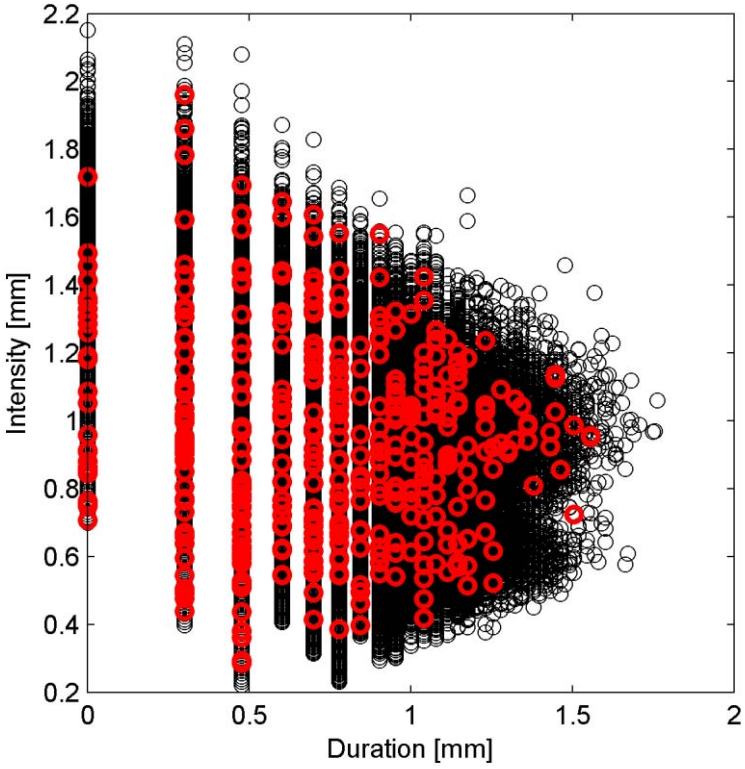

Intensity-duration diagram for TER (black) and for TER of DFs of magnitude=2

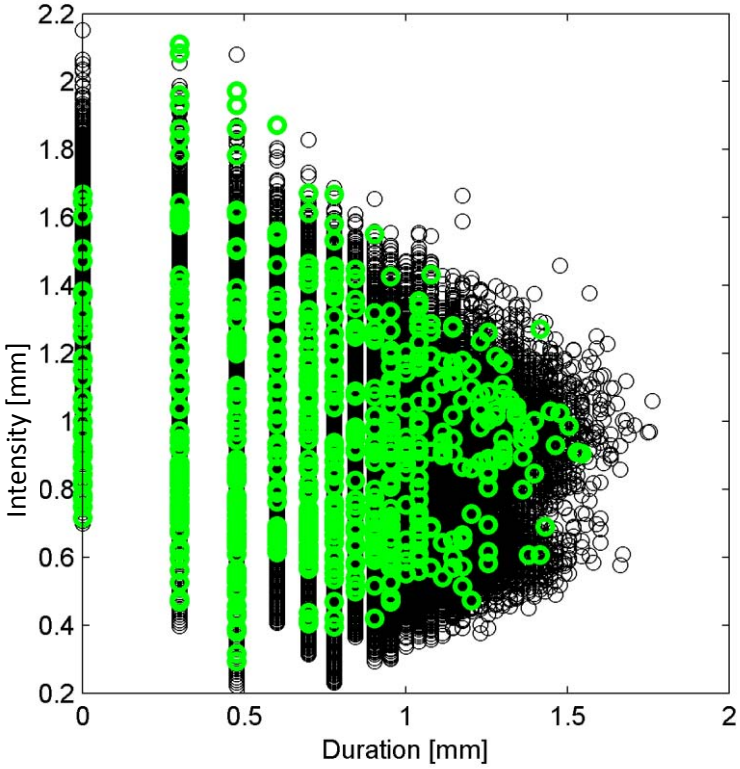

Intensity-duration diagram for TER (black) and for TER of DFs of magnitude=3

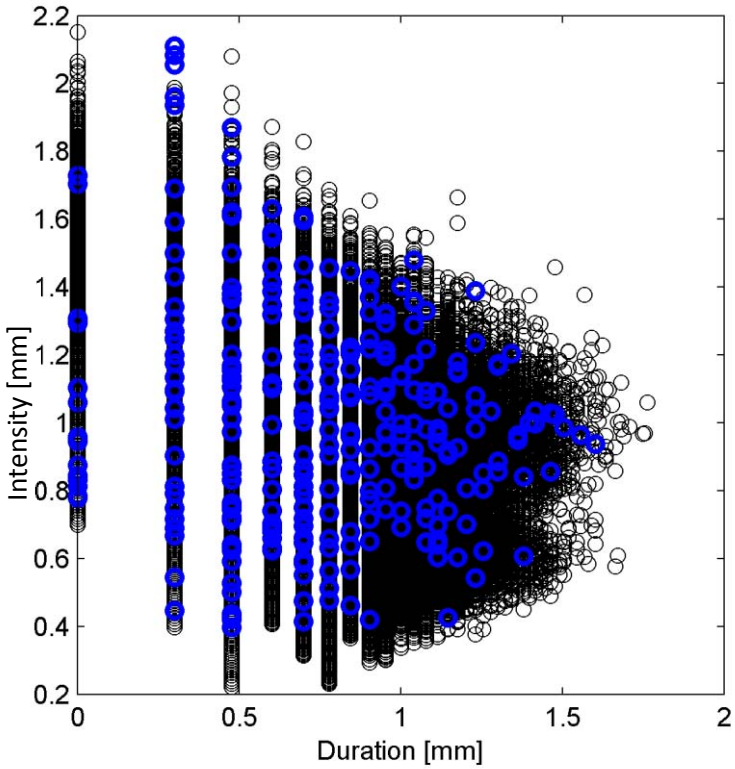

Intensity-duration diagram for TER (black) and for TER of DFs of magnitude=4

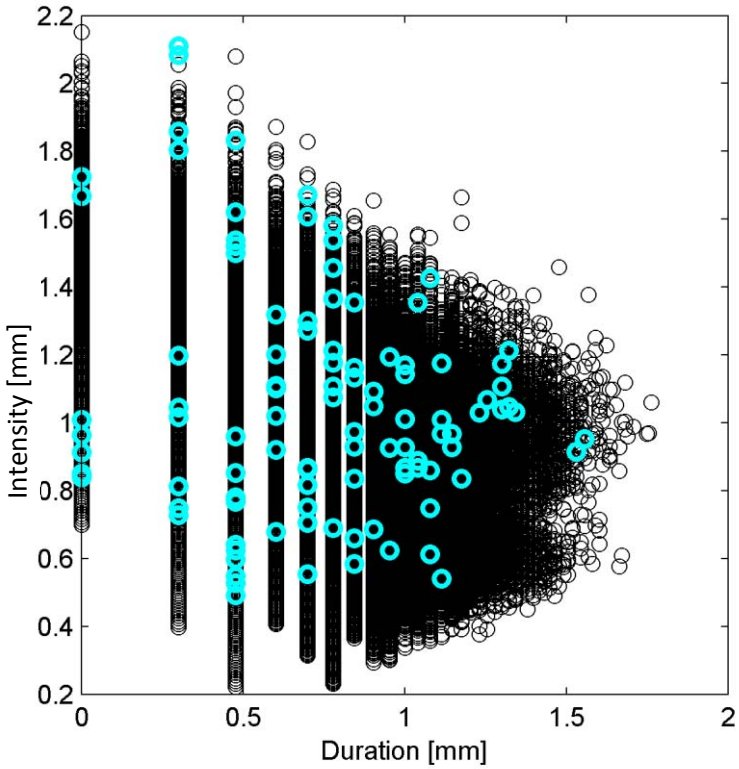

Magnitude-Intensity relationships

Box plots for the TER for different intensity classes

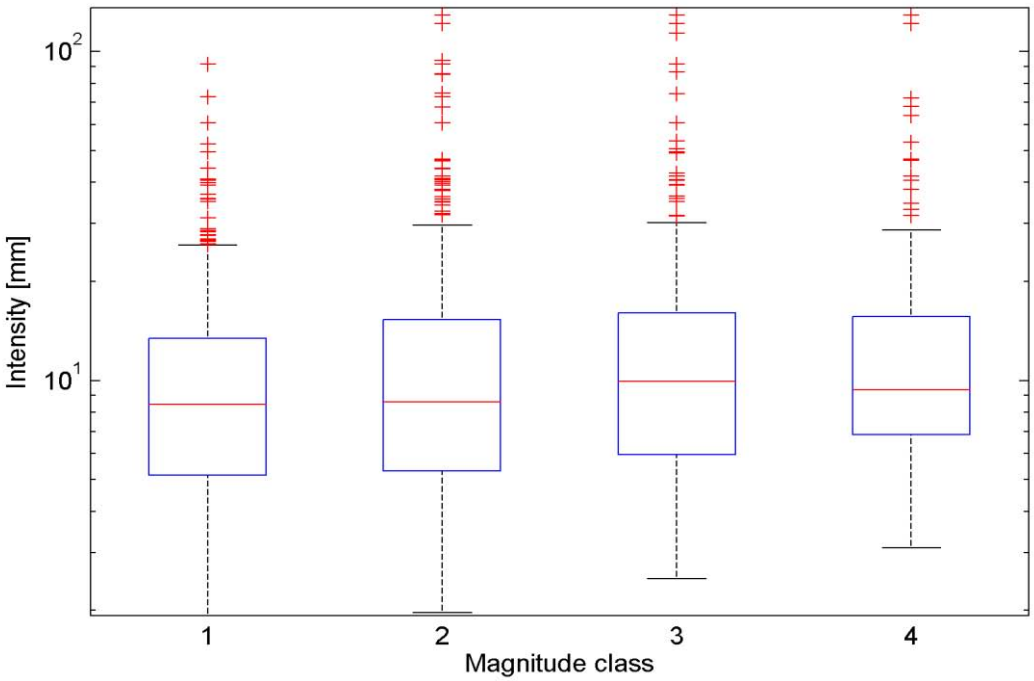

Bayesian analysis

2D Bayesian analysis for all events

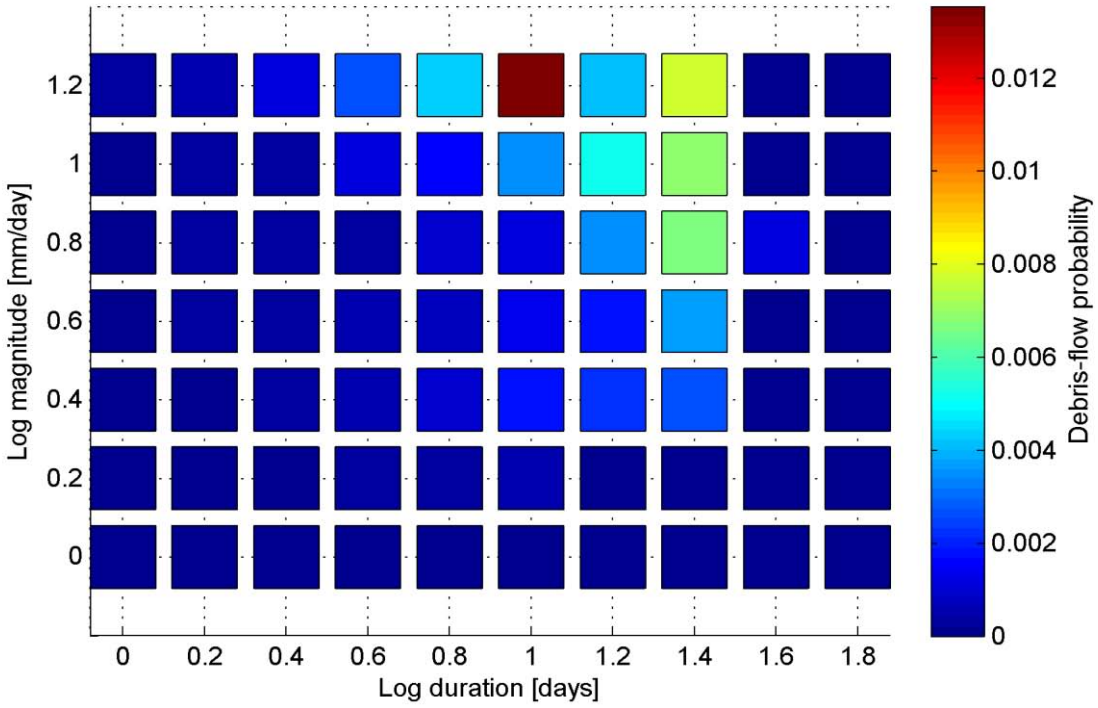

2D Bayesian analysis for all events with assigned magnitudes

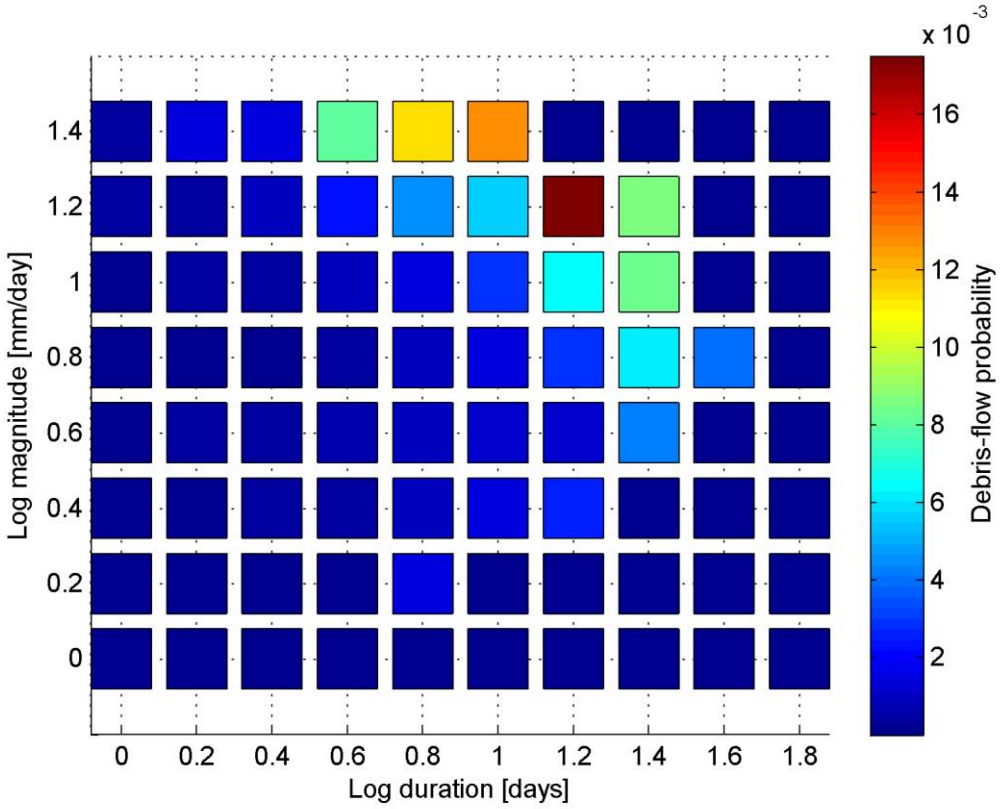

2D Bayesian analysis for all events with magnitude = 1

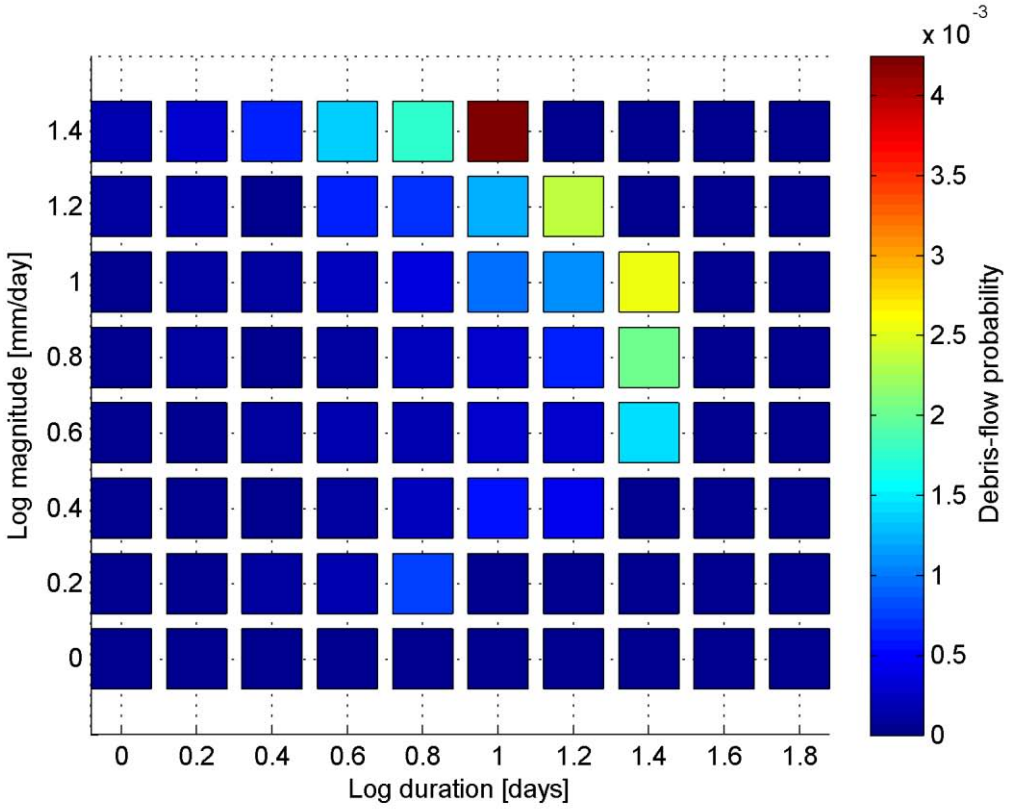

2D Bayesian analysis for all events with magnitude = 2

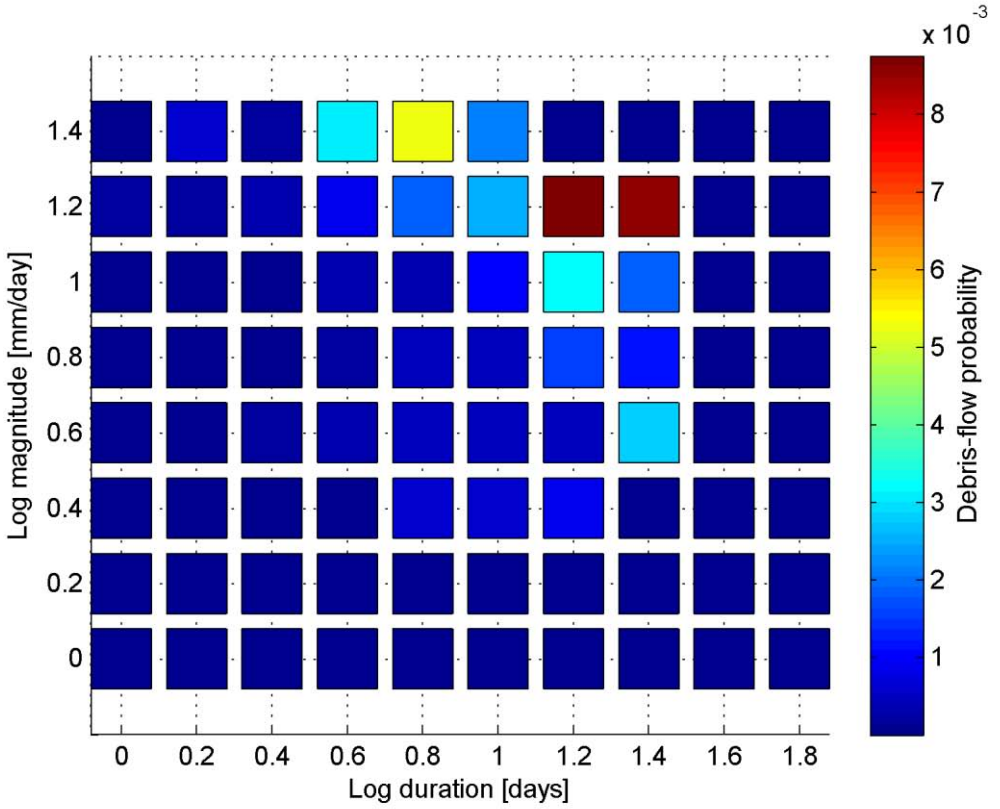

2D Bayesian analysis for all events with magnitude = 3

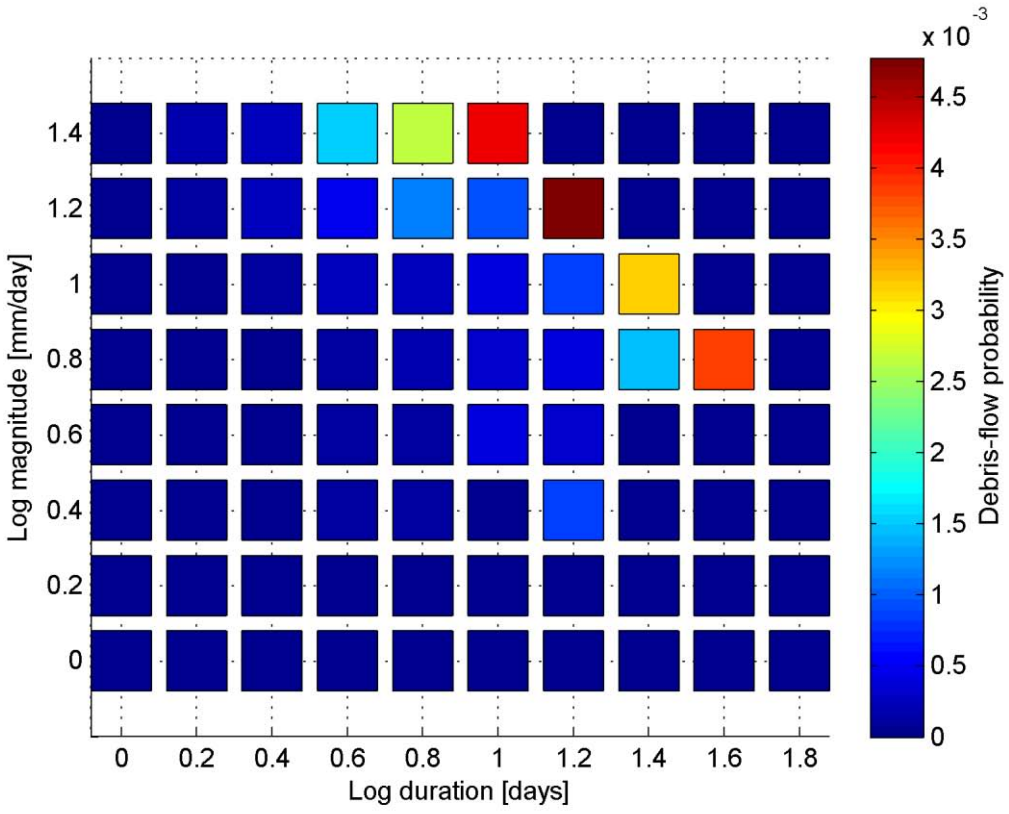

2D Bayesian analysis for all events with magnitude = 4

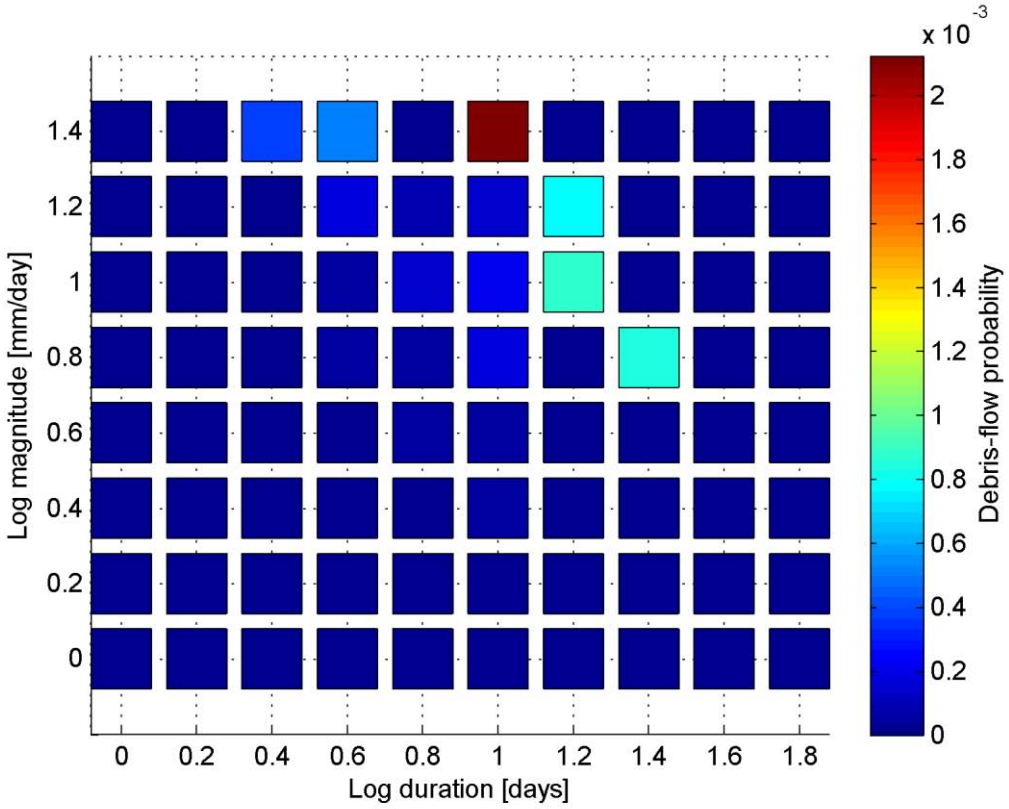

Appendix 2 – Raw data file examples

Example of a ZAMG data-file

name	istnr	laenge	breite	hoehe	datum	tmin	tmax	druckmit	nied	schnee
VILLACH/PERAU	20117	135100	463600	493	19510701	115	150	9652	24	-1
VILLACH/PERAU	20117	135100	463600	493	19510702	90	225	9653	-1	-1
VILLACH/PERAU	20117	135100	463600	493	19510703	117	250	9617	-1	-1
VILLACH/PERAU	20117	135100	463600	493	19510704	100	284	9579	347	-1
VILLACH/PERAU	20117	135100	463600	493	19510705	134	239	9579	88	-1
VILLACH/PERAU	20117	135100	463600	493	19510706	125	229	9623	-1	-1
VILLACH/PERAU	20117	135100	463600	493	19510707	100	257	9636	-1	-1
VILLACH/PERAU	20117	135100	463600	493	19510708	110	276	9597	-1	-1
VILLACH/PERAU	20117	135100	463600	493	19510709	129	276	9565	31	-1
VILLACH/PERAU	20117	135100	463600	493	19510710	138	275	9612	-1	-1
VILLACH/PERAU	20117	135100	463600	493	19510711	136	285	9607	-1	-1
VILLACH/PERAU	20117	135100	463600	493	19510712	130	284	9618	80	-1
VILLACH/PERAU	20117	135100	463600	493	19510713	131	268	9631	4	-1
VILLACH/PERAU	20117	135100	463600	493	19510714	127	284	9615	12	-1
VILLACH/PERAU	20117	135100	463600	493	19510715	122	298	9585	-1	-1
VILLACH/PERAU	20117	135100	463600	493	19510716	128	237	9570	133	-1
VILLACH/PERAU	20117	135100	463600	493	19510717	138	190	9604	50	-1
VILLACH/PERAU	20117	135100	463600	493	19510718	135	235	9613	-1	-1
VILLACH/PERAU	20117	135100	463600	493	19510719	89	281	9613	-1	-1
VILLACH/PERAU	20117	135100	463600	493	19510720	124	259	9606	-1	-1

Example of an eHYD data-file

```
Messstelle:                Forchach
HZB-Nummer:                101212
HD-Nummer:                 HD7000008
DBMS-Nummer:               7000008
Sachgebiet:                NLV
Dienststelle:              HD-Tirol
Messstellenbetreiber:      Hydrographischer Dienst
Höhe:
  gültig seit:             Höhe [m ü.A.]:
   11.09.1895              905
   10.07.1962              905
   24.08.1983              910
   16.11.1989              910
   13.08.1991              910
Geographische Koordinaten (Referenzellipsoid: Bessel 1841):
  gültig seit:             Länge (Grad,Min,Sek):    Breite  (Grad,Min,Sek):
   11.09.1895              10 35 00                 47 25 00
   10.07.1962              10 35 05                 47 25 11
   24.08.1983              10 35 10                 47 25 13
   16.11.1989              10 35 13                 47 25 06
   13.08.1991              10 35 09                 47 25 11
Exportzeitreihe:           Niederschlag,I,Sum,T,1,O,Z,0,,,
Exportqualität:            MAXQUAL
Einheit:                   mm
Exportzeitraum:            01.01.1971 07:00 bis 01.01.2011 07:00
Der Intervallwert gilt bis zum nächsten Zeitpunkt mit einem Wert oder Lücke
Werteformat:               1 Nachkommast.
Werte:
01.01.1971 07:00:00        0.3
02.01.1971 07:00:00        0.0
03.01.1971 07:00:00        0.0
04.01.1971 07:00:00        0.0
05.01.1971 07:00:00        0.0
06.01.1971 07:00:00        0.0
```